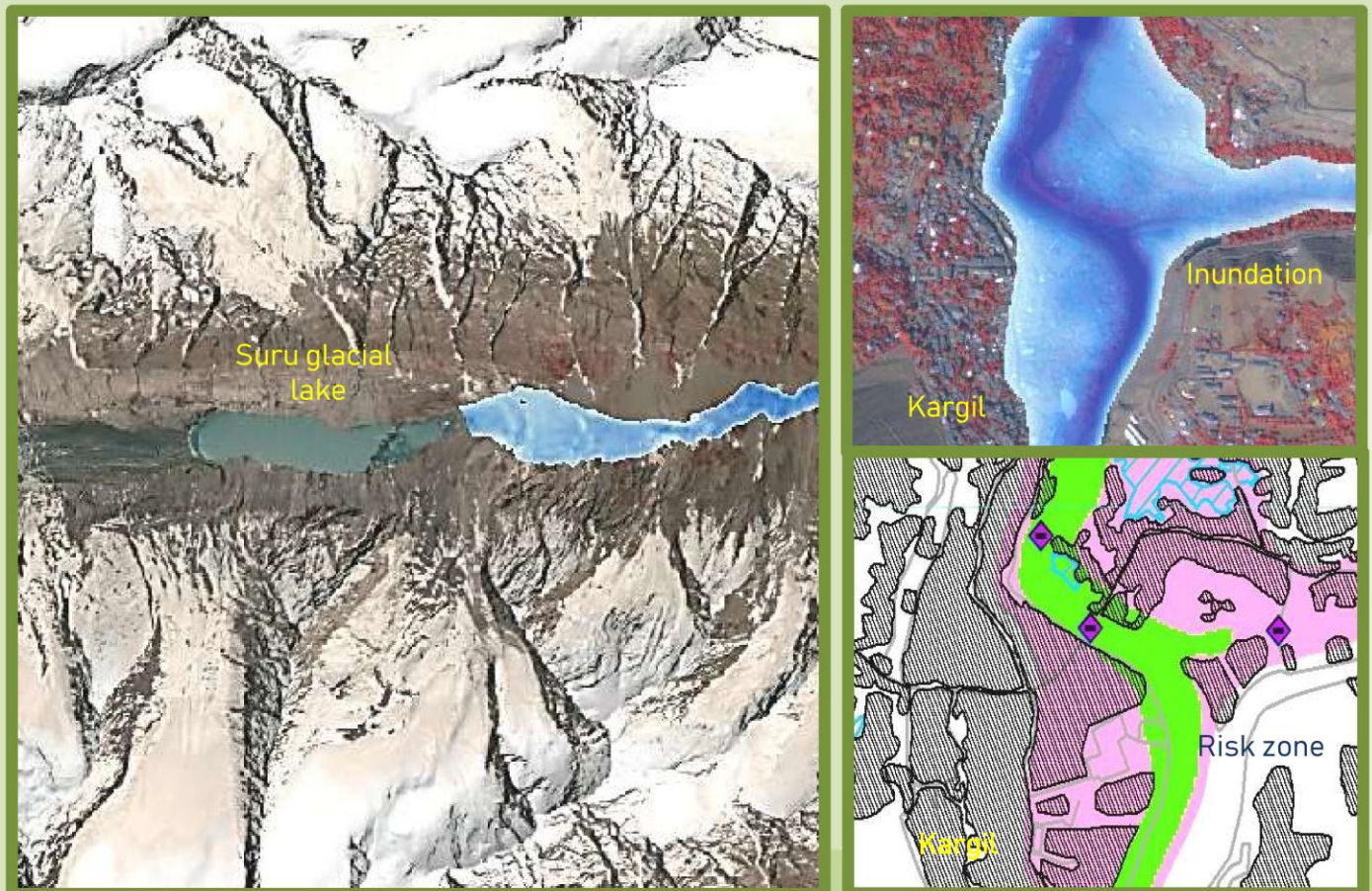


GLOF Risk Assessment of Suru Glacial Lake in Indus River Basin

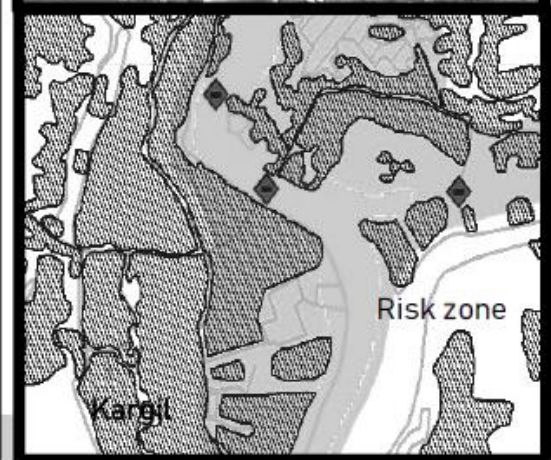
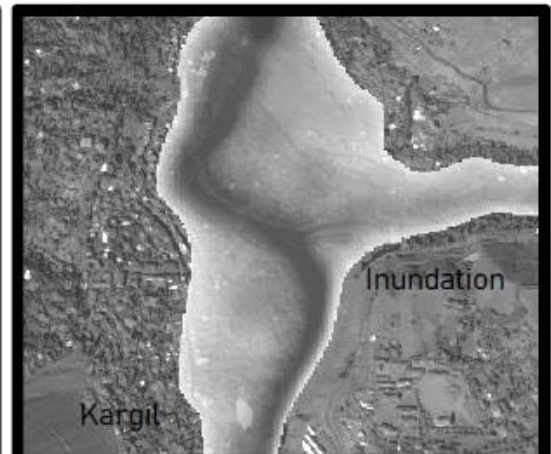
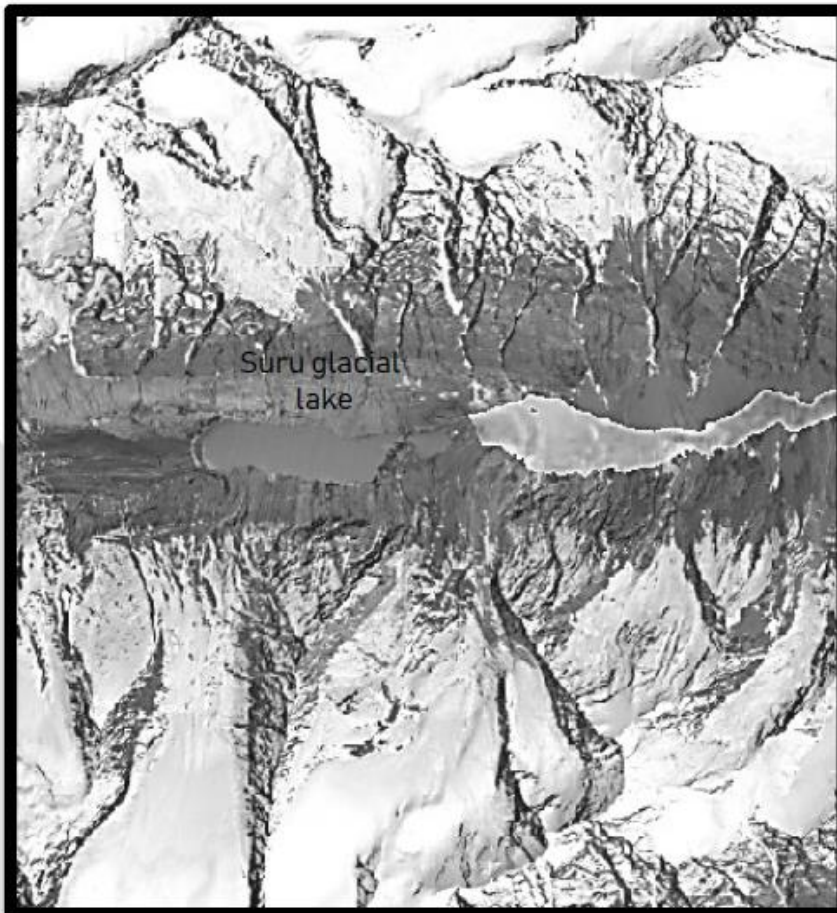
Prepared under National Hydrology Project



National Remote Sensing Centre
Indian Space Research Organisation
Department of Space, Government of India
Hyderabad – 500 037

GLOF Risk Assessment of Suru Glacial Lake in Indus River Basin

Prepared under National Hydrology Project



National Remote Sensing Centre
Indian Space Research Organisation
Department of Space, Government of India
Hyderabad - 500 037



Copyright © 2024

National Remote Sensing Centre, ISRO

Published by

National Remote Sensing Centre, ISRO
Department of Space, Government of India
Hyderabad - 500 037, Telangana, India
<https://www.nrsc.gov.in>

Production

NRSC has taken up several activities under the National Hydrology Project (NHP), sponsored by the Department of Water Resources, River Development and Ganga Rejuvenation (DoWR, RD&GR), Ministry of Jal Shakti, Government of India (GOI) with financial aid from the World Bank.

Reproduction

This publication may be produced in whole or in part and in any form for educational or non-profit purposes without permission from the copyright holder, provided the acknowledgement and citation of the source is made in all type of publications, which include research articles, journal papers, conference proceedings, books, book chapters, scientific reports, dissertation, etc. NRSC would appreciate receiving a copy of any publication that uses this publication as a source. No use of this publication may be made for resale or for any other commercial purposes.

The views and interpretations in this publication are those of the author(s). They are not attributable to NRSC and do not imply the expression of any opinion concerning the legal status of any country, territory, city or area of its authorities, or concerning the delimitation of its frontiers or boundaries, or the endorsement of any product. The administrative boundaries presented in this publication are only for scientific study and not for statutory purpose.

DOCUMENT CONTROL SHEET

1	Security Classification	Official		
2	Distribution	General		
3	Report/Document version	(a) Issue no. 2	(b) Revision & Date	Revision 1 & Dec 09, 2024
4	Report/Document Type	Technical report		
5	Document Control Number	NRSC-RSA-WATER RE-WRAD-MAY 2024-TR-0002436-V2.0		
6	Title	GLOF Risk Assessment of Suru Glacial Lake in Indus River Basin		
7	Particulars of collation	Pages: 104	Figures: 60	Tables: 30
8	Author(s)	B. Simhadri Rao, Saksham Joshi, Abina R and P.V. Raju		
9	Affiliation of authors	Water Resources Assessment Division (WRAD), Water Resources Group, RSAA, NRSC, ISRO, Hyderabad		
10	Project Team	Mr. P.V.Raju	Project Director (NHP) Scientist/Engineer 'G' & Group Director (WRG)	
		Mr. B. Simhadri Rao	Deputy Project Director Scientist/Engineer 'G' & Head, WRAD	
		Mr. Saksham Joshi	Principal Investigator Scientist/Engineer 'SE', WRAD	
		Technical Team	Mrs. Abina R, JRF, WRAD	
11	Scrutiny mechanism	Approved / Controlled by	Dr. K. Sreenivas, Deputy Director (RSAA)	
12	Originating unit	Water Resources Group (WRG) Remote Sensing Applications Area (RSAA) National Remote Sensing Centre, Hyderabad-500 037		
13	Sponsor/Name &Address	National Hydrology Project Ministry of Jal Shakti, New Delhi, Govt. of India		
14	Date of Initiation	January 2024		
15	Date of Publication	May 2024		
16	Abstract:	<p>This report describes the GLOF risk assessment of the Suru glacial lake in the Indus River Basin. It contains detailed description about the study area, data used, and the methodologies for hydrodynamic GLOF simulations and GLOF risk assessment for various GLOF scenarios. High resolution satellite images are used for mapping of infrastructure and other public utilities along the river reach for identifying the elements of exposure due to GLOF. A total of eight GLOF scenarios based on the volume of lake released in case of moraine breach (100%, 75%, and 50%), weather condition (clear weather/PMP), and failure mode (overtopping/piping), were simulated using the 2D hydrodynamic dam-break modelling software. The results of each simulation and consequent GLOF risk maps are also included in this report.</p> <p>Keywords: Glacial Lakes, Remote Sensing, Indus River basin, GLOF modelling and GLOF risk</p>		

Table of Contents

List of Figures	vi
List of Tables	viii
List of Abbreviations.....	ix
Summary	1
1. Introduction.....	3
1.1. About the Project.....	3
1.2. The GLOF Component.....	3
1.3. Organization of the Report.....	5
2. Literature Review.....	6
2.1. Glacial Lake Outburst Floods	6
2.2. Role of Remote Sensing and GIS	7
2.3. GLOF Modelling Approaches	8
2.4. Risk Assessment of GLOFs.....	8
3. Study Area and Data Used	11
3.1. Suru Glacial Lake and its GLOF Potential	11
3.2. Catchment Area of Suru glacial lake	14
3.3. Description of the Lake and its Moraine.....	15
3.4. Data Used.....	16
4. Methodology	18
4.1. GLOF Inundation Modelling.....	19
4.1.1. Study Area Boundaries.....	19
4.1.2. GLOF Scenarios	20
4.1.3. Processing of GLOF Model Inputs.....	22
4.1.3.1. Digital Terrain Model	22
4.1.3.2. Land Cover and Manning's n Values.....	22
4.1.3.3. Dam Breach Parameters.....	23
4.1.3.4. PMP and Runoff.....	24

4.1.4. Dam Breach Model Setup	28
4.1.5. Validation of Peak Discharge.....	31
4.2. Mapping of Exposed Elements.....	31
4.3. GLOF Risk Assessment	33
5. Results.....	37
5.1. GLOF Inundation Modelling.....	37
5.1.1. GLOF Scenarios 1&2 (100% release).....	37
5.1.2. GLOF Scenarios 7&8 (100% release with PMP)	43
5.2. GLOF Risk Assessment	47
5.2.1. GLOF Scenarios 1&7 (100% release& PMP).....	47
5.2.2. GLOF Scenarios 2&8 (100% release & PMP)	50
5.3. Limitations.....	53
6. Conclusions.....	54
References.....	55
Annexure 1: Results of GLOF Scenarios of 3 to 6	65
1. GLOF Scenarios 3&4 (75% release)	65
2. GLOF Scenarios 5&6 (50% release)	69
Annexure 2: Results of GLOF Risk Assessment for Scenarios of 3 to 6	75
1. GLOF Risk for Scenario 3 (75% release-Overtopping failure mode).....	75
2. GLOF Risk for Scenario 4 (75% release- Piping failure mode)	77
3. GLOF Risk for Scenario 5 (50% release- Overtopping failure mode)	80
4. GLOF Risk for Scenario 6 (50% release- Piping failure mode)	82
Annexure 3: GLOF Risk maps for Scenarios of 1 and 7	84

List of Figures

Figure 1: Components of Risk	9
Figure 2: Location of Suru Glacial Lake	11
Figure 3: Suru Glacial Lake and its environs	12
Figure 4: Long-term changes in Suru Glacial Lake water spread area	13
Figure 5: Urban expansion near Kargil	13
Figure 6: Upstream of Suru Glacial Lake	14
Figure 7: Slopes upstream of Suru Glacial Lake	15
Figure 8: DTM of Suru Glacial Lake and its environs.....	16
Figure 9: Flow Chart of Methodology used in the study.....	18
Figure 10: Methodology of GLOF Inundation Modeling used in the study	19
Figure 11: Study Area Boundary of Suru glacial Lake for GLOF Inundation Modelling.....	20
Figure 12: Reconditioned TanDEM-X DTM of Suru Lake.....	22
Figure 13: Probable Maximum Storm used for Runoff Estimation	26
Figure 14: Area Contributing to Rainfall-Runoff Considered in HEC-HMS Model	27
Figure 15: HEC-RAS Grid Cell and underlying Terrain Information	29
Figure 16: Hydraulic properties of Each Cell in HEC-RAS	29
Figure 17: Sample Infrastructure Maps of the study area.....	33
Figure 18: Flow Chart of Methodology of GLOF Risk Assessment	34
Figure 19: GLOF hydrograph for Scenario-1 (100% volume discharge- Overtopping failure)	37
Figure 20: GLOF hydrograph for Scenario-1 (100% volume discharge- Overtopping failure)	38
Figure 21: GLOF hydrograph for Scenario-2 (100% volume discharge - Piping failure)	38
Figure 22: GLOF hydrographs at Different Downstream Locations for scenario-2	39
Figure 23: Map of Flood Inundation Extent for GLOF Scenario-1	40
Figure 24: Map showing extent of inundation for Scenario-2.....	41
Figure 25: Map showing Close View of extent of inundation for Scenarios - 1 and 2	42
Figure 26: GLOF hydrograph for Scenario-7 (100% volume discharge & PMP- Overtopping)	43
Figure 27: GLOF hydrograph for Scenario-8 (100% volume discharge & PMP - Piping).....	43
Figure 28: Map of Flood Inundation Extent for GLOF Scenario-7	45
Figure 29: Map showing extent of inundation for Scenario-8.....	45
Figure 30: Map showing Close View of part of flood inundation for Scenarios - 7 and 8	47
Figure 31: GLOF Risk Map for the Study Area (Scenario-1 and 7)	48
Figure 32: GLOF Risk Map showing Affected Infrastructure near Kargil (Scenario-1 and 7).	49
Figure 33: GLOF Risk Map showing Affected Agricultural Land near Kargil(Scenario-1 and 7)	50
Figure 34: GLOF Risk Map for the Study Area (Scenario-2 and 8)	51
Figure 35: GLOF Risk Map showing Affected Infrastructure near Kargil (Scenario-2 and 8).	52
Figure 36: GLOF Risk Map showing Affected Agricultural Land near Kargil(Scenario-2 and 8)	52
Figure 37: GLOF hydrograph for Scenario-3 (75% volume discharge - Overtopping failure).	65
Figure 38: GLOF hydrographs at Different Downstream Locations for scenario-3	65
Figure 39: GLOF hydrograph for Scenario-4 (75% volume discharge - Piping failure)	66
Figure 40: GLOF hydrographs at Different Downstream Locations for scenario-4	66
Figure 41: Map of Flood Inundation Extent for GLOF Scenario-3	68
Figure 42: Map showing extent of inundation for Scenario-4.....	68

Figure 43: GLOF hydrograph for Scenario-5 (50% volume discharge - Overtopping failure)	70
Figure 44: GLOF hydrographs at Different Downstream Locations for scenario-5	70
Figure 45: GLOF hydrograph for Scenario-6 (50% volume discharge - Piping failure)	71
Figure 46: GLOF hydrographs at Different Downstream Locations for scenario-6	71
Figure 47: Map of Flood Inundation Extent for GLOF Scenario-5	73
Figure 48: Map showing extent of inundation for Scenario-6	73
Figure 49: GLOF Risk Map for the Study Area (Scenario-3)	75
Figure 50: GLOF Risk Map showing Affected Infrastructure near Kargil (Scenario-3)	76
Figure 51: GLOF Risk Map showing Affected Agricultural Land near Kargil (Scenario-3)	77
Figure 52: GLOF Risk Map for the Study Area (Scenario-4)	78
Figure 53: GLOF Risk Map showing Affected Infrastructure near Kargil (Scenario-4)	79
Figure 54: GLOF Risk Map showing Affected Agricultural Land near Kargil (Scenario-4)	79
Figure 55: GLOF Risk Map for the Study Area (Scenario-5)	80
Figure 56: GLOF Risk Map showing Affected Infrastructure near Kargil (Scenario-5)	81
Figure 57: GLOF Risk Map showing Affected Agricultural Land near Kargil (Scenario-5)	81
Figure 58: GLOF Risk Map for the Study Area (Scenario-6)	82
Figure 59: GLOF Risk Map showing Affected Infrastructure near Kargil (Scenario-6)	83
Figure 60: GLOF Risk Map showing Affected Agricultural Land near Kargil (Scenario-6)	83

List of Tables

Table 1: GLOF scenarios simulated in this study.....	21
Table 2: Manning’s n used for different Land cover in this study.....	23
Table 3: Dam Breach Parameters for Various GLOF Scenarios	24
Table 4: Design of the PMS using a Severe Reference Storm from the Himalayan Region ...	25
Table 5: Computations Settings used HEC-RAS Model.....	31
Table 6: Details of Infrastructure Mapped using Satellite data.....	32
Table 7: Flood severity classification.....	34
Table 8: Classification of Flood Wave Arrival Time	35
Table 9: Flood Wave Characteristics of GLOF Scenario 1	39
Table 10: Flood Wave Characteristics of GLOF Scenario 2.....	40
Table 11: Infrastructure affected in GLOF Scenarios 1 and 2.....	41
Table 12: Details of Settlements affected in GLOF Scenarios1 and 2	42
Table 13: Flood Wave Characteristics of GLOF Scenario 7	44
Table 14: Flood Wave Characteristics of GLOF Scenario 8.....	44
Table 15: Infrastructure affected in GLOF Scenarios 7 and 8.....	46
Table 16: Details of Settlements affected in GLOF Scenarios 7 and 8.....	46
Table 17: Zone wise details of Infrastructure affected in GLOF Scenarios 1 and 7	49
Table 18: Zone wise details of Infrastructure affected in GLOF Scenarios 2 and 8.....	51
Table 19: Flood Wave Characteristics of GLOF Scenario 3.....	67
Table 20: Flood Wave Characteristics of GLOF Scenario 4.....	67
Table 21: Infrastructure affected in GLOF Scenarios 3 and 4.....	69
Table 22: Names of Settlements affected in GLOF Scenarios 3 and 4	69
Table 23: Flood Wave Characteristics of GLOF Scenario 5.....	72
Table 24: Flood Wave Characteristics of GLOF Scenario 6.....	72
Table 25: Infrastructure affected in GLOF Scenarios 5 and 6.....	74
Table 26: Names of Settlements affected in GLOF Scenarios 5 and 6	74
Table 27: Zone wise details of Infrastructure affected in GLOF Scenario 3	76
Table 28: Zone wise details of Infrastructure affected in GLOF Scenario 4	78
Table 29: Zone wise details of Infrastructure affected in GLOF Scenario 5	80
Table 30: Zone wise details of Infrastructure affected in GLOF Scenario 6	82

List of Abbreviations

amsl	Above Mean Sea Level
AWiFS	Advanced Wide Field Sensor
CWC	Central Water Commission
DTM	Digital Terrain Model
DoWR, RD&GR	Department of Water Resources, River Development and Ganga Rejuvenation
FCC	False Colour Composite
GL	Glacial Lake
GLOF	Glacial Lake Outburst Flood
GOI	Government of India
ha	Hectare
HEC	Hydrologic Engineering centre
HIS	Hydrological Information System
HKH	Hindu Kush-Himalayas
HP	Himachal Pradesh
I(d)	Glacier Ice-dammed Lake
I(s)	Supra-glacial Lake
ICIMOD	International Centre for Integrated Mountain Development
IHR	Indian Himalayan Region
India-WRIS	India - Water Resources Information System
IRS	Indian Remote Sensing Satellite
ISRO	Indian Space Research Organisation
JK	Jammu& Kashmir (UT)
Km ²	Square Kilometre
LA	Ladakh (UT)
Landsat	Land Resources Satellite
LISS-III	Linear Imaging Self Scanning Sensor - III
LISS-IV	Linear Imaging Self Scanning Sensor - IV
m	Metre
M(e)	End-moraine Dammed Lake
M(l)	Lateral Moraine Dammed Lake
M(lg)	Lateral Moraine Dammed Lake (with ice)
M(o)	Other Moraine Dammed Lake
NDWI	Normalized Difference Water Index
NHP	National Hydrology Project
NIR	Near InfraRed
NRSC	National Remote Sensing Centre
NWIC	National Water Informatics Centre
PMS	Probable Maximum Storm
PMP	Probable Maximum Precipitation
RAS	River Analysis system
RS	Remote Sensing
RS-2	Resourcesat-2
SOI	Survey of India
TM	Thematic Mapper
USGS	United States Geological Survey
UT	Union Territory

Summary

National Remote Sensing Centre (NRSC), Indian Space Research Organisation (ISRO), Hyderabad as one of the Central Implementing Agency under the National Hydrology Project (NHP), is carrying out hydrological studies using satellite data and geo-spatial techniques. As part of NHP, a detailed glacial lake inventory, prioritization of glacial lakes, Glacial Lake Outburst Flood (GLOF) inundation simulation and GLOF risk assessment for selected lakes are taken up for entire catchment of Indian Himalayan Rivers covering Indus, Ganga, and Brahmaputra River basins.

A total of 28,043 glacial lakes have been mapped in the entire catchment area of Indian Himalayan River basins using a total of 397 high resolution multispectral Resourcesat-2 LISS-IV satellite images, with a total lake water spread area of 1,31,070ha and further details are available in Glacial lake atlas of Indian Himalayan River Basins(https://www.nrsc.gov.in/Atlas_Glacial_Lake). Technical reports on inventory and prioritization of glacial lakes in Indus, Ganga and Brahmaputra river basins are published describing the details of prioritization methodologies. In each river basin, top five prioritized glacial lakes are selected for further detailed study of GLOF inundation simulation and GLOF risk assessment. This technical report provides the details of GLOF inundation simulation for various scenarios and GLOF risk assessment of Suru lake which is one of the five prioritized glacial lakes in Indus river basin.

The Suru Glacial Lake is located at an elevation of 4,355 m a.m.s.l. in the Union Territory of Ladakh, India. The stream emerging from this lake flows for about 7 km and joins the Suru river on left side. The Suru river originates from Panzella glacier near the Drang Drung Glacier and traverses about 11 km where this Suru glacial lake stream joins from left side. A change analysis of the lake water spread area carried out using Hexagon KH-9 of 1980 and Sentinel-2 of 2023 multi-temporal optical imagery revealed a 216% increase in size from 17.16 ha to 54.14 ha. Such alarming rate of lake expansion and the rapid urbanization of its downstream settlements have increased the possibilities of a catastrophic impact due to GLOF event by many folds. This necessitated a detailed GLOF risk assessment in case of a breach of the natural moraine dam holding about 14.41 MCM of water. A high resolution Digital Terrain Model of Tandem-X with a spatial resolution of 5 m was used in the study to simulate GLOF inundations of various scenarios. A series of 2D hydrodynamic dam-breach simulations in HEC-RAS software are developed for 8 different failure modes (overtopping and piping), different volumes of water released in case of a failure of the lake moraine (100%, 75%, and 50%), and under two weather conditions (clear-weather and Probable Maximum Precipitation). The worst-case scenario (scenario 7) was the one with a 100% discharge of the lake water under overtopping failure due to PMP occurrence over the catchment area of glacial lake. The breach depth in the worst-case was calculated as 26.61 m with an average breach width of 91.97 m, and it formed within 44 minutes since the start of breach. The GLOF peak hydrograph of 5,005.09 cumecs propagated from the moraine dam to the nearest partly affected settlement of Thulus in 7hr46 minutes where it was estimated as 923 cumecs. The simulated GLOF peak of flood hydrographs for 100%, 75% and 50% of lake water releases scenarios (scenario 1, 3 and 5) yielded 871 cumecs, 576 cumecs and 338 cumecs near Thulus village for overtopping failure. The GLOF hydrograph was routed downstream up to a distance of about 160 km from the glacial lake where it was attenuated near to the normal average flow of the stream. Suru lake GLOF outputs of flood depth, flood velocity, inundation extent, and

flood wave arrival time were used to generate hazard and risk maps for the downstream areas along the river reach. GLOF hazard maps are prepared by integrating flood depth and flood velocity for different scenarios.

High resolution satellite images (spatial resolution of 0.5 m) are used for mapping of settlements, agriculture lands, road network, road bridges, hydropower projects and other utilities along the river reach for identifying the elements of exposure due to the various Suru lake GLOF scenarios. The mapped infrastructure was integrated with GLOF simulated inundation extent to identify the affected elements. The total number of settlements, agricultural land, bridges, and road length inundated in the worst-case scenario (scenario 7) are 31, 255.6 ha, 65 and 67.3 km respectively. All the 31 settlements are partially flooded by the GLOF inundation extent.

Finally, GLOF risk maps are prepared by integrating flood hazard (flood depth X flood velocity) and flood wave arrival time, which was classified, into zones of high, medium, and low risk. The combination of flood hazard and flood wave arrival time for flood risk mapping presents a unique approach to flood risk assessment as demonstrated in this study. Zones of high risk are defined as those regions where flood severity was either medium or high, and the flood wave arrival time was within 2 hours since the start of the breach. For this GLOF scenario, there is no settlement affected in the high-risk zone while Thulus village and nearby areas fall under the medium-risk zone, and further downstream, the risk reduces to low near Gyaling at distance of 96 km from lake for scenarios 1 & 2, 7 & 8. The medium risk zone extends for a distance of 90 km along the river reach from lake covering the settlements of Thulus, Pranti, Kargee, Namsuru, and Damshna.

1. Introduction

1.1. About the Project

The National Hydrology Project (NHP) sponsored by the Department of Water Resources, River Development and Ganga Rejuvenation (DoWR, RD&GR), Ministry of Jal Shakti, Government of India, with financial aid from the World Bank. It aims to improve the extent and accessibility of water resources information and strengthen institutional capacity to improve water resources planning and management across India. Its mission is to establish a sound and effective hydrologic database and a Hydrological Information System while also developing scientific and consistent tools/aids to assist the concerned stakeholders in effective water resources planning and management of the Implementing Agencies.

National Remote Sensing Centre (NRSC) as one of the Central Implementing Agency under NHP is engaged with generation of geo-spatial products & services pertaining to water resources sector. The activities include generation of high resolution Digital Elevation Models (DEM), development of flood early warning systems, Glacial Lake Outburst Flood (GLOF) risk assessment, spatial snowmelt runoff modelling, decision support system development for irrigation water management, modeling & dissemination of hydrological products to support water resources management and capacity building to NHP stakeholders. The satellite data based geo-spatial products & services, mainly encompassing the following:

- Satellite Data/Geo-Spatial Data Hosting & Services through Bhuvan Web Portal
- Water Resources Information Products & Services (Satellite/Model derived - Bhuvan/India- Water Resources Information System (India-WRIS)/National Water Informatics Centre (NWIC))
- Customized Applications Development (Flood Forecasting, Irrigation Water Management)
- Hydro-conditioned Digital Elevation Model (Satellite & Aerial)
- Capacity Building (Customized Training & Hand Holding)

As part of various NHP technical studies carried out, NRSC has taken up “Glacial Lake Outburst Flood (GLOF) Risk Assessment of Glacial Lakes in the Himalayan Region of Indian River Basins”. Under this activity, it was proposed to prepare an updated inventory of glacial lakes, prioritization and selection of critical glacial lakes based on certain characteristics, GLOF modelling and flood inundation simulation for selected few lakes using high resolution Digital Terrain Model (DTM) for downstream of the lakes along their river reach, and to assess GLOF risk.

1.2. The GLOF Component

Glaciers are essentially huge masses of ice slowly moving under the influence of gravity. Glacial lakes are water bodies that are fed by glacier melt water and extend with a free surface on, in, under, in front, or beside the glaciers, and are usually dammed by glacial

ice or loosely consolidated moraine deposits. At times, the glacial lake dams breach due to various reasons such as failure of the unstable moraine, avalanches/landslides into the lake, heavy rainfall, etc., the torrential amounts of water and debris released from the lake causes catastrophic flooding in its downstream. This phenomenon is called a Glacial Lake Outburst Flood and it is a common disaster occurring in the Himalayan Region of the Indian River Basins. Many GLOF events are reported in Himalayan mountain region resulting in loss of lives and damages to public infrastructure.

The risk of catastrophic GLOF events in the Indian Himalayan Region (IHR) has increased due to the rise in global temperatures. The glacier ice and snow in the IHR serves as a direct indicator of climate change and global warming. Many studies have noted the accelerated melting of glaciers and their retreat in the last few decades due to climate change. Consequently, the glacial lakes have generally increased in number and size indicating a spike in their damage potential in case they undergo a GLOF event. It is a fact that GLOFs are an emerging threat to the socio-economy of the high mountain regions of the world, particularly in India where they tend to cause significant damage. Therefore, it is imperative to identify those glacial lakes that pose a significant threat to the downstream communities and assess the risk well in advance so that detailed Disaster Management Plans (DMPs) can be created to mitigate the damages due to GLOFs.

Towards the assessment of risk of GLOFs, NRSC/ISRO has taken up the following tasks under this component:

- i. To prepare a comprehensive inventory of glacial lakes of size greater than 0.25 hectare using Resourcesat-2 LISS-IV multispectral satellite images of spatial resolution of 5.8 m in entire Himalayan region
- ii. Prioritization of inventoried glacial lakes to identify the critical glacial lakes
- iii. GLOF modelling (dam breach modelling) for the prioritized glacial lakes and identification of infrastructure elements which gets exposed due to simulated GLOF events
- iv. GLOF risk assessment for selected glacial lakes

A total of 28,043 glacial lakes have been mapped in the Indian Himalayan Region (IHR) covering Indus, Gang and Brahmaputra river basins using a total of 397 high resolution Resourcesat-2 LISS-IV multispectral images with a total lake water spread area of 1,31,070.90 hectare. Each of these glacial lakes has been assigned a unique ID along with several key attribute information related to its hydrology, geometry, geography and topography. Based on the process of lake formation, location, and type of damming material, the glacial lakes has been classified into four major categories viz. moraine-dammed, ice-dammed, glacier erosion, and other glacial lakes. Using glacial lake database, basin-wise atlases of Indus, Ganga and Brahmaputra are published on December 2020 (NRSC-RSAA-WRG-WRAD-Nov2020-TR-0001702-V1.0), June 2021 (NRSC-RSAA-WRG-WRAD-Mar2021-TR-0001818-V1.0), and July 2022 (NRSC-RSAA-WRG-WRAD-May2022-TR-0002026-V1.0) respectively. Combined atlas for the entire IHR was published on March 2023 (NRSC-RSA-WATER RE-WRAD-Mar2023-TR-0002176-V1.0). All these glacial lake atlases are freely available to download at the official websites of the NRSC (https://www.nrsc.gov.in/Atlas_Glacial_Lake) and NHP (<https://nhp.mowr.gov.in>).

The inventoried glacial lakes were prioritized for further detailed study through a rigorous two-step procedure i.e. preliminary screening followed by ranking. Preliminary screening of glacial lakes was carried out based on four parameter criteria sequentially comprising lake type, lake area, lake association with glacier and lake with settlements enroute river reach. The preliminary screened in glacial lakes were ranked based on a total of 6 criteria viz. lake area, lake type, distance between glacier snout and lake inlet, slope between glacier snout and lake inlet, distance between lake outlet and nearest settlement, and slope between lake outlet and nearest settlement. Three technical reports on inventory and prioritization of glacial lakes in Indus (NRSC-RSA-WATERRE-WRAD-FEB2021-TR0001805-V1.0), Ganga (NRSC-RSA-WATER RE-WRAD-NOV2022-TR-0002116-V1.0) and Brahmaputra (NRSC-RSA-WATER RE-WRAD-JAN2024-TR-0002339-V1.0) river basins are published describing the details of prioritization methodologies. In each river basin, top five prioritized glacial lakes are selected for further detailed study of GLOF inundation simulation and GLOF risk assessment. This technical report provides the details of GLOF inundation simulation for various scenarios and GLOF risk assessment of Suru lake which is one of the five prioritized glacial lakes in Indus river basin.

The Suru glacial lake dam breach was simulated using HEC-RAS 2D hydrodynamic modelling to estimate the flood extents, flood depths, flood peak discharges, flood velocities, and flood wave arrival time in case of a probable GLOF event. A series of 2D hydrodynamic dam-breach simulations in HEC-RAS software are developed for 8 different failure modes (overtopping and piping), different volumes of water released in case of a failure of the dam (100%, 75%, and 50%), and under different weather conditions (clear-weather and Probable Maximum Precipitation). The results of HEC-RAS simulations were used for generating hazard maps of flood severity (depth x velocity) and GLOF risk assessment. A method of generating GLOF risk maps was devised in this study, which combines flood severity with flood wave arrival time using a matrix method. The details of the study are given in appropriate sections.

1.3. Organization of the Report

This technical report provides details on the hydrodynamic modelling of Glacial Lake Outburst Floods (Dam Break modelling), and the risk assessment of GLOFs in the downstream areas. The key elements of this report include:

- Review of Literature on GLOF modelling and Risk Assessment
- Study Area and Data Used
- Hydrodynamic Modelling of GLOF (Dam Break Modelling):
 - Selection of appropriate study area limits
 - Description of Dam Breach Scenarios
 - Data Requirements of the Hydraulic Model
 - Estimation of Dam Breach Parameters
 - Development of the model
- Flood Inundation and Hazard Mapping
- Elements of Exposure due to GLOF
- GLOF Risk Assessment
- Conclusions

2. Literature Review

2.1. Glacial Lake Outburst Floods

The IHR houses the largest volume of glaciers and perennial snow outside the Poles thus receiving the name ‘Third Pole’ (Rao et al., 2023; Zheng et. al., 2021). Being densely glaciated, the IHR is very sensitive to climate change and serves as a good indicator of its impacts (Maskey et al., 2020; Kraaijenbrink et al., 2017; Haeberli et al., 2013; ICIMOD, 2011). Recent decades have witnessed rapid global land surface warming rates (+0.03 °C/year) that exceed the global mean surface temperature rate (0.011 °C/year) from 1951 to 2012 (Zhang et al., 2015; IPCC, 2014). This rapid warming phenomena has induced an extensive shrinkage of glaciers causing a significant reduction of glacier length in the IHR (Dubey and Goyal, 2020; Maurer et al., 2019; Sakai & Fujita, 2017; Cogley, 2016). This reduction in length of glaciers is known as glacial retreat which aids in the formation of new glacial lakes, and expansion of existing ones (Nie et al., 2018; Song et al., 2017; Westoby et al., 2014; Kang et al., 2010). Glacier bed topographies have been modeled in the Himalayas, and it has been predicted that around 5,000 depressions may turn into glacial lakes in the near future (Linsbauer et al., 2016). The International Centre for Integrated Mountain Development (ICIMOD) prepared an inventory of around 9,000 glacial lakes of size > 0.3 hectares in the Himalayas between 1999 and 2005 (Mool, 2005). The latest and most comprehensive glacial lake inventory showing 28,043 glacial lakes in the IHR of size ≥ 0.25 hectares has been published by NRSC, ISRO (Rao et al., 2023). These inventories highlight the marked increase in the number of glacial lakes over time in the IHR. The formation of pro-glacial lakes accelerates the melting of glaciers further in what is called a positive-feedback mechanism that results in more expansion of the lakes (Tsutaki et al., 2019; King et al., 2018). An increase in the number and areal extent of glacial lakes brings both large opportunities and risks (Zheng et. al., 2021; Farinotti et al., 2019; Haeberli et al., 2016). Glacial lakes are important water resources as they serve as sources of pristine water for the downstream communities (Rawat et al., 2022; Brighenti et al., 2021; Huss et al., 2017). Unfortunately, glacial lakes also behave as sources of great danger to the lives and livelihoods in their downstream in the form of catastrophic Glacial Lake Outburst Flood (GLOF) events (Dubey et al., 2020; Cook et al., 2018).

Glacial lakes are mostly bound by loosely consolidated glacial deposits called moraines, or glacial ice dams, or moraines with ice cores, and surrounded by unstable slopes or hanging glaciers (Rinzin et al., 2023; Otto, 2019). Mass movements into the lake as a result of slope failure may cause impulse waves that would overtop the moraine or ice dam causing its overtopping failure. Overtopping of the dam may also be caused due to pluvial, nival, and glacial runoff induced overfilling of the lake (Taylor et al., 2023; Rounce et al., 2016; Emmer et al., 2013). Overtopping failure occurs when water flows over the damming material and erodes the downstream face of the dam. Another mode of dam failure occurs due to piping failure under which the hydrostatic pressure of the water tends to create a pipe-like hole that eventually grows big enough to cause the dam to collapse (Chowdhury et al., 2021; Schmidt et al., 2020). Moraines may also fail due to slope undercutting by glacio-fluvial erosion and heavy monsoonal rainfall (Barnard et al., 2001; Owen et al., 1996). Ice-dam failures are mostly concentrated in the Pamir and Karakoram regions

(Bhambri et al., 2019; Hewitt and Liu, 2010), while moraine-dam failures are more common in the IHR (Nie et al., 2018). In the event of failure of the dam, there is a sudden high magnitude discharge of water with a high velocity of flow from the glacial lake that tends to flood the downstream areas (Rinzin et al., 2021; Begam et al., 2018). This phenomenon is termed Glacial Lake Outburst Flood (GLOF) and it can devastate entire towns and settlements in its way downstream (Dubey and Goyal, 2020; Cook et al., 2018). Fifty-one incidents of GLOFs have been reported from the IHR (Nie et al., 2018). An inventory of GLOFs reported that the maximum number of casualties have occurred in the Central Himalayas with fewer floods but higher damage (Carrivick and Tweed, 2016). GLOFs have been recognized as one of the most serious natural hazards in the IHR (Chen et al., 2021; Veh et al., 2020). These events are more catastrophic in the IHR due to the steep slopes and narrow flow channels in the terrain (Sattar et al., 2019; Worni et al., 2012). GLOFs are significantly hazardous and destructive causing widespread damage to property, infrastructure, agricultural land and livelihoods, thereby resulting in extensive loss of life (Rinzin et al., 2023; Taylor et al., 2023; Allen et al., 2019). One of the most notable examples of GLOFs in the IHR was the Chorabari Lake GLOF that occurred on 16th June 2013 in Kedarnath, Uttarakhand. This GLOF event was triggered by heavy rainfall induced mass movements into the lake and it devastated the villages of Kedarnath, Rambara, and Gaurikund on its way (Das et al., 2015; Martha et al., 2014). Around 6,000 people were killed in the region, and most of the deaths were directly linked to the GLOF (Allen et al., 2015; Guha-Sapir et al., 2014). Countless bridges and roads were washed away or damaged, and about thirty hydropower plants were affected or completely devastated (Sati and Gahalaut, 2013). In light of the highly hazardous nature of GLOF events, it becomes necessary to lay out risk management and mitigation plans in advance to prevent loss of life.

2.2. Role of Remote Sensing and GIS

The preparation of GLOF risk management plans, however, requires a lot of data to analyze the susceptibility of the lake to outburst, its geometry, how the failure would be triggered, what magnitude of discharge would be expected, how the flood wave will propagate downstream, and how it would impact the lives and livelihood on its course. Considering the challenging terrain where these lakes are usually situated, gathering in-situ data becomes very tedious and often impossible (Guru et al., 2019; Pratap et al., 2016). In such scenarios, Remote Sensing (RS), and Geographical Information Systems (GIS) serve as highly indispensable tools in providing the required information on glacial lakes (Gupta et al., 2019; Cogley et al., 2011). High spatio-temporal and spectral resolution satellites provide extremely valuable information on glacial lake location, geometry, water spread area, type, etc. (Rao et al., 2023; Sharma et al., 2013). RS and GIS techniques coupled with hydrologic and hydraulic modelling approaches allow rapid investigation of these challenging glaciated terrains and they could play a key role in prioritizing critical glacial lakes and monitoring GLOF events in near real-time (Ahmed et al., 2022; Ahmed et al., 2021; Gilany and Iqbal, 2020).

There is a plethora of research on the applications of RS and GIS for glacial lakes and GLOF studies. The studies include preparation of glacial lake inventory and assessment of glacial

lake distribution, GLOF susceptibility analysis, GLOF modelling, and GLOF risk assessment. Worni et al. (2013) inventoried glacial lakes in the Indian Himalayas and also carried out risk assessment for those lakes. ICIMOD (Ives et al., 2010) has a similar inventory of glacial lakes for the Hindu Kush Himalayas. Many regional glacial lake studies were also conducted (Sattar et al., 2019; Aggarwal et al., 2017; Raj et al., 2013). All these studies extensively use remotely sensed data such as Landsat, Sentinel, RS-2 imagery, etc., that have been processed using GIS software and tools.

2.3. GLOF Modelling Approaches

GLOFs have been modeled using different approaches in various studies. Many researchers apply analytical and numerical models to simulate the impact waves generated due to mass movements into the lake (L'Heureux et al., 2011; Biscarini, 2010; Heller et al., 2008a; Falappi and Gallati, 2007) that can trigger GLOFs. Some of the numerical models used for impact wave modelling include 2D-BING (L'Heureux et al., 2011), LS3D (Ataie-Ashthiani and Yavari-Ramshe, 2011), and FUNWAVE (Wei et al., 1995). Other studies simulate the dam breach process and outflow discharges using various different approaches and models, often combined with the impact wave effects (Sattar et al., 2023; Psomiadis et al., 2021; Worni et al., 2014; Westoby et al., 2014). Various dam breach models were used even before the year 2000, such as Lou Model, BEED, BRDAM, BREACH, NWS DAMBRK (Singh, 1996, Fread, 1982). There are empirical models that use regression equations based on the analyses of real dam failures to estimate dam breach parameters like breach formation time, breach geometry, and peak discharges (Wahl, 2010; Xu and Zhang, 2009; MacDonald and Langridge-Monopolis, 1984; Froehlich 1995a, b). Parametric models apply user defined dam breach parameters to provide breach hydrographs, such as HEC-RAS, MIKE 11, and NWS DAMBRK. Physical models on the other hand use hydraulic principles, erosion rates and geotechnical considerations to model the breach (Worni et al., 2014), e.g., BREACH, BRDAM, BEED, etc. BASEMENT (Faeh et al., 2012) and HR-BREACH (Morris et al., 2008) are some other models to simulate embankment failures. In addition, there are various models to simulate the flows occurring from a dam break such as HEC-RAS, NWS-FLDWAV, TELEMAC-2D, DASSFLOW, SOBEK, Delft3D, FLO-2D, RAMMS, IBER, and BASEMENT. The state-of-the-art models mostly use 1-D and/or 2-D hydrodynamic models to simulate GLOFs. HEC-RAS and MIKE 11 are widely used software that provide dam break modelling capabilities to the user. These applications can solve the St. Venant Equations to simulate the GLOF process and flood wave hydrodynamic routing.

2.4. Risk Assessment of GLOFs

Assessment of risk of GLOFs requires the understanding of the terms risk, hazard, vulnerability, and exposure. The terms can be defined as:

Risk is the probability of a loss that depends on hazard, vulnerability, and exposure (Figure 1). The most common definition of risk is the combination of flood hazard and flood vulnerability at a given location.

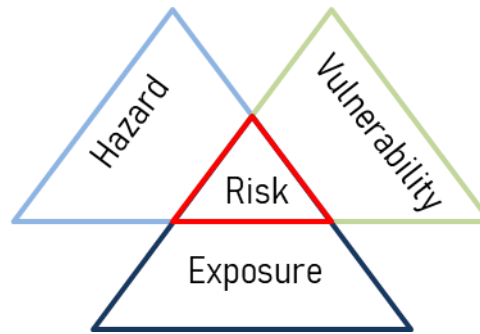


Figure 1: Components of Risk

Mathematically, risk can be defined as (Lie et al., 2012; UN, 1992):

$$\text{Risk} = \text{Hazard} \times \text{Vulnerability}$$

Hazard reflects the consequence of damage that could result from a flood of a given intensity. Or, it may also be defined as the potential occurrence of a natural or anthropogenic event that may cause loss of life, injury, health impacts, and damage to property, infrastructure, livelihoods, service provision, ecosystems, and environmental resources.

Vulnerability in simple terms is the extent of harm that may occur to the elements exposed to the hazardous event. It can be expressed as:

$$\text{Vulnerability} = \text{Exposure} + \text{Susceptibility} - \text{Resilience}$$

Therefore, vulnerability is highly context specific. It varies with the element under consideration, e.g. Physical vulnerability for physical elements such as houses, roads, infrastructure, etc. Other types of vulnerability are social and economic vulnerability related to the society and the economy respectively.

Exposure is the presence of vulnerable elements within the extent of flood inundation. It is assessed based on an inventory of anthropogenic elements such as villages, roads, bridges, hydropower stations, etc. that may be affected by the hazard.

There are various sources that describe the different risk assessment methodologies, among which the latest ones are NDMA Guidelines on Management of GLOFs (NDMA, 2020), CWC Guidelines for Mapping Flood Risks Associated with Dams (CWC, 2018), GAPHAZ Assessment of Glacier and Permafrost Hazards in Mountain Regions - Technical Guidance Document (GAPHAZ, 2017), and AEMI Australian Emergency Management Handbook Series, Technical Flood Risk Management Guideline (AEMI, 2014). In general, to assess the GLOF risk, firstly, hazard assessment is carried out involving (i) estimation of peak discharge and breach hydrographs, (ii) estimating water depths, velocities, inundation extent, and severity of flooding, and (iii) identifying the inundated elements. It can be carried out using 1D or 2D unsteady flow hydrodynamic modelling in HEC-RAS or similar software. Secondly, vulnerability assessment can be carried out to estimate the damages likely to be caused by GLOFs. It involves the use of depth-damage curves (Huizinga et al., 2017) to assess the susceptibility of exposed elements to undergo damage. Finally, risk assessment is carried out by combining the hazard and vulnerability assessments to generate GLOF risk maps that represent the adverse consequences associated with the GLOF events. Many studies have been conducted to assess the GLOF risks such as GLOF risk assessment in Nepal (Washakh et al., 2019; Shrestha et al., 2010), Bhutan (Rinzin et al., 2023), and in

the Indian Himalayan regions (Rawat et al., 2023; Pandey et al., 2022; Ahmed et al., 2022; Sattar et al., 2021; ICIMOD, 2010), etc. It has been observed that most of the glacial lake outburst flood risk assessment methodologies differ from each other, and a common methodology is not available. GLOF risk assessment studies commonly terminate up to the assessment of hazard and do not generate risk maps due to the lack of vulnerability data. Therefore, it is proposed a unique approach to GLOF risk assessment in this study. The approach can be followed even when detailed vulnerability information is lacking, or the information is incomplete. In the present study risk assessment approach involves the generation of risk maps directly using hazard maps (hydrodynamic modelling outputs of depth, velocity) and flood wave arrival time. An overview of the approach and details are given in Chapter 3 and Chapter 8 correspondingly.

3. Study Area and Data Used

3.1. Suru Glacial Lake and its GLOF Potential

Suru glacial lake is one the top five prioritized glacial lakes in Indus river basin and hence taken up for further detailed study. The glacial lake is located at an elevation of 4,355 m a.m.s.l in the upper reaches of in the Indus upper sub-basin of the Indus Basin, Union Territory of Ladakh, India (Figure-2). The geographical co-ordinates of Suru Glacial Lake are 33° 56' 42'' N and 76° 13' 39'' E. The river Suru is flowing near to it that originates from the Panzella glacier which lies at Pensi La pass near the Drang Drung Glacier. The stream emerging from this glacial lake flows for about 7 km and joins the Suru river on left side (11 km from river origin). The river flows westwards along with the Kargil-Zanaskar Road from its source and forms the Suru valley, which is towered by the massif of Nun Kun mountain. Most of its part covers within the jurisdiction of Kargil district forms the western and northern boundary of the Zanskar range and Kargil town is the largest city situated on the banks of the Suru river, also being the second largest city in the Ladakh region after Leh.

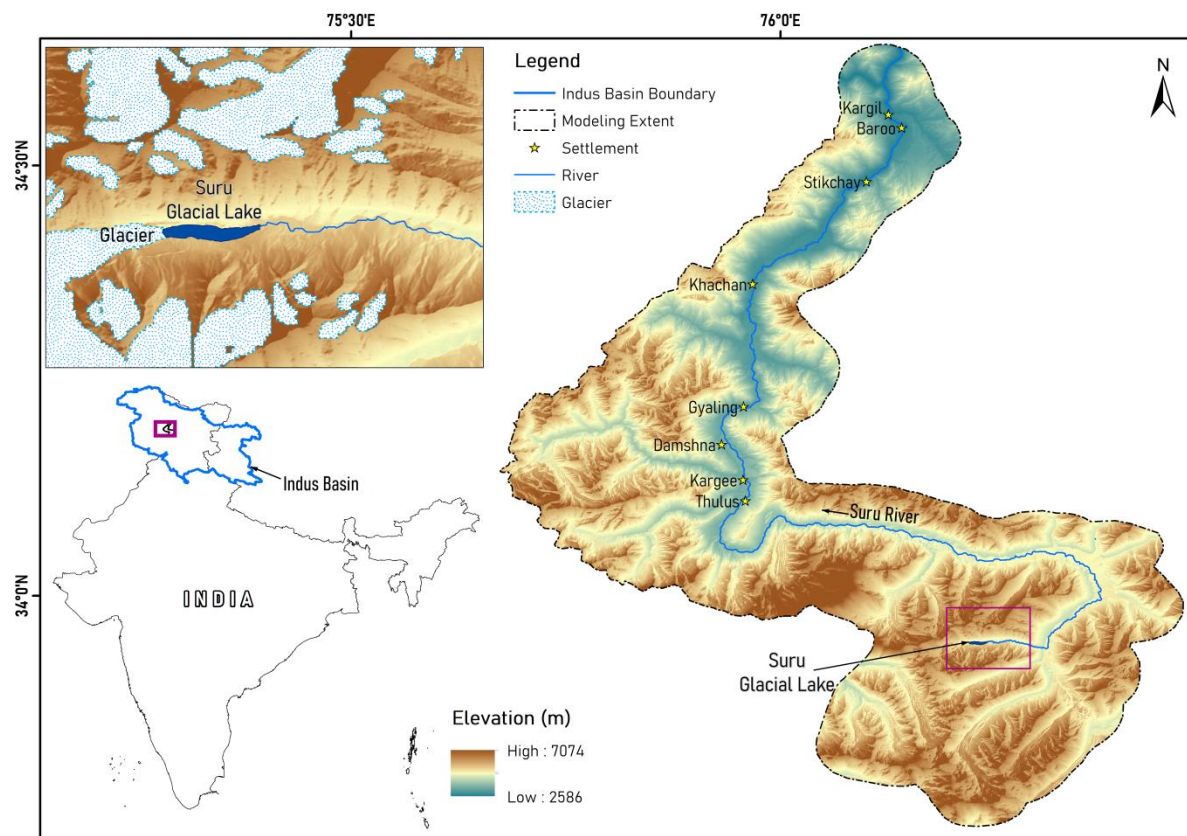


Figure 2: Location of Suru Glacial Lake

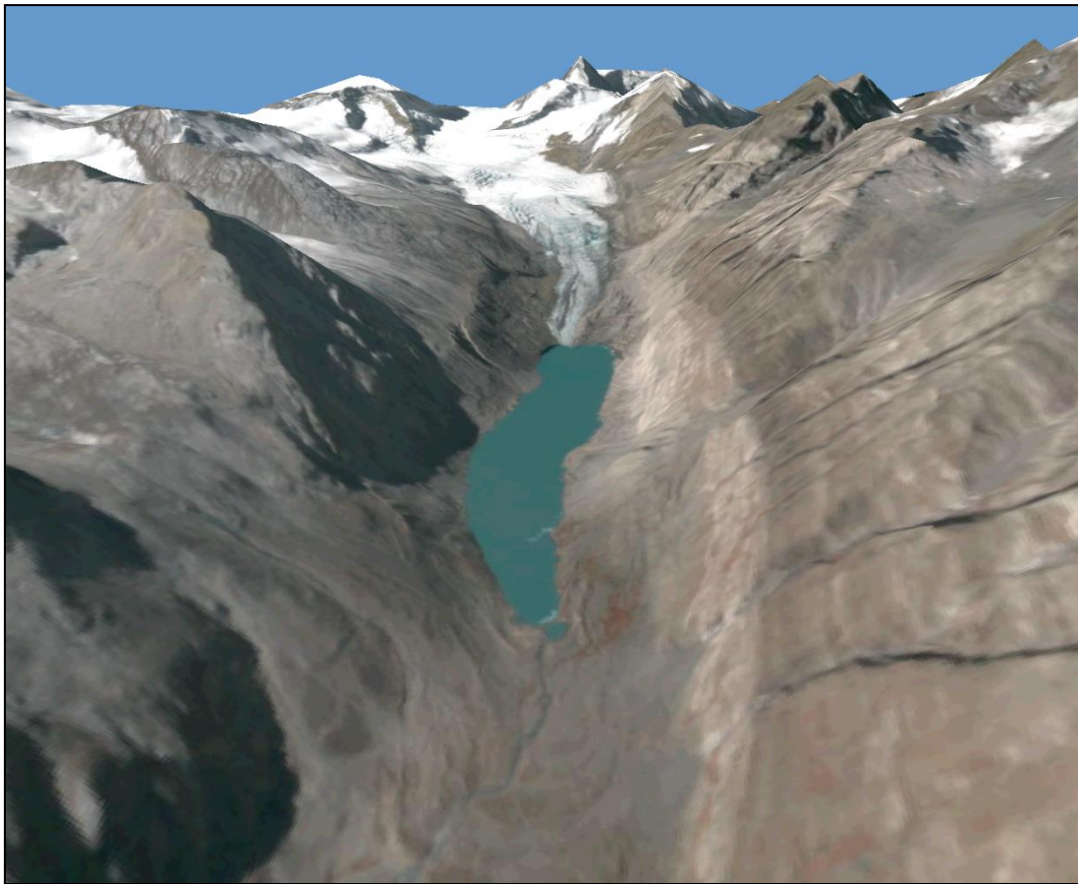


Figure 3: Suru Glacial Lake and its environs

Figure 3 shows Resourcesat-2 LISS-IV multispectral satellite image of Suru glacial lake and its surroundings. The nearest settlement of Thulus lies around 74 km downstream of the lake at an elevation of 3,228 m a.m.s.l, i.e., 1,127 m below the lake. The stream has an average slope of about 1 in 63 between the lake and Thulus settlement. In addition to that, the channel is also narrow leading to higher flow depths. These conditions are highly favorable for catastrophic flooding in case of a GLOF event.

An analysis of multi- temporal satellite data using Hexagon KH-9 of 1980 and Sentinel 2 of 2023 revealed a 216% increase in size. Figure 4 shows the lake water-spread area at different time periods, which increased from 17.16 hectare to 54.14 hectare in a span of 43 years. Such alarming rate of lake expansion and the rapid urbanization of its downstream settlements have increased the chances of a catastrophic GLOF event by many folds. Figure 5 shows the typical example of urban expansion near Kargil town (source: Google Earth Images).

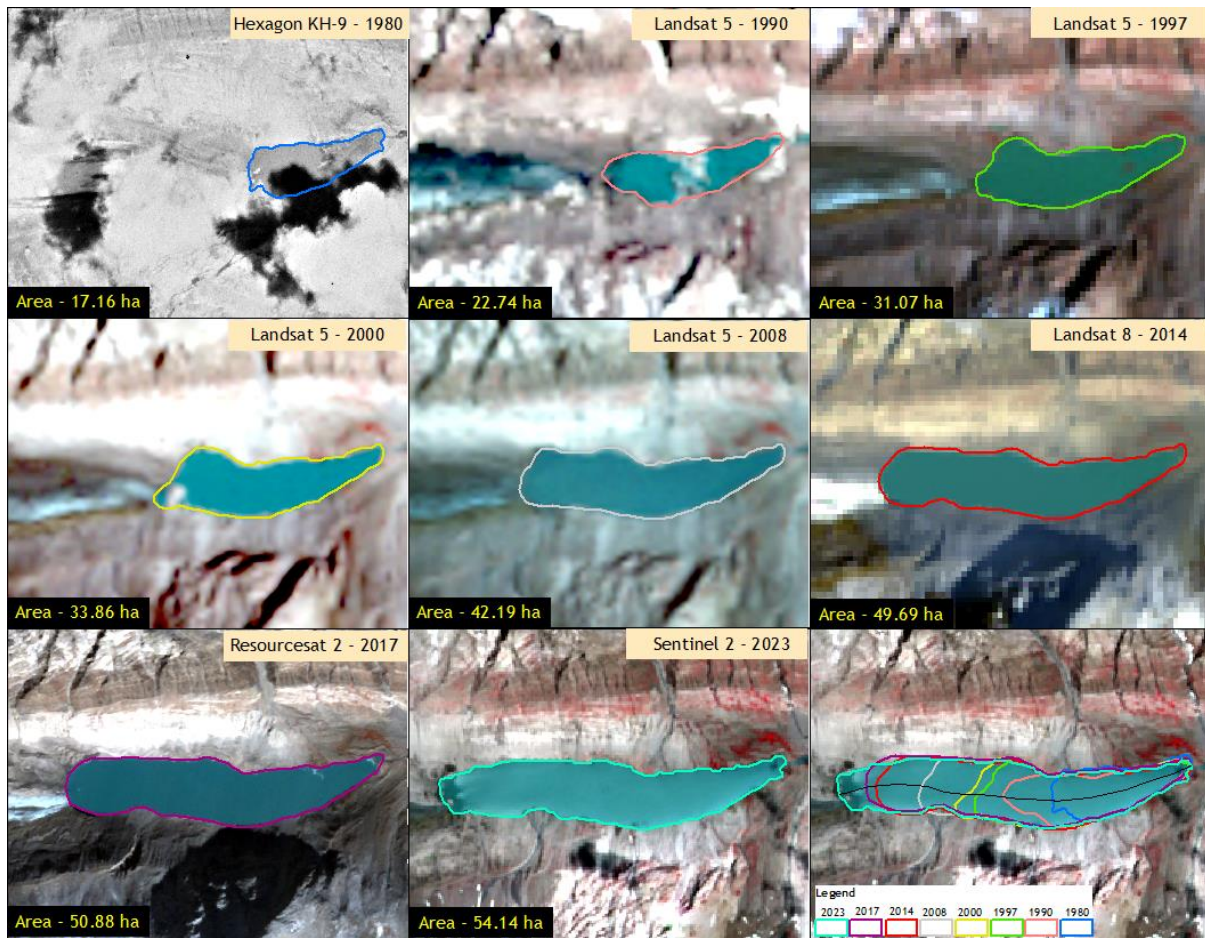


Figure 4: Long-term changes in Suru Glacial Lake water spread area

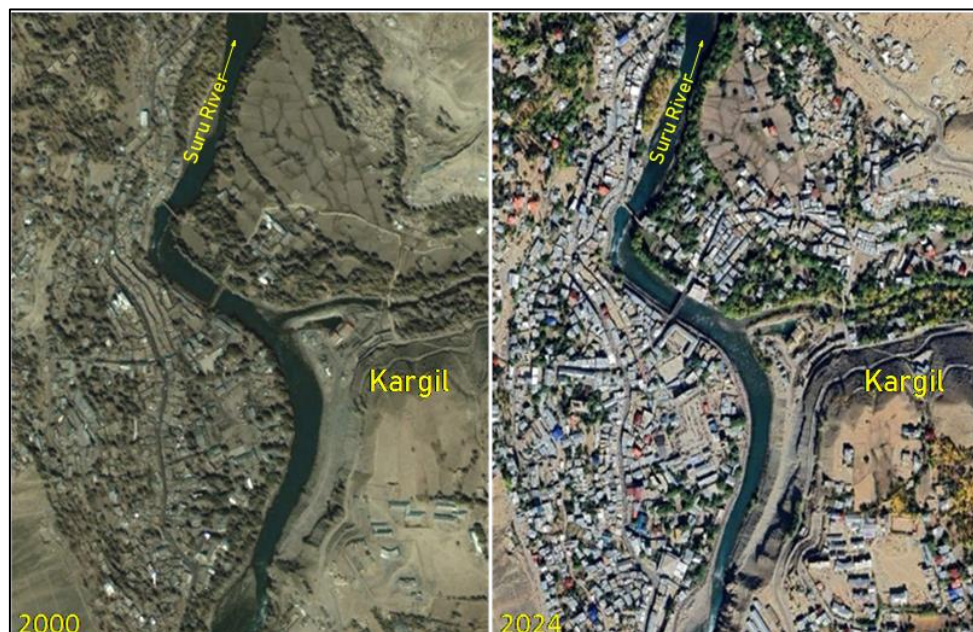


Figure 5: Urban expansion near Kargil

3.2. Catchment Area of Suru glacial lake

Suru glacial lake is fed by glacier melt, snowmelt and rainfall-runoff from a catchment of area 3,187 hectare. Assuming rainfall occurs below 4,500 m elevation, about 159 hectare of catchment area contributes to rainfall runoff into the lake. The minimum and maximum elevations of the catchment area up to lake are 4,363 m and 5,852 m respectively. The catchment area of the lake is located in the Kargil district of Ladakh, and it is located in Indus Upper sub-basin of the Indus Basin. Figure 6 shows the drainage pattern upstream of the lake. Slopes in the catchment range from 0° to 72° near the peaks (Figure 7). Many studies mention the occurrence of ice and rock-ice avalanches over slopes $\geq 25^\circ$ or 30° (Mohanty and Maiti, 2021; Allen et al., 2019; Alean, 1985) that act as the most common cause of GLOFs in the Himalayas (Wang et al., 2011).

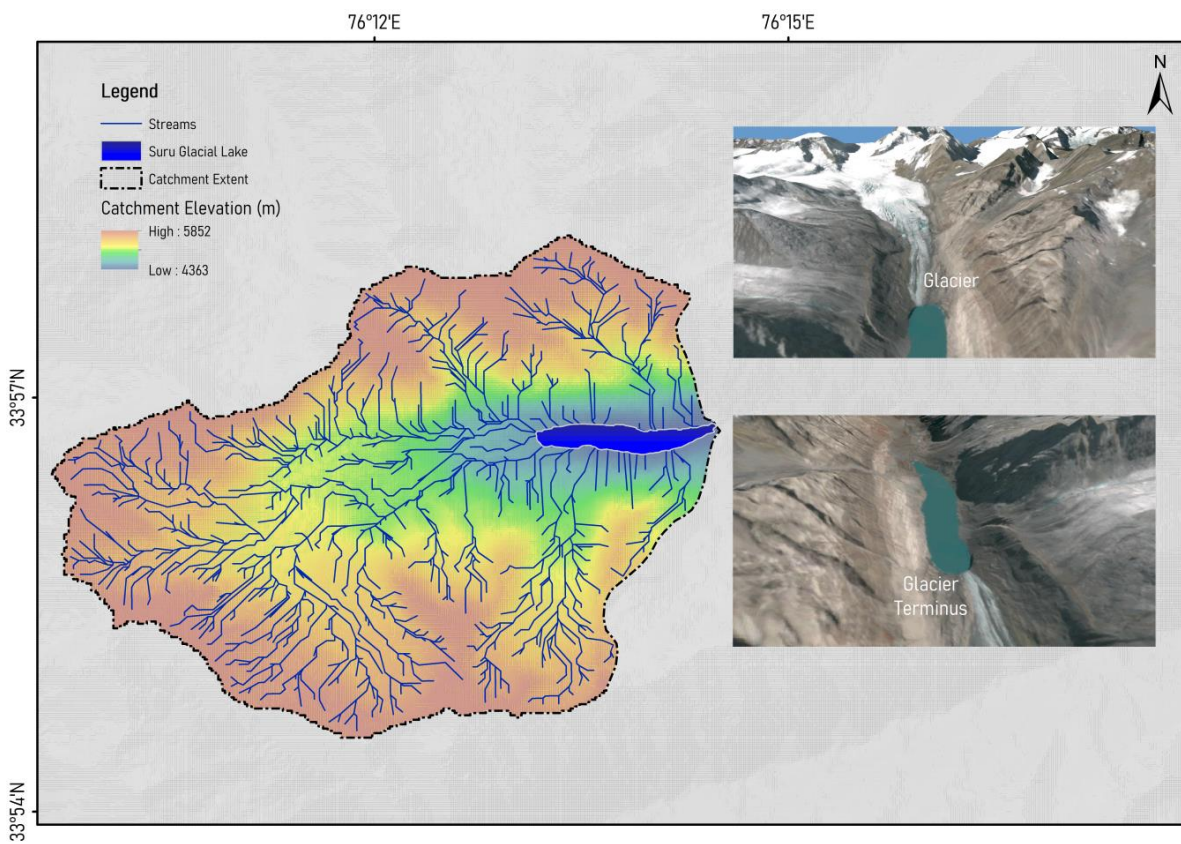


Figure 6: Upstream of Suru Glacial Lake

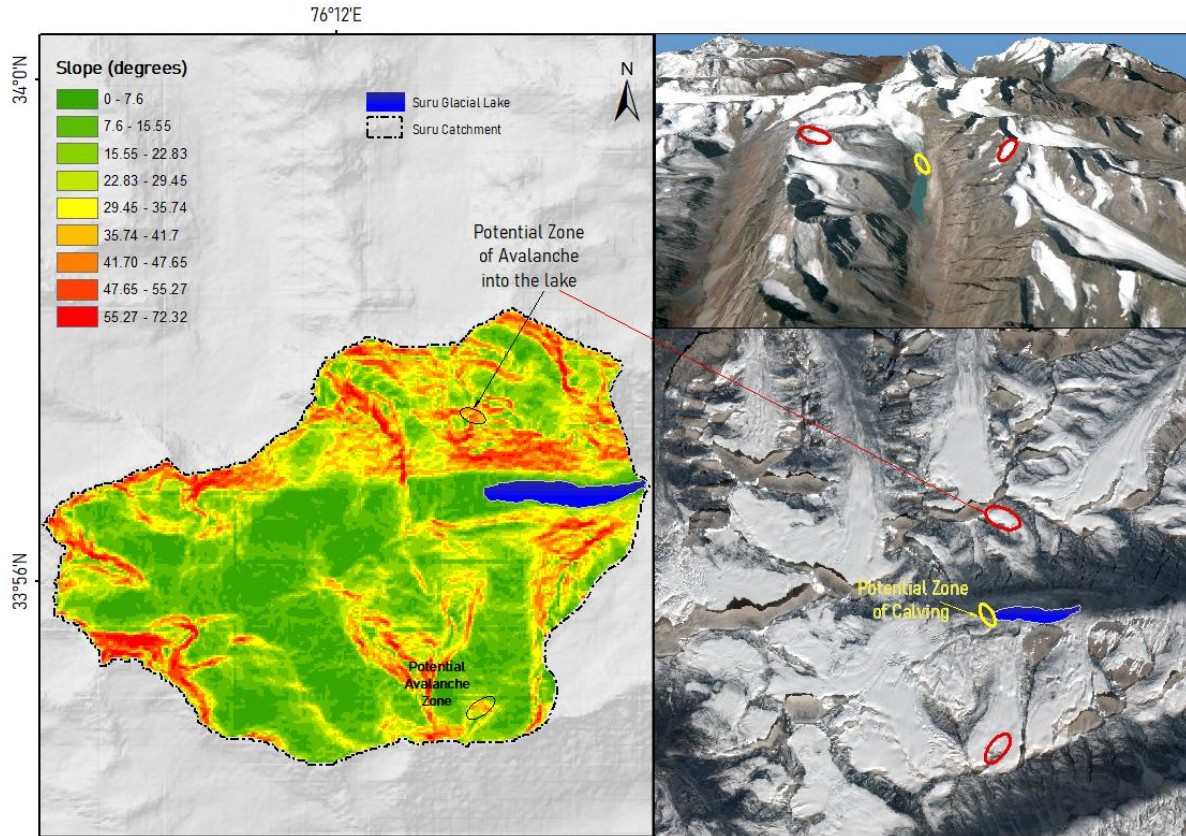


Figure 7: Slopes upstream of Suru Glacial Lake

3.3. Description of the Lake and its Moraine

Suru glacial lake has a water spread area of 54.14 hectare (ha) as on July 2023 at an elevation of 4,382.1 m. It has a length of 2,027 m with a maximum width of 347 m. Due to the absence of the actual volume of water stored in the lake, Huggel et al.’s empirical formula is used for estimating the lake volume. According to Huggel et al. (2002), the average depth (D) and volume (V) of a glacial lake can be related to its water spread area (A) by the following empirical relationships:

$$D = 0.104 \times A^{0.42} \quad \dots \text{(i)}$$

$$V = 0.104 \times A^{1.42} \quad \dots \text{(ii)}$$

where, A is in m², D is in m, and V is in m³.

Using equations (i) and (ii), the average depth of the lake was estimated to be 26.61 m, and the volume of the lake estimated as 14.41 million cubic meters (MCM). The TanDEM-X Digital Terrain model (DTM) was reconditioned to represent lake bed profile that gave 14.41 MCM of water volume when the initial water surface elevation was set to 4,382.1 m. The reconditioned DTM has an elevation of 4,355.5 m at the bed of the lake outlet. Elevation of the lakebed at the glacier terminus was 4,356.5 m, i.e., 1 m above the outlet, which will facilitate 100% drainage of lake volume during dam-breach simulation. Figure 8 shows the reconditioned DTM lake elevation details. Modification of the DTM to contain lakebed elevation values is a prerequisite for performing full-hydrodynamic simulation of Glacial Lake Outburst Floods. We assume that the lake contains clear water at a density of 1,000 kg/m³ throughout the simulation process.

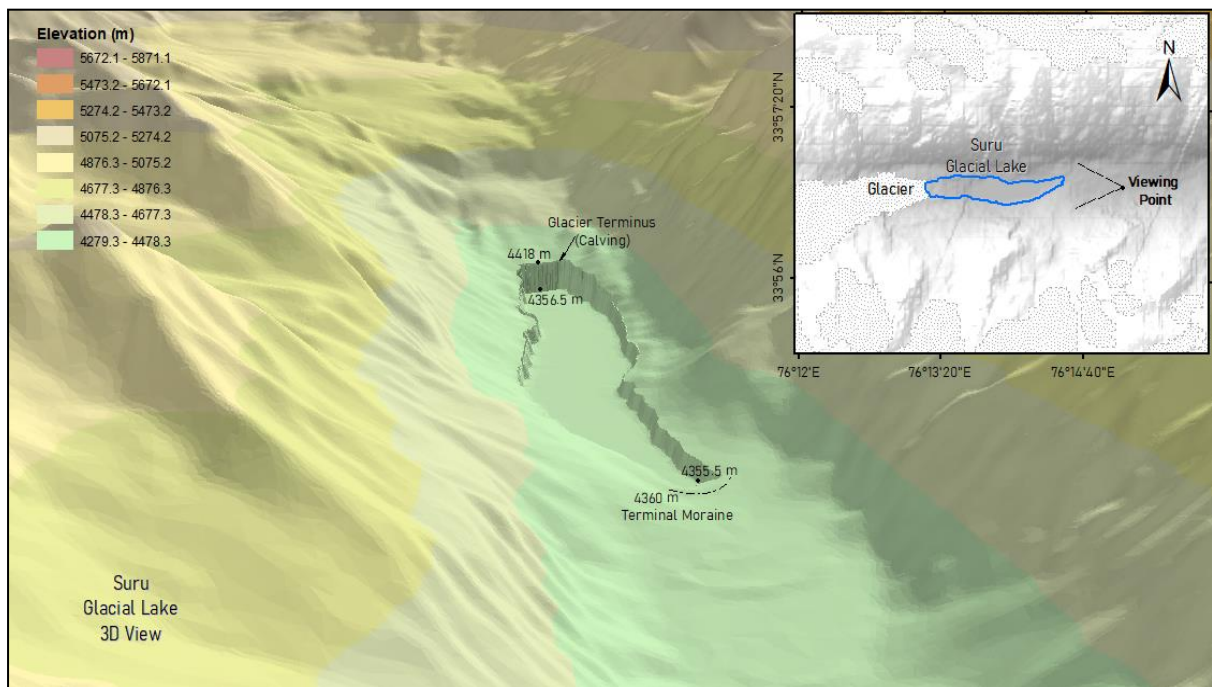


Figure 8: DTM of Suru Glacial Lake and its environs

Suru glacial lake is bound by a terminal moraine at its frontal end. The elevation of the crest of the frontal moraine is around 4,360 m, i.e., 4.5 m above the bed of the lake at its outlet. Width of the crest of the moraine is ~131m. It has slopes of 25% and 8.5% at the upstream and downstream faces respectively. The downstream face of the moraine dam is slightly vegetated and the absence of dense vegetation makes it prone to erosion even in case of a small overtopping wave. An overtopping wave could significantly erode the downstream face of the moraine dam and eventually cause its failure (Worni et al., 2013). In the absence of field data about the moraine, we have assumed that the moraine material is made of loosely consolidated glacial deposits and is in an unstable condition undergoing some seepage through the moraine dam, and therefore, it is susceptible to both piping and overtopping failures. Under these conditions, both the modes of failure are possible and hence proposed to study the hydrodynamic characteristics of the GLOF in each of these failure modes.

3.4. Data Used

Accuracy of hydrodynamic model depends on the resolution and accuracy of the terrain dataset used for the study. In this study, the German Aerospace Center's (DLR) TanDEM-X 5 m high resolution Digital Terrain Model (DTM) is used for simulating GLOF inundation. TanDEM-X DTM is an X-band SAR based interferometric DTM dataset. TanDEM-X and TerraSAR-X are twin satellites for radar based Earth observation for digital elevation measurements. TerraSAR-X and TanDEM-X orbited together in a close formation with a typical separation between 120 m and 500 m operating in bistatic SAR interferometric mode. Data acquisition was carried out between 2010 and 2015, and the 3D elevation model it produced was of absolute accuracy with 4 m. The DTM used for the study is

hydrologically corrected DTM representing bare-earth model devoid of human-made and natural features, such as infrastructure and vegetation. Cartosat DEM is used in delineating the sub basin boundaries and their outlets for computing lateral inflows along the river reach for GLOF scenarios due to extreme precipitation.

Very high-resolution satellite data of Kompsat of 0.5 m spatial resolution of recent period was procured to identify elements of infrastructure that are affected GLOF inundation for various scenarios. The details of infrastructure such as settlements, road network, agriculture land, bridges, and other public utilities is mapped using this satellite data along the river reach.

Both the TanDEM-X DTM and Kompsat satellite data are procured for the study for a distance of about 160 km from the Suru glacial lake along the river reach.

4. Methodology

The GLOF risk assessment of Suru glacial lake is carried out in a three step process of GLOF inundation modelling, mapping of vulnerable infrastructure elements and risk assessment. The first step of GLOF modeling is carried out using TanDEM-X 5 m high-resolution DTM for various scenarios. The GLOF scenarios include release of 50%, 75% and 100% volume of water stored in the lake. In addition, a GLOF scenario of extreme rainfall event due to Probable Maximum Precipitation occurring over catchment area of lake with simultaneous breach of lake is also simulated. In the second step, using very high resolution Kompsat satellite data elements of infrastructure affected by various flood scenarios are mapped. In the third step, GLOF risk assessment is carried out by integrating GLOF inundation scenarios and vulnerable elements of infrastructure. Figure 9 shows the flow chart of methodology used in this study.

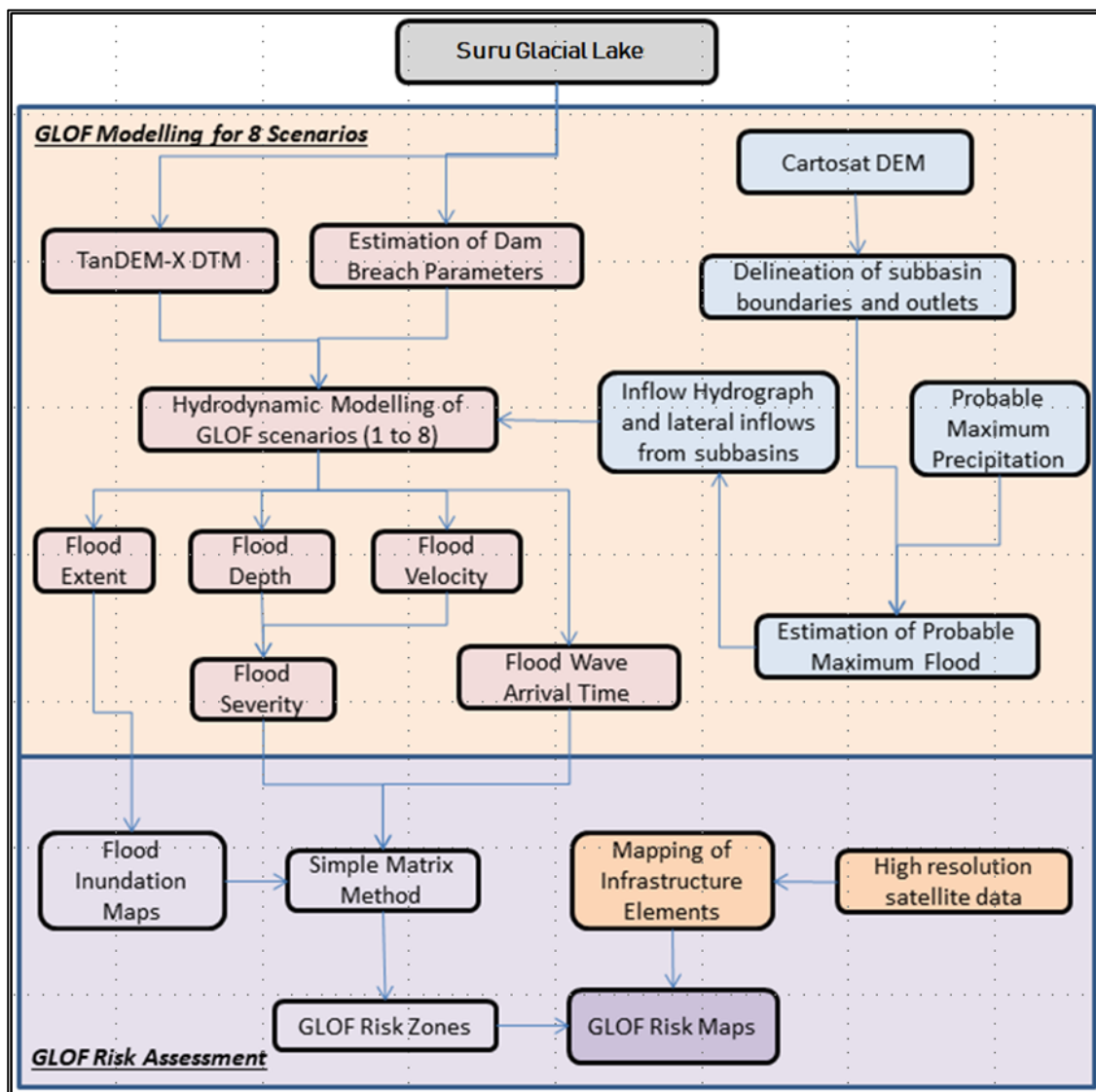


Figure 9: Flow Chart of Methodology used in the study

4.1. GLOF Inundation Modelling

Glacial Lake Outburst Floods (GLOF) are simulated as dam break hydrodynamic models in which a breach is created in the dam causing an uncontrolled flow of the stored water out of the lake. Hydrologic Engineering Center - River Analysis System (HEC-RAS) has been widely used for dam break hydrodynamic modelling due to its free availability and 1D and 2D modelling capabilities (Rawat et al., 2022; Psomiadis et al., 2021; Hussain et al., 2020; Kougkoulos et al., 2018; Klimeš et al., 2016). HEC-RAS version 6.3.1 was used to carry out the hydrodynamic GLOF simulations in this study. Full St. Venant partial differential equation sets are used for unsteady flow routing of the flood wave in a 2D hydrodynamic model established using 2D flow areas for the lake as well as the downstream areas. 2D models account for the water movement in a direction perpendicular to the direction of wave propagation, which is neglected in 1D models (Dasallas and Kim, 2019; Teng et al., 2017). The 2D unsteady hydrodynamic model was used to determine the hydrodynamic parameters of the glacial lake outburst flood wave such as flood depth, flood velocity, flood discharge, flood wave travel time at the downstream areas. The process for developing the GLOF model in HEC-RAS has been illustrated in Figure 10. TanDEM-X 5 m resolution DTM was preprocessed with Arc Map and HEC-RAS GIS tools for correction of DTM errors like sinks, and anomalies in the terrain.

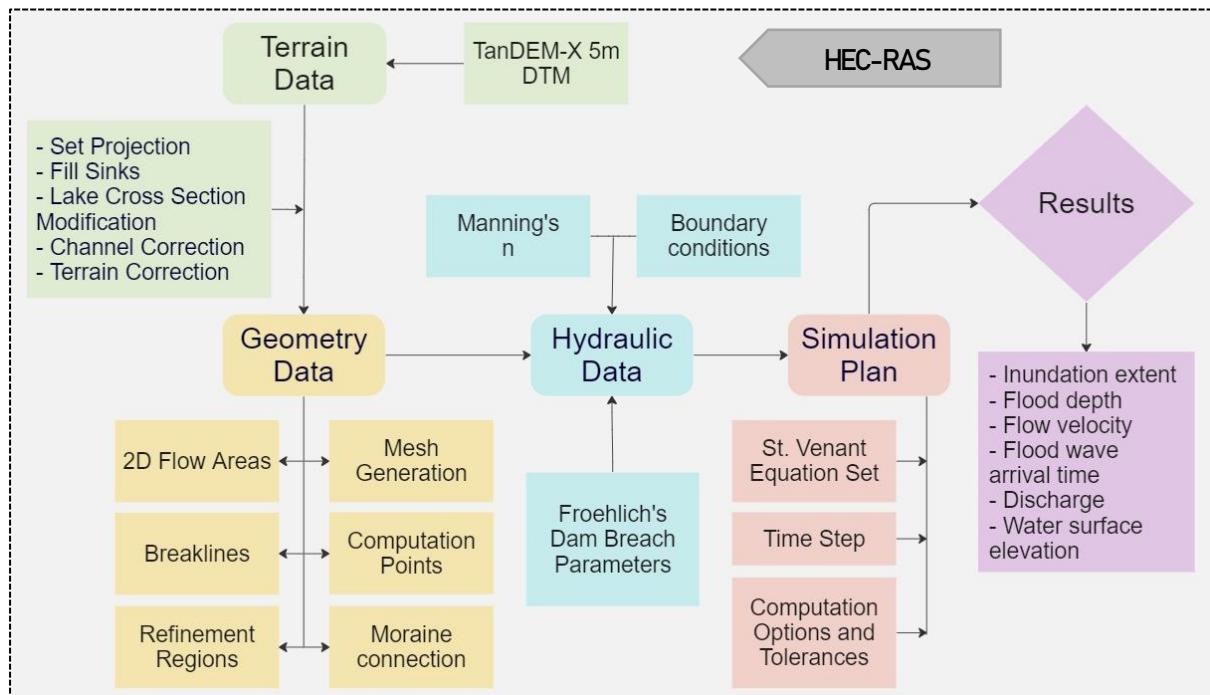


Figure 10: Methodology of GLOF Inundation Modeling used in the study

4.1.1. Study Area Boundaries

The selection of the study area boundary is an important step in the GLOF modelling process. In order to capture the entire inundation area of the GLOF, the study area boundaries must be enough to accommodate the total flow length of the flood wave, or atleast capture the flood wave until it attenuates to the normal no-flood stream flow.

Moreover, the study area must also account for the backwater flows into lateral streams or reservoirs to determine the inundation in such areas. Another important consideration in defining the study area extent is the computation time required for simulation. Too large of a study area will increase the complexity of the model, and hence, the computation time. The study area for 2D hydrodynamic simulation is defined by 2D flow areas in HEC-RAS which currently has a maximum cell limit of 2 million cells. Taking the above factors into consideration, the study area is taken from lake outlet to 160 km downstream along the river reach assuming that the flood wave will attenuate to a no-flood stream flow within this flow length. The boundaries of the study area of Suru glacial lake has been illustrated in Figure 11.

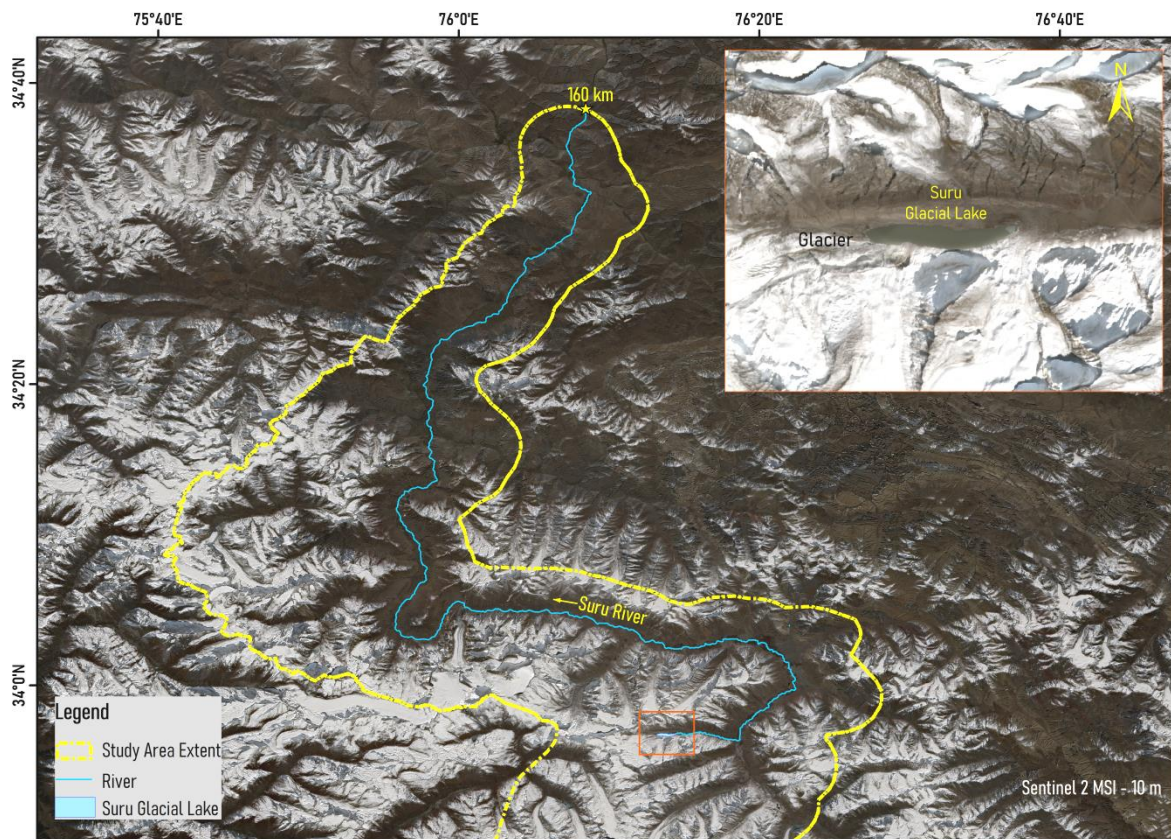


Figure 11: Study Area Boundary of Suru glacial Lake for GLOF Inundation Modelling

4.1.2. GLOF Scenarios

Pluvial and fluvial floods are usually modeled with different scenarios based on the return period of the flood under consideration (5 years, 10 years, 100 years, etc.). In contrast, Glacial Lake Outburst Floods are very low-frequency rare-events and therefore, scenarios based on return period may not be suitable for modelling GLOFs. One way of defining GLOF modelling scenarios can be based on the lake volume drained after breach (50%, 75% and 100%). HEC-RAS software has capabilities to simulate two types of failure modes i.e. piping and overtopping. In addition to dry weather conditions, dam breaches can also occur due to extreme rainfall events. Considering the above possibilities of failure scenarios, in this study eight GLOF scenarios based on the percentage volume of water discharged from the lake after failure of the moraine, the weather conditions, and the

failure modes are simulated. Table 1 describes various GLOF scenarios simulated in the study.

Table 1: GLOF scenarios simulated in this study

Scenario	Definition (based on volume discharged)	Failure Mode	Weather Condition
Scenario-1	100% volume discharged from lake	Overtopping	Fair
Scenario-2		Piping	
Scenario-3	75% volume discharged from lake	Overtopping	
Scenario-4		Piping	
Scenario-5	50% volume discharged from lake	Overtopping	
Scenario-6		Piping	
Scenario-7	100% volume discharged from lake with PMS	Overtopping	Inclement
Scenario-8		Piping	

To simulate extreme rainfall events, Probable Maximum precipitation (PMP) is considered to occur in the catchment areas of the glacial lake. The resultant runoff generated due to PMP is estimated using rainfall-runoff modeling in HEC-HMS software. The stream runoff is then hydrodynamically modeled along with simultaneous breach of the lake.

Each of these scenarios has been modeled using 2D unsteady flow hydrodynamic modelling in HEC-RAS that essentially solves the St. Venant partial differential equations (Saint Venant, 1871). The St. Venant equations in 2D, also known as the Shallow Water Equations (SWE) can be written as:

A. Continuity Equation (Conservation of Mass):

$$\partial h / \partial t + \partial(hv_x) / \partial x + \partial(hv_y) / \partial y = 0 \quad \dots(\text{iii})$$

B. Momentum Equations (Conservation of momentum in x and y directions):

$$\partial(hv_x) / \partial t + \partial(hv_x^2 + (1/2) gh^2) / \partial x + \partial(hv_x v_y) / \partial y = - gh \partial z / \partial x + \tau_x \quad \dots(\text{iv})$$

$$\partial(hv_y) / \partial t + \partial(hv_x v_y) / \partial x + \partial(hv_y^2 + (1/2) gh^2) / \partial y = - gh \partial z / \partial y + \tau_y \quad \dots(\text{v})$$

where, h = water depth, t = time, v_x = component of velocity in x-direction, v_y = component of velocity in y-direction, x and y = horizontal spatial coordinates, z = bed elevation, τ_x and τ_y are bed shear stresses in the x and y directions, respectively.

Equation (iii) is known as the continuity equation which basically accounts for the volume of water in a river reach, and equations (iv) and (v) are known as the momentum equations which account for all the forces acting on the body of fluid in an open channel. HEC-RAS employs a finite difference approximation of the partial differential equations in which the SWE are discretized into a grid or a mesh transforming them into a set of algebraic equations. These algebraic equations are then solved iteratively for each grid cell using an implicit numerical solution scheme in which the unknown values of depth and velocities are calculated based on their known values at the neighboring cells and the current time step. The 2D flow areas of the glacial lake and the downstream serve as the mesh/grid having ‘n’ number of cells on which the iterative implicit finite difference solution scheme solves the SWE to compute a water surface elevation error that is within a user specified tolerance for each cell.

4.1.3. Processing of GLOF Model Inputs

4.1.3.1. Digital Terrain Model

The TanDEM-X DTM requires few corrections for hydrodynamic modeling. Firstly, the DTM was preprocessed by filling the sinks using ArcMap software. The original TanDEM-X DTM did not have lake bathymetric information as DEMs can only provide elevation of the top surface of water. In addition, the TanDEM-X DTM was acquired between 2010 and 2015, and hence, did not have the current lake extent. For 2D hydrodynamic modelling of the lake, it is necessary to correct the lake area of the DTM to include its underlying lakebed topography. Therefore, next step in DTM preprocessing was the modification of the lake area using cross-sections in HEC-RAS.

The original TanDEM-X DTM of the lake (left) procured depicts area of about 47.01 ha, and the TanDEM-X DTM (right) is reconditioned to represent the lake area extent as 54.14 ha (as on 2023) have been shown in Figure 12. Changes in the longitudinal profile of the lake post-correction are plotted on the graph.

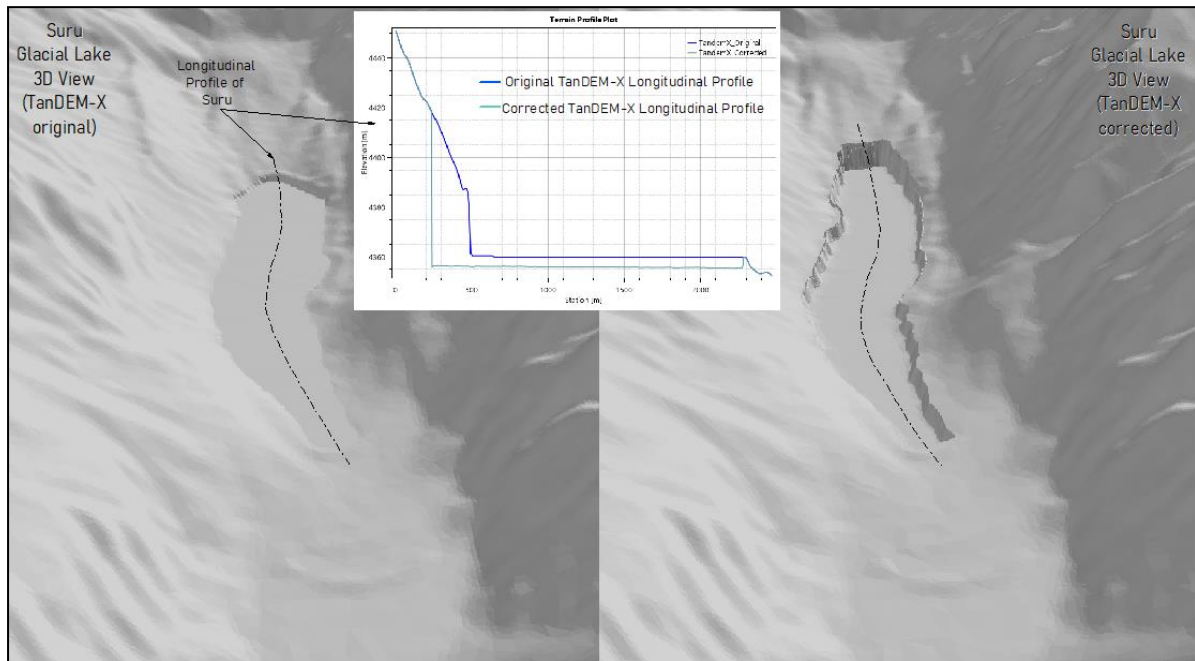


Figure 12: Reconditioned TanDEM-X DTM of Suru Lake

4.1.3.2. Land Cover and Manning’s n Values

Manning’s roughness coefficient plays a very significant role in the accuracy of computed water surface elevations in HEC-RAS. It represents the resistance to flow in channels and floodplains. The value of Manning’s n is highly variable and depends on several factors such as surface roughness; vegetation; channel irregularities; channel alignment; scour and deposition; obstructions; size and shape of the channel; stage and discharge; seasonal changes; temperature; and suspended material and bed load. Manning’s n values can be associated with Landcover data, and typical values of n for different streams and floodplain landcover types can be found in the book “Open Channel Hydraulics” by Chow, 1959. In this study, the landcover map of 1:10,000 generated by NRSC is used. Based on

literature, Manning’s n values assigned to the different landcover classes as provided in Table 2.

Table 2: Manning’s n used for different Land cover in this study

Landcover Class	Manning’s n
Waterbody	0.035
Snow and Glacier	0.06
Forest	0.10
Riverbed	0.04
Built-up area	0.12
Cropland	0.04
Bare Soil and Rock	0.03
Grassland	0.05

4.1.3.3. Dam Breach Parameters

The moraine of Suru glacial lake described in section 4.1.3.1 has a crest elevation of 4,360 m. It is around 131 m in width and is assumed to hold a water volume of 14.41 MCM at full capacity estimated using Huggel’s formula. In the absence of in-situ data regarding the moraine, it is assumed to be in poor condition readily susceptible to failure even with the slightest of overtopping depth. The average depth of the lake computed using Huggel’s formula was 26.61 m. Based on the average depth of the lake, the bed elevation of the lake at its outlet is calculated as 4,355.5 m.

With this data, the moraine dam breach parameters are estimated using the widely used Froehlich’s empirical equation set (Sattar et al., 2021; Majeed et al., 2021; Wang et al., 2018; Anacona et al., 2015). Wahl (2004) reported that Froehlich’s empirical formulae have the lowest prediction uncertainty, and hence, Froehlich’s empirical equations are used in this study. A dam breach analysis requires the estimates of dam breach parameters like breach formation time (t_f) and average breach width (B_{ave}) as inputs. t_f and B_{ave} can be computed using the empirical equations (vi) and (vii) given by Froehlich (1995a, b):

$$t_f = 0.00254 \times V_w^{0.53} \times h_b^{-0.90} \quad \dots(vi)$$

$$B_{ave} = 0.1803 \times K_0 \times V_w^{0.32} \times h_b^{0.19} \quad \dots(vii)$$

where, t_f = breach formation time in hours, B_{ave} = average breach width in metre, V_w = volume of water at the time of failure in cubic metre, h_b = height of breach in metre, K_0 = constant (1.4 for overtopping and 1.0 for piping failures).

Using these two parameters, we can estimate the breach progression rate (r) and the breach bottom width (B_{bw} , meters) with equations (viii) and (ix):

$$B_{bw} = B_{ave} - (h_b \times S_s) \quad \dots(viii)$$

$$r = 1 / [(B_{bw}/t_f) / (h_b/t_f)] \quad \dots(ix)$$

where, S_s is the average side slope of the breach = 1.4H:1V for overtopping failures and 0.9H:1V for piping failures.

Breach parameters are estimated for each scenario using equations (vi) to (ix), and are provided in Table 3.

Table 3: Dam Breach Parameters for Various GLOF Scenarios

Scenario	Failure Mode	Volume Discharge	Breach bottom elevation (m)	h_b (m)	B_{ave} (m)	t_f (hrs)	B_{bw} (m)	r
Scenario-1	Overtopping	100%	4355.5	26.61	91.97	0.82	54.72	0.49
Scenario-2	Piping				65.69		41.74	0.64
Scenario-3	Overtopping	75%	4364.6	17.51	84.94	1.2	60.43	0.29
Scenario-4	Piping				60.67		44.91	0.39
Scenario-5	Overtopping	50%	4371.14	10.97	77.72	3.33	62.36	0.18
Scenario-6	Piping				55.51		45.64	0.24
Scenario-7	Overtopping	100% with PMP	4355.5	26.61	91.97	0.82	54.72	0.49
Scenario-8	Piping				65.69		41.74	0.64

These breach parameters are fed into HEC-RAS moraine connection data to obtain a breach hydrograph and peak discharge from the breach during simulation. This breach hydrograph is then hydrodynamically routed as unsteady flow in HEC-RAS using 2D flow areas to assess the effects of the flood wave downstream.

4.1.3.4. PMP and Runoff

Scenarios 7 and 8 as described under section 4.1.2 consider a glacial lake outburst event and simultaneous occurrence of Probable Maximum Precipitation (PMP) over its catchment. A PMP is defined as the maximum depth of rainfall meteorologically possible at a location over a given duration. There are various physical and statistical methods for estimation of PMP such as the moisture maximization method, storm transposition method, generalized method, atmospheric moisture budget method, Hershfield method, etc. The India Meteorological Department (IMD) has published a gridded PMP atlas for the Indus River Basin using some of these methods, however it does not have any gridded PMP data within Kargil district where the study area is located. Therefore, the PMP value over the Suru River catchment is estimated using the Annual Maximum Daily Precipitation (AMDP) series data over the past 51 years (1972-2023) from IMD. The World Meteorological Organization (WMO) recommended Hershfield statistical method is applied to calculate the PMP from the AMDP series (Hershfield, 1965). Hershfield's equation for estimation of PMP is based on Chow's general frequency equation (1951), given as:

$$A_{PMP} = \bar{A} + K \times S_N \quad \dots(x)$$

where, A_{PMP} is the PMP estimate for the location under consideration, \bar{A} is the mean of the AMDP series for N years at that location, S_N is the standard deviation of the AMDP series, K is the frequency factor which can be determined from equation (xi):

$$K = (A_m - \bar{A}_{N-1})/S_{N-1} \quad \dots(xi)$$

where, A_m is the maximum value of the AMDP series, \bar{A}_{N-1} and S_{N-1} are the mean and standard deviation of the AMDP series respectively for N-1 years after removing the year with the maximum value.

Using equations (x) and (xi), the value of PMP for the catchment is computed to be 148 mm/day. This value of PMP is converted to a Probable Maximum Storm (PMS) by taking the time distribution of a 1-day severe storm from the Himalayan Region as reference (Table 4 and Figure 13).

Table 4: Design of the PMS using a Severe Reference Storm from the Himalayan Region

Time (hrs)	Cumulative Rainfall of Reference Storm (mm) [i]	Proportion of Total Rainfall (i/335.3) [ii]	PMP Cumulative distribution (mm) [148 x ii]	Incremental Rainfall (mm)	Bell Curve Arrangement (mm)
1	55	0.164	24.28	24.28	0.00
2	90	0.268	39.73	15.45	0.31
3	119	0.355	52.53	12.80	0.88
4	154	0.459	67.97	15.45	2.21
5	193	0.576	85.19	17.21	2.47
6	228	0.68	100.64	15.45	3.97
7	243	0.725	107.26	6.62	3.97
8	252	0.752	111.23	3.97	4.41
9	262	0.781	115.65	4.41	6.62
10	267	0.796	117.85	2.21	15.45
11	275	0.82	121.38	3.53	17.21
12	284	0.847	125.36	3.97	24.28
13	294	0.877	129.77	4.41	15.45
14	296	0.883	130.65	0.88	15.45
15	301.4	0.899	133.04	2.38	12.80
16	307	0.916	135.51	2.47	5.30
17	316	0.942	139.48	3.97	4.41
18	328	0.978	144.78	5.30	3.97
19	332.8	0.993	146.90	2.12	3.53
20	332.8	0.993	146.90	0.00	2.38
21	332.8	0.993	146.90	0.00	2.12
22	333.5	0.995	147.21	0.31	0.79
23	335.3	1	148.00	0.79	0.00
24	335.3	1	148.00	0.00	0.00

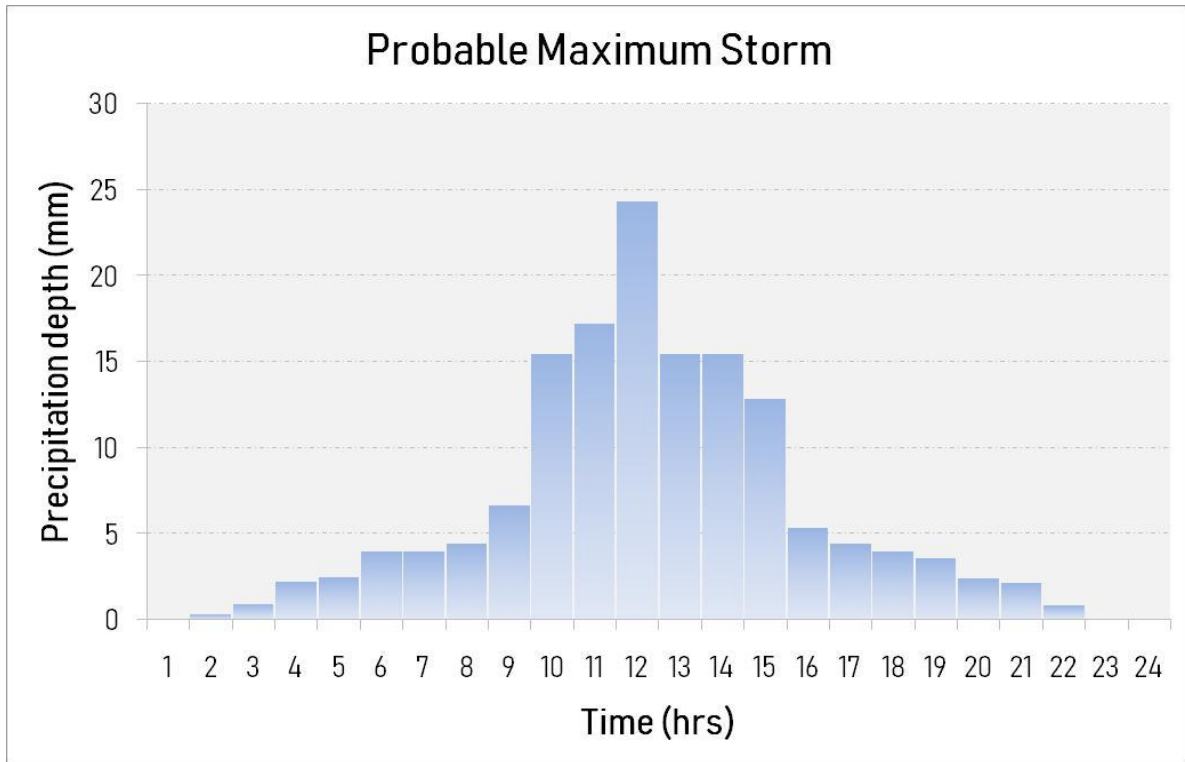


Figure 13: Probable Maximum Storm used for Runoff Estimation

To incorporate the effect of the PMS on Suru GLOF, a rainfall-runoff model is developed in HEC-HMS software to derive the PMS induced inflow hydrographs at various lateral streams contributing to the lake as well as the downstream flow path of the flood wave. The rainfall-runoff model is developed to include the runoff generated from entire catchment of the Suru river up to the study area boundary (Figure 14). This ensured a comprehensive assessment of the lateral inflows contributing to the flood wave in case of failure of Suru’s moraine. Cartosat DEM is used in delineating the subbasin boundaries and their outlets for computing lateral inflows along the river reach. A total of nine lateral inflows in the catchment are considered. Rainfall is assumed to occur below the 4,500 m elevation in the study area. The total area of the catchment was 10,437 km², out of which 5,931 km² area was below 4,500 m elevation.

Generating the lateral stream flow hydrographs in HEC-HMS requires the specification of a loss model that computes the excess precipitation after deducting the losses, a transform model that converts the excess precipitation into a direct runoff hydrograph, a base flow model (optional) to simulate sub-surface drainage, and a routing model to simulate the 1D open channel flow using continuity equation and produce the routed direct runoff hydrograph as the output. In this study, the following models are used:

- i. Loss Model - SCS Curve Number
- ii. Transform Model - SCS Unit Hydrograph
- iii. Routing Model - Muskingum Routing

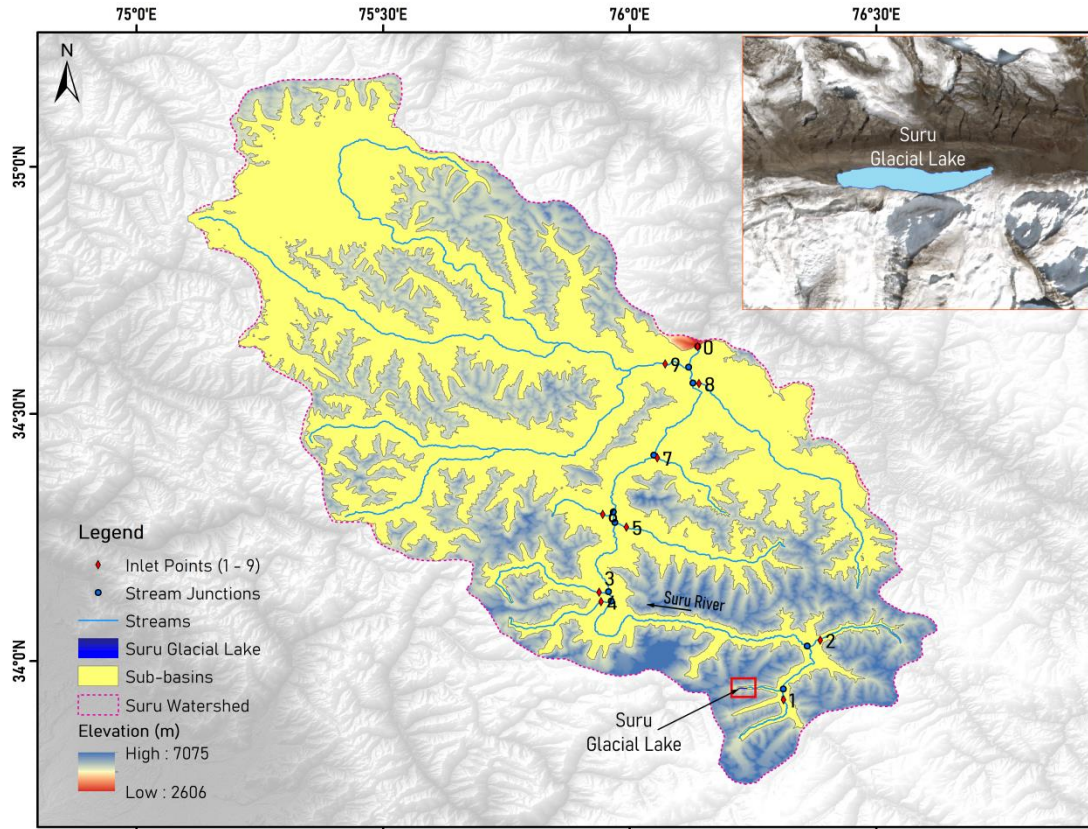


Figure 14: Area Contributing to Rainfall-Runoff Considered in HEC-HMS Model

The SCS Curve Number (CN) is a dimensionless parameter that represents the combined effects of soil type, land use, and antecedent moisture conditions on the runoff potential of a particular area. It ranges from 0 to 100 (40 - 98), with lower values indicating better infiltration losses and higher values indicating more runoff. The CN value can be estimated using CN tables provided by the SCS. In GIS raster data, the CN value is estimated for each picture element “pixel”. Once the CN value is calculated, the maximum potential retention (R) can be calculated using equation (xii) given by the Soil Conservation Service (1971):

$$R = (25400 - 254 \times CN)/CN \quad \dots(xii)$$

where, R = maximum potential retention in the area represented by the pixel (mm). Then, we can determine the accumulated precipitation excess at time t (P_e) using equation (xiii):

$$P_e = (P - 0.2 R)^2 / (P + 0.8 R) \quad \dots(xiii)$$

where, P = accumulated rainfall depth at time t.

HEC-HMS uses equations (xii) and (xiii) to give the excess precipitation at time t. This excess precipitation is transformed to a direct runoff hydrograph using the SCS Unit Hydrograph (UH) transform method in HEC-HMS. The SCS UH is also a dimensionless hydrograph with ordinate Q_t/Q_p (discharge at any time t/peak discharge of UH), and abscissa t/T_p (time/time of UH peak). The SCS suggests that the UH peak and the time of UH peak are related by (equation xiv):

$$Q_p = C \times A/T_p \quad \dots(xiv)$$

where, A = watershed area, and C = conversion constant (2.08 in SI).

The time of peak is related to the duration of excess precipitation as (equation xv):

$$T_p = (\Delta t/2) + t_{lag} \quad \dots(xv)$$

where, Δt = excess precipitation duration (computational interval of model run), t_{lag} = basin lag defined as the time difference between the centre of mass of rainfall excess and the peak of UH. When the lag time is specified, HEC-HMS solves equation (xiv) to find Q_p and T_p . The basin lag is related to the time of concentration in the basin (t_c) and calculated using equation (xvi):

$$t_{lag} = 0.6 t_c \quad \dots(xvi)$$

where, t_c is the time taken by a drop of water to reach the basin outlet from the farthest point in the watershed. t_c (hrs) was computed in HEC-HMS using equation (xvii):

$$t_c = l^{0.8} \times (R + 1)^{0.7} / (1140 \times Y^{0.5}) \quad \dots(xvii)$$

where, R = maximum potential retention (inch), Y = sub-basin slope (%), l = maximum flow length in sub-basin.

Routing of the direct runoff hydrograph obtained by SCS UH transform method was done using Muskingum's hydrologic channel routing equation (xiv):

$$S = K [x I + (1 - x) Q] \quad \dots(xviii)$$

where, S = total storage in a channel reach, I = inflow rate, Q = outflow rate, x = weighting factor (0 - 0.5), and K = storage-time constant having dimensions of time.

In this model, K = 0.5, and x = 0.25 are used for the Muskingum Routing that simulates channel flow and gives the routed direct runoff hydrograph at specified locations within the stream. The model is used to derive the lateral inflow hydrographs for each of the nine points shown in Figure 14. These inflow hydrographs are specified as boundary conditions in HEC-RAS for simulating hydraulic channel routing and estimation of the hydrodynamic parameters.

4.1.4. Dam Breach Model Setup

A two-dimensional unsteady flow full hydrodynamic model is set-up in HEC-RAS to simulate the dam breach phenomenon. Setting up of a HEC-RAS 2D unsteady flow dam breach model requires the following inputs:

- i. Terrain data
- ii. Geometry data
- iii. Dam breach parameter data
- iv. Unsteady flow data (initial and boundary conditions)
- v. Computational plan settings

Terrain Data is one of the most important inputs of a good hydrodynamic model. The accuracy of a hydrodynamic model greatly depends on the accuracy and resolution of the terrain data used in the study. When 2D meshes are generated in HEC-RAS to model

the flow areas, each cell face contains the information of the terrain underneath it (Figure 15).

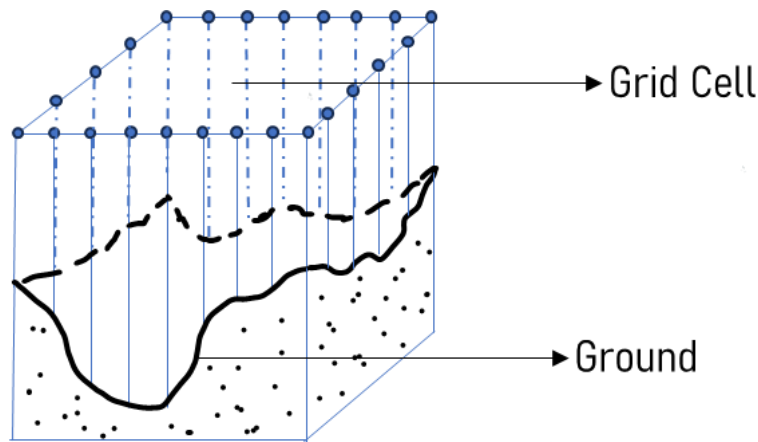


Figure 15: HEC-RAS Grid Cell and underlying Terrain Information

Each cell and cell faces of the computational mesh are pre-processed automatically in HEC-RAS to generate a detailed elevation-volume relationship for each cell along with station elevation data for each face. Other hydraulic property tables are also generated for each cell such as elevation vs wetted perimeter, elevation vs area, etc. (Figure 16)

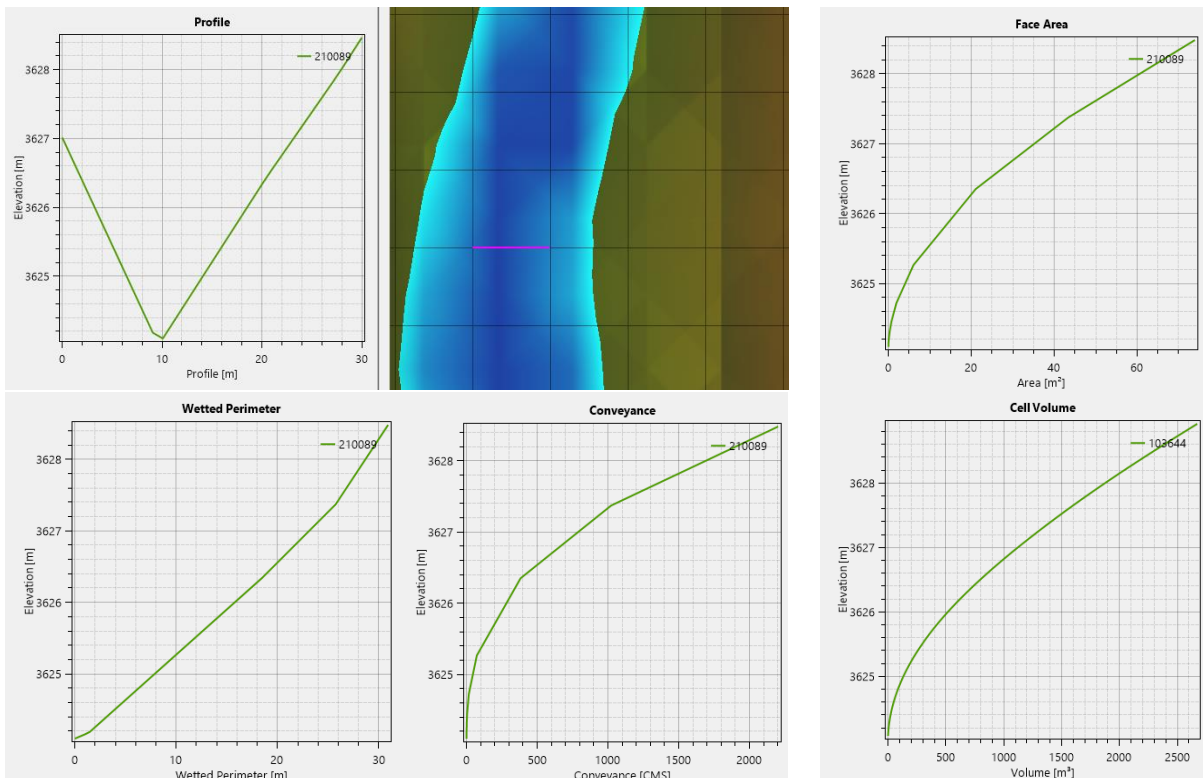


Figure 16: Hydraulic properties of Each Cell in HEC-RAS

Finer resolution of terrain data will give more accurate hydraulic properties of each cell. High-resolution TanDEM-X 5 m DTM is used to generate the terrain data as described under section 4.1.3.1.

Geometry Data contains the 2D computational mesh that defines the area within which HEC-RAS will solve the Shallow Water Equations and give hydrodynamic parameters such as discharge, depth, and velocity as output. As mentioned earlier, for fully hydrodynamic 2D simulation, the lake as well as the downstream with 2D flow areas needs to be setup. It is very important to select the extents of the 2D flow areas properly to include the backwater flows of the flood wave into the lateral streams, and it must also cover the maximum distance of flooding so that even the most downstream flood affected location is included in the 2D flow area. So, a 160 km long 2D flow area for the downstream of Suru glacial lake along its river reach to include all lateral flows, and one 2D flow area covering the full extent of the glacial lake itself are setup in the model. Each cell face of the 2D mesh acts as a cross section, and so, the elevation values between two cross sections are interpolated. Therefore, to accurately model the terrain underneath, the cell size should be selected suitably. It is recommended that for highly varying terrain geometry, smaller cell sizes be used, and for floodplains where the elevations don't vary much over space, larger cells may be sufficient. A cell size of 15 m to model the channel, and a 30 m cell size for modelling the overbank areas area used. Cell sizes were also chosen by considering the time taken to solve the model, and the HEC-RAS cell limit of 2 million cells. Also, the cells need to be aligned perpendicular to the direction of flow to capture the cross-sectional geometry of the terrain accurately. Breaklines in the lake as well as the downstream 2D flow areas to align the cells properly are used. The 2D flow areas were also associated with the Manning's n values as described in section 4.1.3.2.

Dam breach Parameter Data is entered into the 2D flow area connection editor that describes the moraine geometry. The parameter calculations are shown in section 4.1.3.3. The moraine is defined as a 2D flow area connection in HEC-RAS which transfers flow between the two flow areas. During the formation of the breach, the moraine behaviour oscillates between that of a broad-crested weir and a sharp-crested one. A breach weir coefficient of 1.44 (SI units), and additionally, in case of piping failure, a piping coefficient of 0.5 are used to simulate pressurised orifice flow.

Unsteady Flow Data is manually entered in HEC-RAS unsteady flow data editor. A downstream boundary condition of "Normal Depth" with a friction slope of 0.012 is used. The friction slope value was roughly taken as the slope of the channel from the most upstream point to the most downstream point. The initial water surface elevation of the glacial lake 2D flow area was set as 4,382.11 m. For simulating scenarios 7 and 8, the HEC-HMS rainfall-runoff model derived lateral inflows were also input into the unsteady flow data editor as upstream boundary conditions at their respective locations in the channel.

Computational Plan Settings in HEC-RAS are extremely important to ensure model stability and accurate results. From equations (iii), (iv) and (v), as described in section 4.1.2, HEC-RAS solves derivatives with respect to time and space. The time step for model computations can be selected by the Courant condition (C), equation (xix) and (xx):

$$C = (v \times \Delta t) / \Delta x \quad \dots(xix)$$

where, v = velocity of flow (m/s), Δt = time step (s), and Δx = cell size (m).

For St. Venant equations, the value of C should ideally be ≤ 1.0 , and maximum 3.0. That gives us the time step as:

$$\Delta t \leq \Delta x/v \text{ (For } C \leq 1.0) \quad \dots(xx)$$

Too small time-steps give breach hydrographs with steep rising limb until the point of oscillation and instability. On the contrary, larger time steps induce numerical diffusion that results in the attenuation of the peak discharge and a flatter broadly spread hydrograph. So, using the Courant condition, a computational time step of 1 second is selected to remove time step induced errors in the model results. All the computation parameters are given in Table 5.

Table 5: Computations Settings used HEC-RAS Model

Parameter	Value
Computation Time Step (s)	1
Theta	1
Water Surface Tolerance (m)	0.003
Volume Tolerance (m)	0.003
Equation Set	SWE-ELM
Turbulence Model	None
Coriolis Effect	None
Matrix Solver	PARDISO (Direct)
Maximum Iterations	30

4.1.5. Validation of Peak Discharge

The breach hydrograph obtained from HEC-RAS simulation is validated by comparing the simulated peak discharge with the peak discharge computed using Froehlich’s (1995b) empirical equation (xxi):

$$Q_p = 0.607 \times V_w^{0.295} \times h_b^{1.24} \quad \dots(xxi)$$

where, Q_p = peak discharge, V_w = volume of water at the time of failure in cubic meters, h_b = height of breach in meters.

The simulated peak discharge value was similar to the value of peak discharge estimated using equation (xxi), and hence, the model is considered to give reasonable results for the hydrodynamic parameters.

4.2. Mapping of Exposed Elements

Areas of exposure are those places along the flood plain with buildings, infrastructure, and services where people are settled for their livelihood (Rinzin et al., 2023; Allen et al., 2019). Flood exposure can be estimated by overlaying the flood inundation extent map on the maps of population, structures, livestock, and agricultural land (Rinzin et al., 2023; Tate et al., 2021). In this study, infrastructure maps are generated within a buffer of 500 m from the maximum flood extent derived using GLOF hydrodynamic simulations in HEC-RAS. South Korean satellite KOMPSAT-3/3A 0.5 m data of very high-resolution multispectral imagery was procured for mapping of infrastructure. Using visual interpretation techniques, elements such as settlements, agriculture lands, road network, road bridges, hydropower projects and other public utilities along the river reach are mapped from KOMPSAT-3/3A imagery (Figure 17).In Figure 17, locations 1 &2 show

thematic information generated from the image and location 3 on satellite image shows the Kargil city. In addition, infrastructure information was taken from the Geofabrik's free download server (<https://download.geofabrik.de>). The information was extracted from the OpenStreetMap project, which contains buildings, roads, and bridges and is normally updated periodically. Table 6 shows the detailed information of the mapped infrastructure with reference to the type, counts and their details. These maps and information can be used to carry out a detailed assessment of exposure for downstream infrastructure, farmland, and population against GLOFs (Zhang et al., 2021).

Table 6: Details of Infrastructure Mapped using Satellite data

Sl. No	Infrastructure	Shapefile Type	Details
1	Road Network	Polyline	377 km
2	Bridges	Point	71
3	Dams and power projects	Point	3
4	Settlements	Polygon	50
5	Agricultural Land	Polygon	1,858 ha

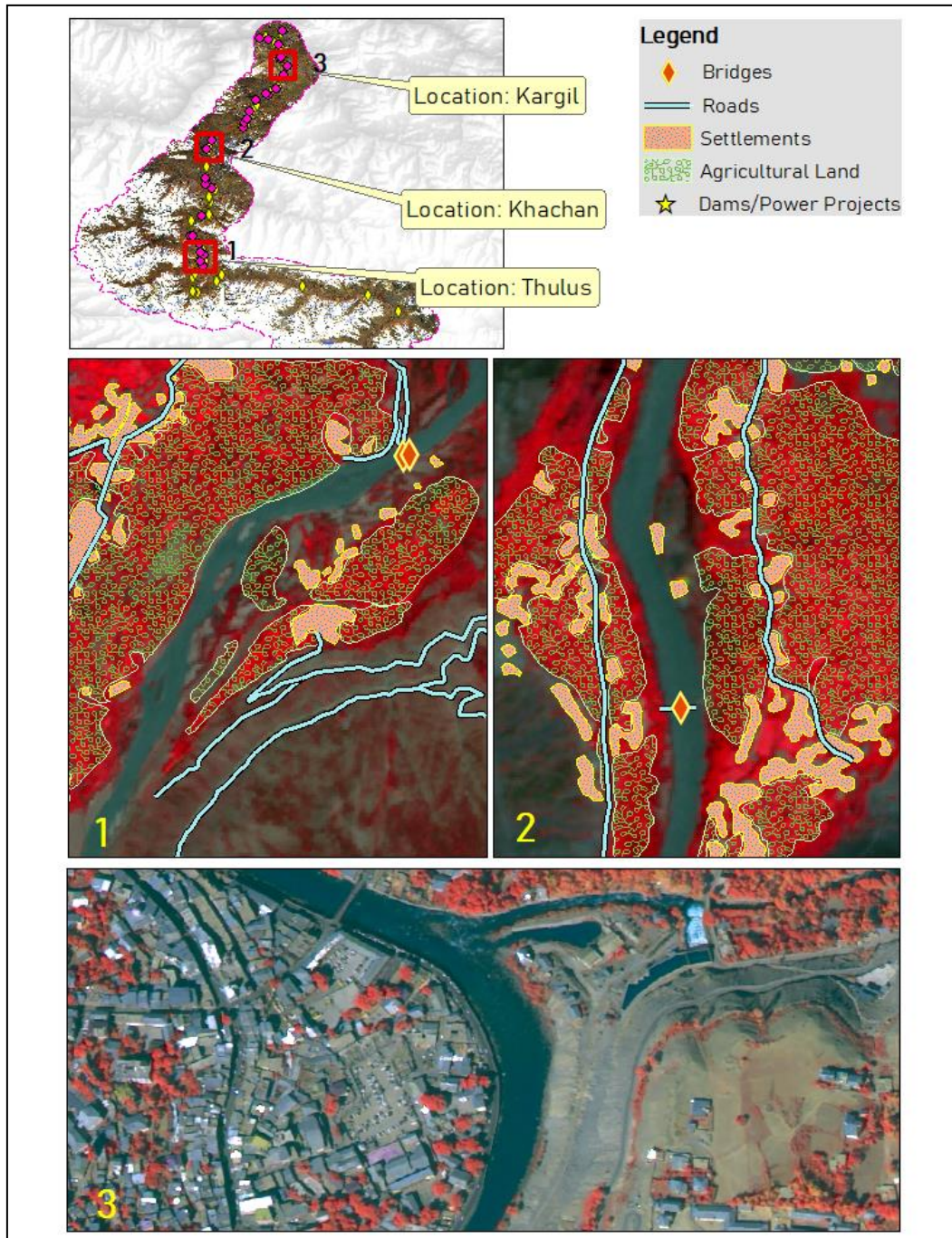


Figure 17: Sample Infrastructure Maps of the study area

4.3. GLOF Risk Assessment

A review of literature indicates the lack of a common approach or methodology for risk assessment. The Water Research Laboratory’s technical report of September 2014 describes about hazard-vulnerability thresholds depending upon stability criteria for people, vehicles, and buildings, but does not mention about risk classification (WRL, 2014). On similar lines, the GAPHAZ (2017) technical guidance document also mentions about Hazard Assessment of GLOFs without any risk assessment methodology. The CWC (2018) “Guidelines for mapping flood risk associated with dams” contains general guidelines for mapping hazard and risk, and it also mentions commonly used tools for risk

assessment. However, detailed procedure or thresholds for risk level classification are lacking in this guideline. NDMA’s GLOF Management Report (NDMA, 2020) mentions the same hazard assessment methodology of the GAPHAZ technical guidance document. Additionally, it has some general guidelines for risk assessment. Other studies on GLOF risk assessment are available, but they differ in the methodologies and data used for risk assessment. So, it is decided to carry out GLOF risk assessment using only the results of hydrodynamic simulation and a detailed analysis of the downstream infrastructure maps. Figure 18 shows the flow chart of methodology for GLOF risk assessment adopted for Suru glacial lake. In this study GLOF risk assessment is proposed by combining flood severity and flood wave arrival time using a simple matrix method to generate flood risk maps.

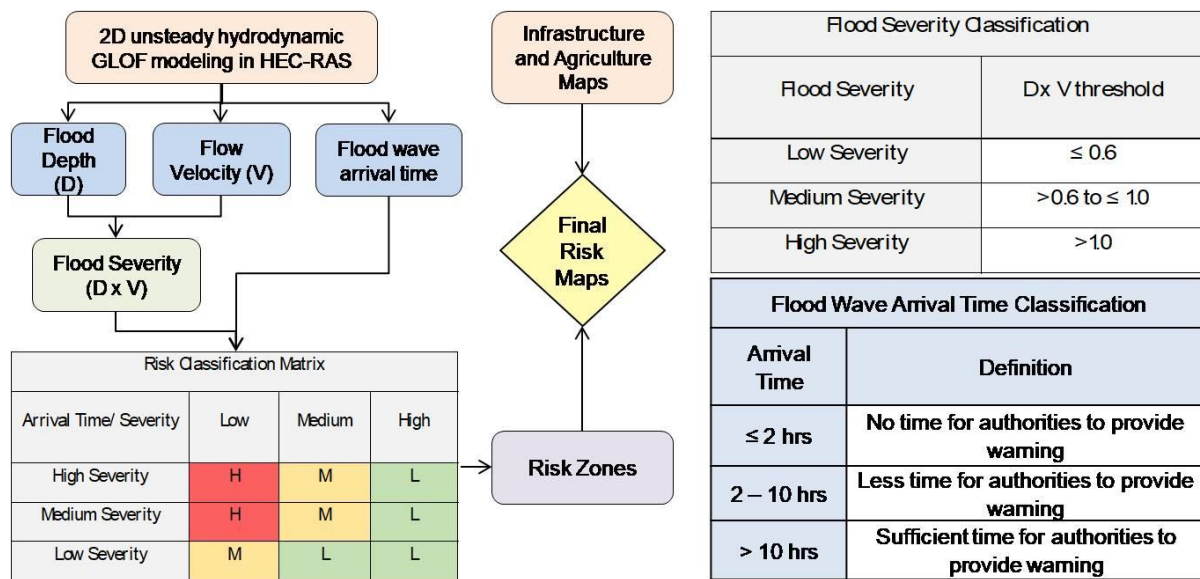


Figure 18: Flow Chart of Methodology of GLOF Risk Assessment

The flood risk classification is based on flood severity and flood wave arrival time. Flood severity can be defined as a product of flood depth and flow velocity (Graham, 1999), and it mainly represents flood hazard. The flood wave arrival time is defined as the time taken for a flood to add 0.3 m of water depth at the location under consideration. It is also derived from the results of the hydrodynamic simulation. The flood wave arrival time is categorized into 3 classes based on engineering judgment. The classification of flood wave arrival time would vary on a case-to-case basis depending upon the peak discharge of the flood, the terrain geometry, and the average discharge of the flooded stream in no-flood conditions. As per literature on flood severity classification (CWC, 2018; AEMI, 2014; Escuder-Bueno et al., 2012; Graham, 1999), it is decided to arrive at three levels of severity classification as defined in Table 7.

Table 7: Flood severity classification

Flood Severity Class	Definition	D x V (m ² /s) threshold
Low Severity	People survive, with some loss of stability, no fatalities expected. Children, elderly and small	≤ 0.6

	vehicles may be in danger. All buildings are safe.	
Medium Severity	Significant loss of stability. All vehicles and people are in danger.	> 0.6 and ≤ 1.0
High Severity	High risk for people and vehicles. All buildings vulnerable to structural damage and some less robust buildings susceptible to failure.	> 1.0

The definition of the severity classes are based on interpretation of the literature on flood severity. These severity thresholds are based on the stability criteria for people, vehicles, and buildings affected by flood inundation, and oriented on similar lines with the AEMI, 2014 handbook on flood risk management guidelines. As the stability criteria of the exposed elements are taken into consideration, the severity classes also represent the susceptibility and resilience of the exposed elements to damage. Therefore, this severity classification also serves as a proxy for vulnerability. So, in locations where the flood severity is high, the exposed elements may be highly vulnerable to undergo greater extents of harm. Usually, high severity areas will face very high loss of life and almost complete washing-out of habitations and infrastructure, thereby indicating high risk.

For Suru glacial lake, the flood wave arrival time thresholds are defined in Table 8. The arrival time indicates the time difference between the initiation of breach and the arrival of the flood wave at a particular location. So, if the flood wave arrival time is low, it indicates that the flood wave arrives very quickly at the location.

Table 8: Classification of Flood Wave Arrival Time

Flood Wave Arrival Time	Threshold	Description
High	> 10 hours	Sufficient time for the authorities to provide warning
Medium	2 to 10 hours	Less time for the authorities to provide warning
Low	≤ 2 hours	No time for the authorities to provide warning

To define the thresholds of flood wave arrival time, the time of warning and evacuation available to the people in case of a GLOF event have been considered. It is assumed that the first two hours since the initiation of a GLOF event are extremely critical as the time available for warning and evacuating people is insufficient. Therefore, any inhabitant in the flood affected areas irrespective of their age or physical capacity are prone to the flood adversity, and hence, may not be able to escape the flood. Hence, the combination of low arrival time (≤ 2 hours) and a high to moderate flood severity automatically renders the exposed population under high risk. Another threshold value of 10 hours of arrival time was defined to delineate the low risk zones. In essence, any exposed population beyond the 10 hours of arrival time have sufficient time to evacuate the zones after warning is issued from the concerned authorities. So, irrespective of the flood severity in this region, the people’s exposure to the flooding is expected to be near zero, and hence, the risk level is low. The time between 2 - 10 hours is assumed to have moderate impacts to the

exposed population. Depending on the effectiveness of warning communication, people exposed to the flood may or may not be alerted/evacuated. Therefore, the time between 2 hrs and 10 hours after the initiation of the GLOF event along with the flood severity would create a zone of moderate risk where exposed people may or may not be catastrophically affected.

In summary, arrival time indicates the effective warning time available for people to evacuate the flood inundated areas, and therefore, it serves a proxy for the exposure of people and movable assets to a flood. If flood wave arrival time is high, people will get more time to evacuate with their movable assets leading to lower flood exposure. Therefore, moderately-high flood wave arrival times with effective warning will lead to lower risk. The same flood wave arrival times are considered for all GLOF scenarios while assessing the risk.

Finally, the risk zone maps are overlaid on the infrastructure maps of exposed elements to generate the GLOF risk maps. These maps can be used to identify those locations in the study area which require immediate attention for flood risk management.

An important point to note in the GAPHAZ (2017) technical document is that extreme scenarios like Scenarios 7 and 8 are not assessed separately for hazard due to their extremely low frequency of occurrence. The inundation extents of these scenarios exceeding the maximum inundation extents of the other scenarios mark zones of residual hazard. Therefore, we have considered the zones of residual risk as the additional inundation zones caused due to PMP, and we haven't assessed the risk for Scenarios 7 and 8 separately.

5. Results

The results of Suru glacial lake GLOF inundation modelling and risk assessment are described in the following sections. The results of GLOF scenarios of 1 and 2 (100% of lake volume release) and 7 and 8 (100% of lake volume release with PMP) are discussed here whereas results of other scenarios are provided in annexure 1.

5.1. GLOF Inundation Modelling

5.1.1. GLOF Scenarios 1&2 (100% release)

The GLOF scenarios 1 and 2 are simulated for 100% of lake volume release (14.41 MCM) in two failure modes (scenario 1 for overtopping and scenario 2 for piping). Figure 19 shows GLOF hydrograph downstream of the lake for scenario 1 (overtopping failure mode). The flood hydrograph reached its peak of 5,005 cumecs in 44 minutes after the initiation of breach in the lake. Figure 20 shows GLOF hydrographs downstream of the lake at various locations on the river reach for scenario 1. The peak of the flood hydrograph is attenuated from 5,005 cumecs to 490 cumecs over river reach length of 149 km at Kargil.

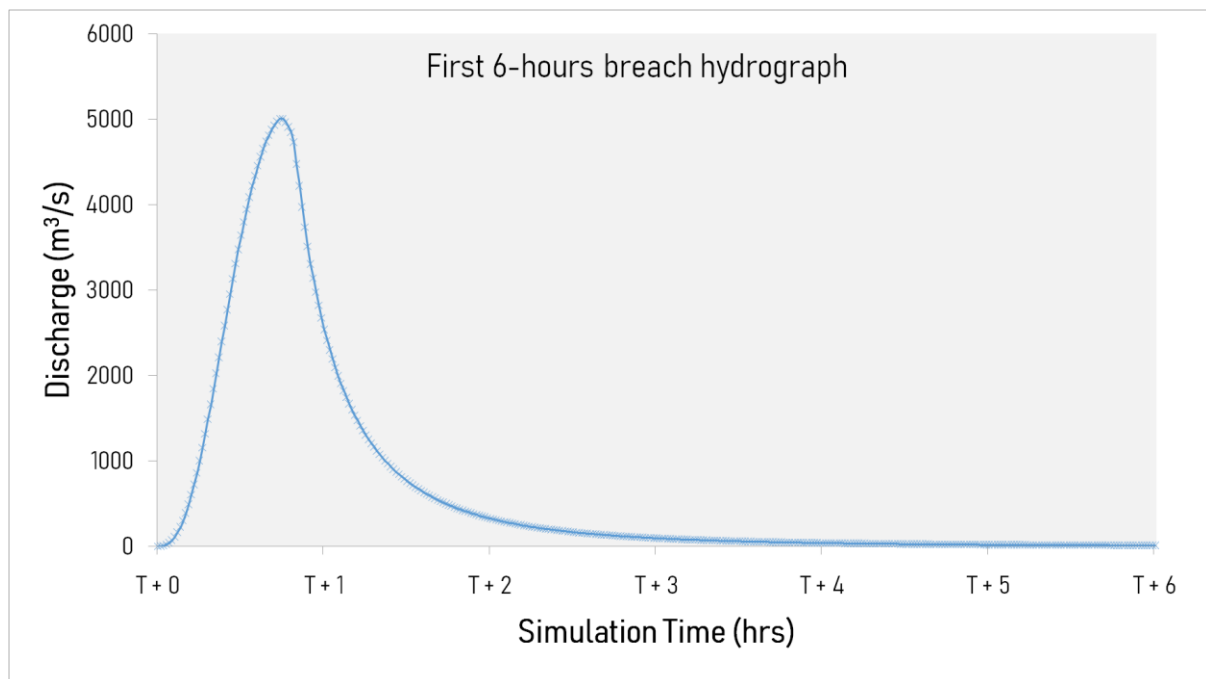


Figure 19: GLOF hydrograph for Scenario-1 (100% volume discharge- Overtopping failure)

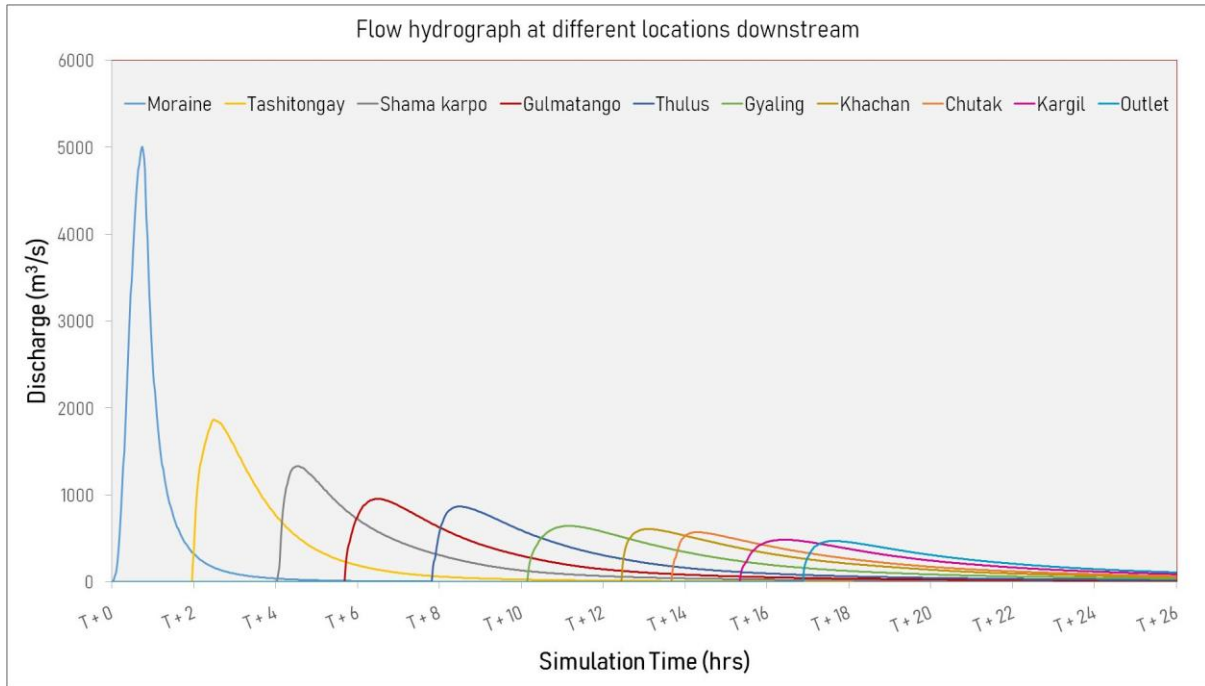


Figure 20: GLOF hydrograph for Scenario-1 (100% volume discharge- Overtopping failure)

Figure 21 shows GLOF hydrograph downstream of the lake for scenario 2 (piping failure mode). The flood hydrograph reached its peak of 4,878 cumecs in 37 minutes after the initiation of breach in the lake. Figure 22 shows GLOF hydrographs downstream of the lake at various locations on the river reach for scenario 2. The peak of the flood hydrograph is attenuated from 4,878 cumecs to 485 cumecs over river reach length of 149 km at Kargil.

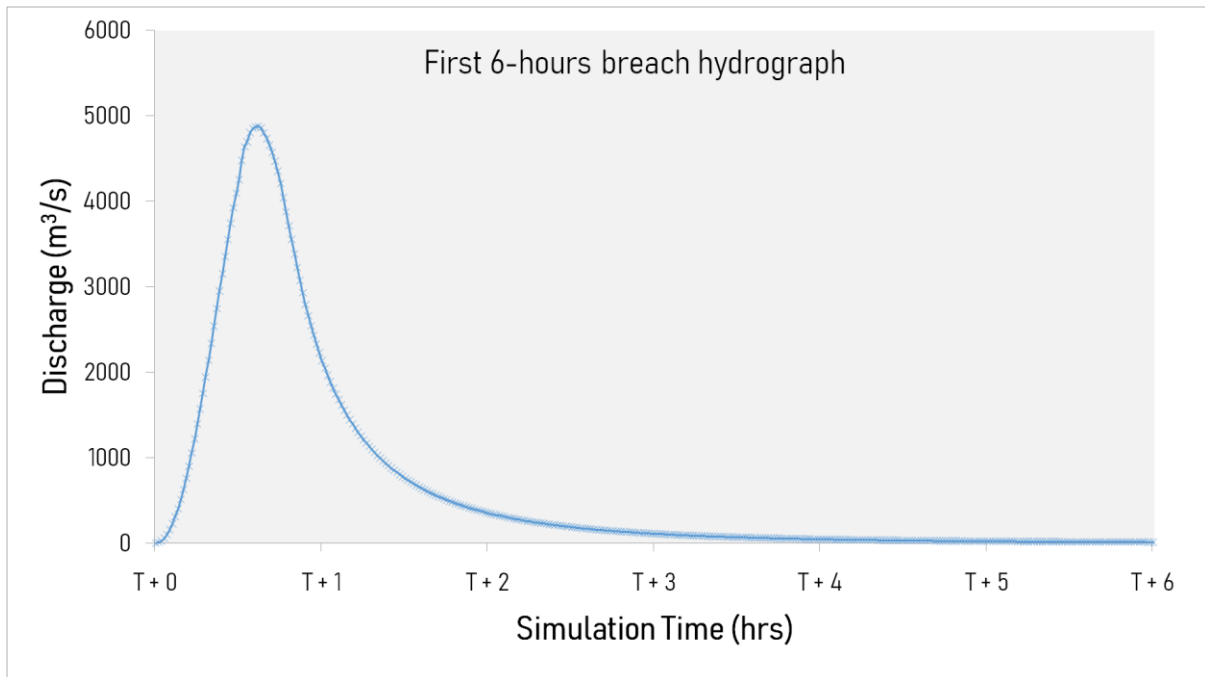


Figure 21: GLOF hydrograph for Scenario-2 (100% volume discharge - Piping failure)

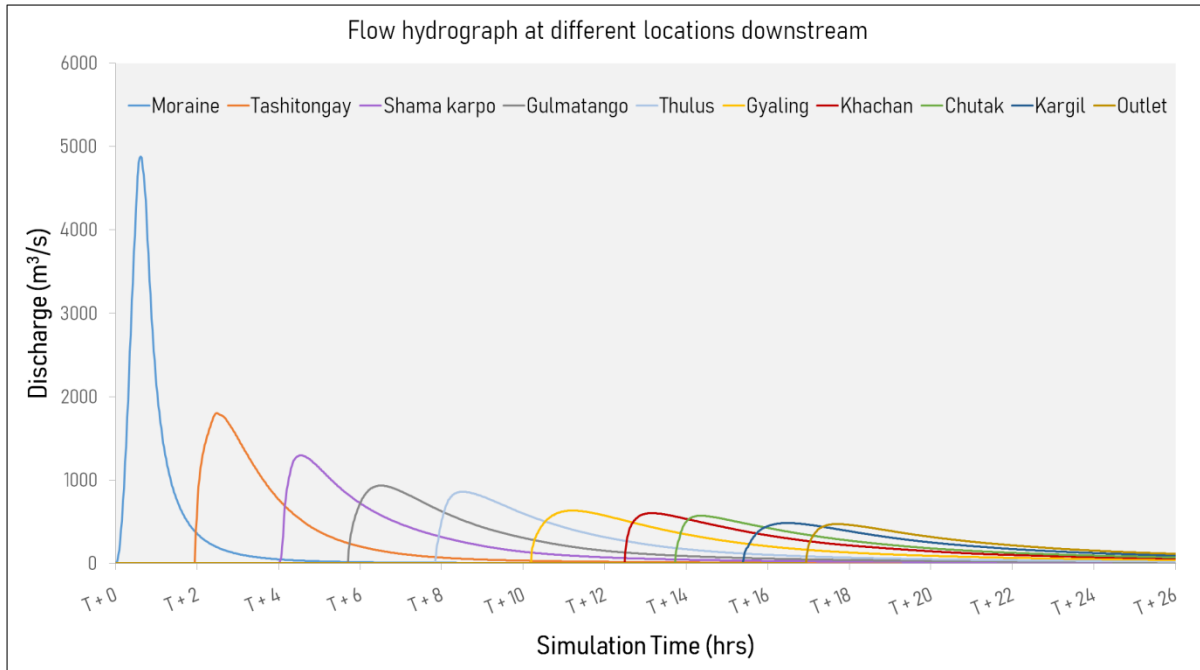


Figure 22: GLOF hydrographs at Different Downstream Locations for scenario-2

Table 9 describes the flood wave characteristics of GLOF scenario 1. After the breach of lake, the flood wave reaches nearest village of Thulus located at a distance of 74 km with peak discharge of 871 cumecs (maximum depth: 5.6 m; maximum velocity: 5.5 m/s) and as the flood wave traverses further downstream gets attenuated.

Table 9: Flood Wave Characteristics of GLOF Scenario 1

Location	Distance from Lake (km)	Time to peak	Peak Discharge (m ³ /s)	Max Depth (m)	Max Velocity (m/s)
Tashitongay	19	02hr 30mins	1,871	3.9	4.8
Shama karmo	33	04hr 32mins	1,330	2.5	2.1
Gulmatango	46	06hr 30mins	954	4.6	4.7
Thulus	74	08hr 30mins	871	5.6	5.5
Gyaling	96	11hr 09mins	644	3.6	4.6
Khachan	120	13hr 07mins	608	3.5	5.1
Chutak	134	14hr 18mins	576	4.7	1.7
Kargil	149	16hr 25mins	490	4.1	2.3
Outlet	160	17hr 38mins	475	2.2	4.2

Table 10 describes the flood wave characteristics of GLOF scenario 2. After the breach of lake, the flood wave reaches nearest village of Thulus located at a distance of 74 km with peak discharge of 855 cumecs (maximum depth: 5.6 m; maximum velocity: 5.5 m/s) and as the flood wave traverses further downstream gets attenuated.

Table 10: Flood Wave Characteristics of GLOF Scenario 2

Location	Distance from Lake (km)	Time to peak	Peak Discharge (m ³ /s)	Max Depth (m)	Max Velocity (m/s)
Tashitongay	19	02hr 29mins	1,801	3.9	4.6
Shama karmo	33	04hr 32mins	1,295	2.4	2.1
Gulmatango	46	06hr 31mins	936	4.6	4.8
Thulus	74	08hr 32mins	855	5.6	5.5
Gyaling	96	11hr 12mins	635	3.6	4.6
Khachan	120	13hr 09mins	600	3.5	5.1
Chutak	134	14hr 21mins	569	4.7	1.7
Kargil	149	16hr 29mins	485	4.1	2.2
Outlet	160	17hr 42mins	470	2.2	4.2

Flood inundation maps for all the GLOF scenarios were created by overlaying the inundation extents derived from HEC-RAS simulation on Resourcesat-2 LISS-IV 5.8 m multispectral imagery. Figure 23 shows the map of flood inundation extent along with major settlements affected due to the flood for GLOF scenario 1. The inset images show flood depth and flood velocity near Kargil city along with GLOF affected settlements, roads, bridges and other infrastructure.

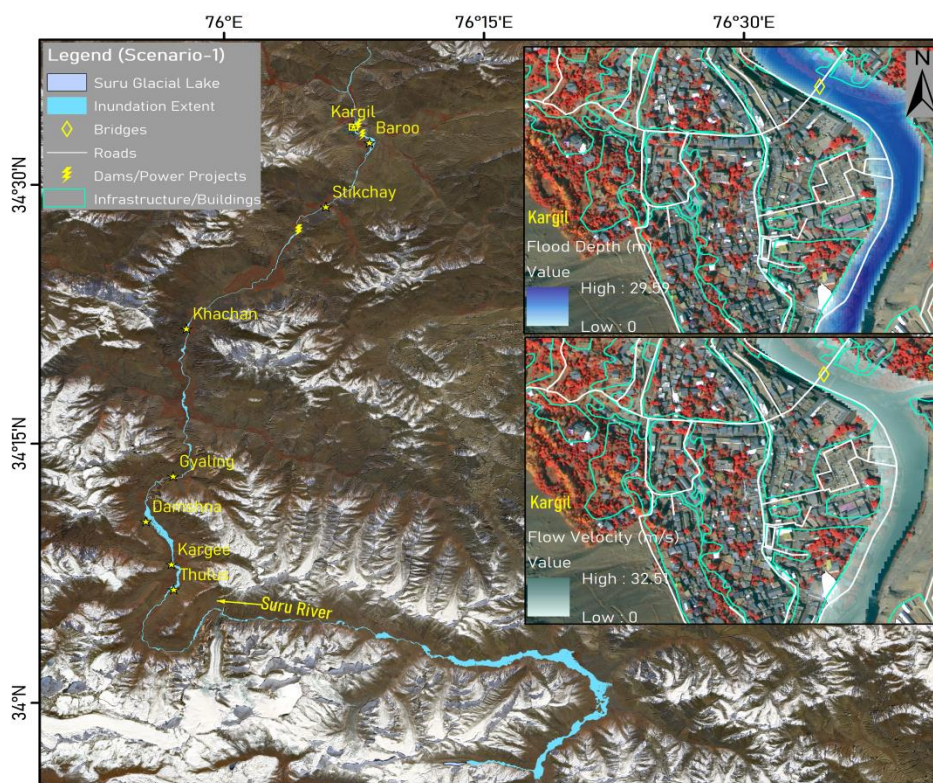


Figure 23: Map of Flood Inundation Extent for GLOF Scenario-1

Figure 24 shows the map of flood inundation extent along with major settlements affected due to the flood for GLOF scenario 2. The inset images show flood depth and flood velocity near Kargil city along with GLOF affected settlements, roads, bridges and other infrastructure.



Figure 24: Map showing extent of inundation for Scenario-2

Table 11 provides number of settlements, extent of agricultural land, number of bridges and length of road network affected by scenarios 1 and 2. Table 12 provides names of settlements affected by scenarios 1 and 2. All the settlements (13) are partly affected by the GLOF inundation.

Table 11: Infrastructure affected in GLOF Scenarios 1 and 2

Scenario	No. of Affected Settlements	Area of Agricultural Land Affected (ha)	No. of Bridges Affected	Length of Roads affected (km)	Inundated Area (ha)
Scenario-1	13	41.1	54	13.1	3260
Scenario-2	13	40.6	54	12.7	3244

Table 12: Details of Settlements affected in GLOF Scenarios1 and 2

S. No.	Settlement Name	Distance from lake (km)
1	Thulus	74
2	Kargee	84.9
3	Namsuru*	85
4	Damshna	90.68
5	Gyaling*	96
6	Khachan*	120
7	Zambakha*	129.3
8	Sarchay*	131.2
9	Stikchay*	138
10	Zamistang*	143.48
11	Baroo	147.43
12	Kargil	149
13	Poyen	150

Note: * indicate few buildings, which are affected close to the river channel near the mentioned settlement.

Figure 25 shows close view of partly affected settlements and other infrastructure at Thulus (Left) and Kargil (Right) in both scenarios 1 and 2.

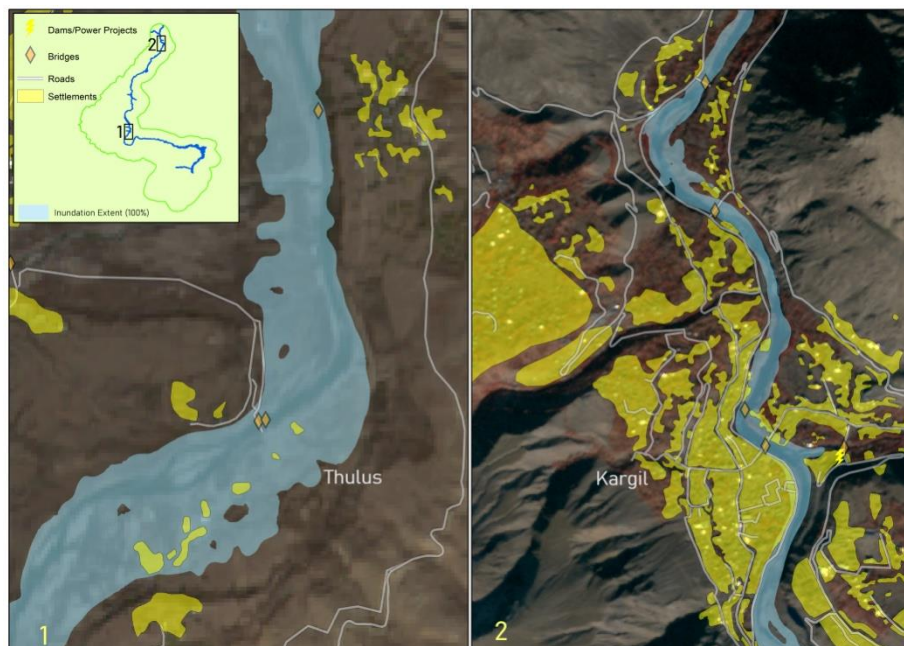


Figure 25: Map showing Close View of extent of inundation for Scenarios - 1 and 2

5.1.2. GLOF Scenarios 7&8 (100% release with PMP)

The GLOF scenarios 7 and 8 are simulated for 100% of lake volume release (14.41 MCM) along with rainfall-runoff due to PMP in two failure modes (scenario 7 for overtopping and scenario 8 for piping). Figure 26 shows GLOF hydrograph downstream of the lake for scenario 7 (overtopping failure mode) along with runoff generated due to PMP. The flood hydrograph reached its peak of 5,005 cumecs in 44 minutes after the initiation of breach in the lake as in the case of scenario 1.

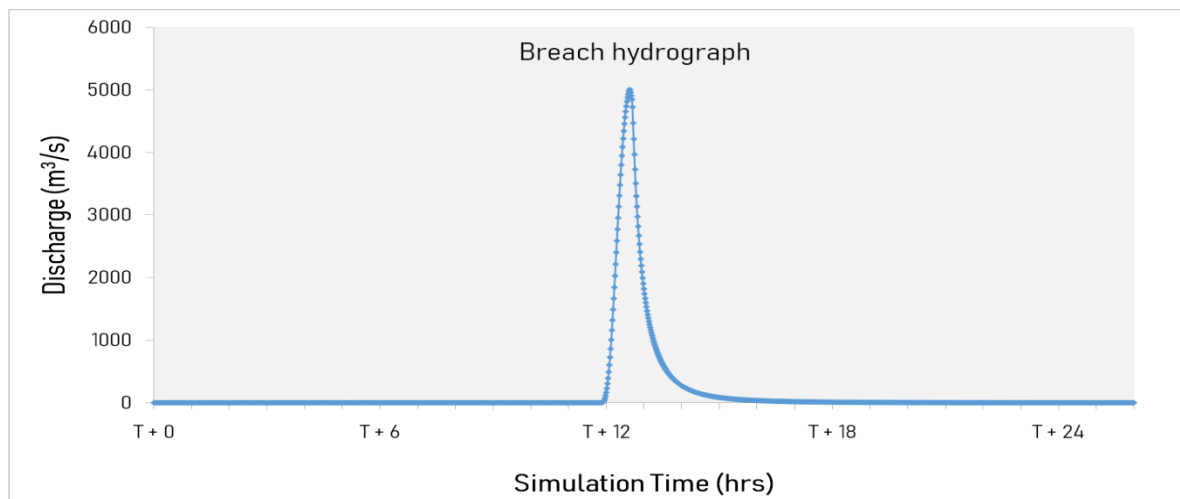


Figure 26: GLOF hydrograph for Scenario-7 (100% volume discharge & PMP-Overtopping)

Figure 27 shows GLOF hydrograph downstream of the lake for scenario 8 (piping failure mode) along with runoff generated due to PMP. The flood hydrograph reached its peak of 4,878 cumecs in 37 minutes after the initiation of breach in the lake as in the case of scenario 2.

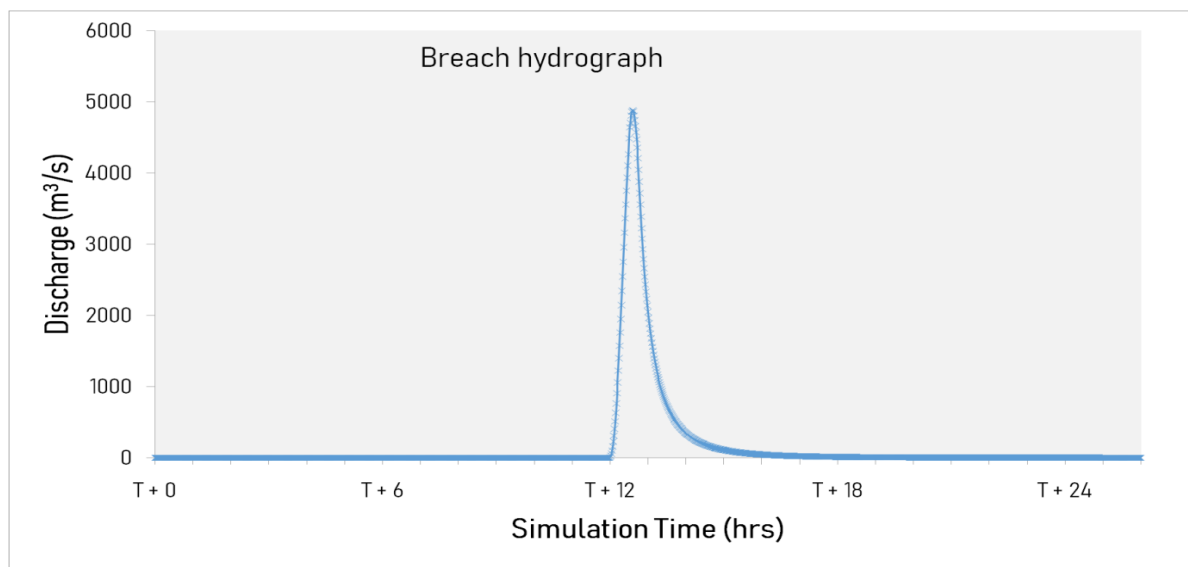


Figure 27: GLOF hydrograph for Scenario-8 (100% volume discharge & PMP - Piping)

Table 13 describes the flood wave characteristics of GLOF scenario 7. After the breach of lake, the flood wave reaches nearest village of Thulus located at a distance of 74 km with peak discharge of 923 cumecs (maximum depth: 5.6 m; maximum velocity: 5.7 m/s) and the flood wave traverses further downstream.

Table 13: Flood Wave Characteristics of GLOF Scenario 7

Location	Distance from Lake (km)	Time to peak	Max Depth (m)	Max Velocity (m/s)
Tashitongay	19	08hr 30mins	3.8	4.7
Shama karmo	33	10hr 33mins	2.4	2
Gulmatango	46	12hr 30mins	4.6	5.2
Thulus	74	14hr 30mins	5.6	5.7
Gyaling	96	16hr 14mins	5.1	6.1
Khachan	120	14hr28mins	9.3	5.8
Chutuk	134	14hr 44mins	10.9	3.9
Kargil	149	15hr 48mins	11.4	3.3
Outlet	160	15hr 39mins	15.4	17.9

Table 14 provides the flood wave characteristics of GLOF scenario 8. After the breach of lake, the flood wave reaches nearest village of Thulus located at a distance of 74 km with peak discharge of 901 cumecs (maximum depth: 5.6 m; maximum velocity: 5.7 m/s) and the flood wave traverses further downstream.

Table 14: Flood Wave Characteristics of GLOF Scenario 8

Location	Distance from Lake (km)	Time to peak	Max Depth (m)	Max Velocity (m/s)
Tashitongay	19	08hr 25mins	3.8	4.7
Shama karmo	33	10hr 29mins	2.4	2
Gulmatango	46	12hr 28mins	4.6	5.2
Thulus	74	14hr 25mins	5.6	5.7
Gyaling	96	16hr 11mins	5.1	6.1
Khachan	120	14hr 27mins	9.3	5.8
Chutuk	134	14hr 45mins	10.9	3.9
Kargil	149	15hr 49mins	11.4	3.3
Outlet	160	15hr 38mins	15.4	17.9

Figure 28 shows the map of flood inundation extent along with major settlements affected due to the flood for GLOF scenario 7. The inset images show flood depth and flood velocity near Kargil city along with GLOF affected settlements, roads, bridges and other infrastructure.

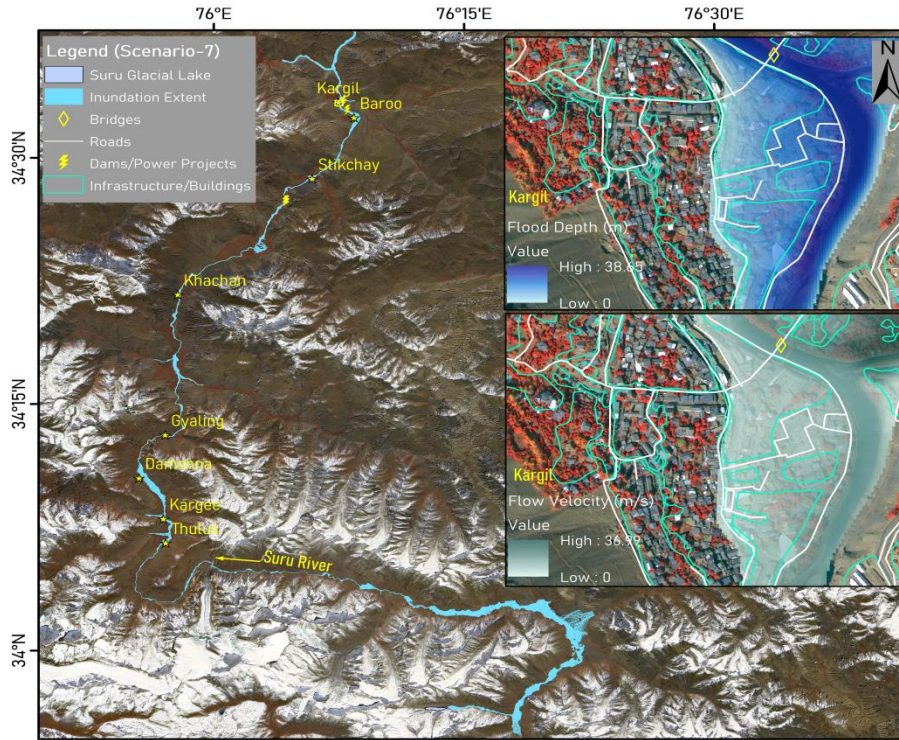


Figure 28: Map of Flood Inundation Extent for GLOF Scenario-7

Figure 29 shows the map of flood inundation extent along with major settlements affected due to the flood for GLOF scenario 8. The inset images show flood depth and flood velocity near Kargil city along with GLOF affected settlements, roads, bridges, and infrastructure.

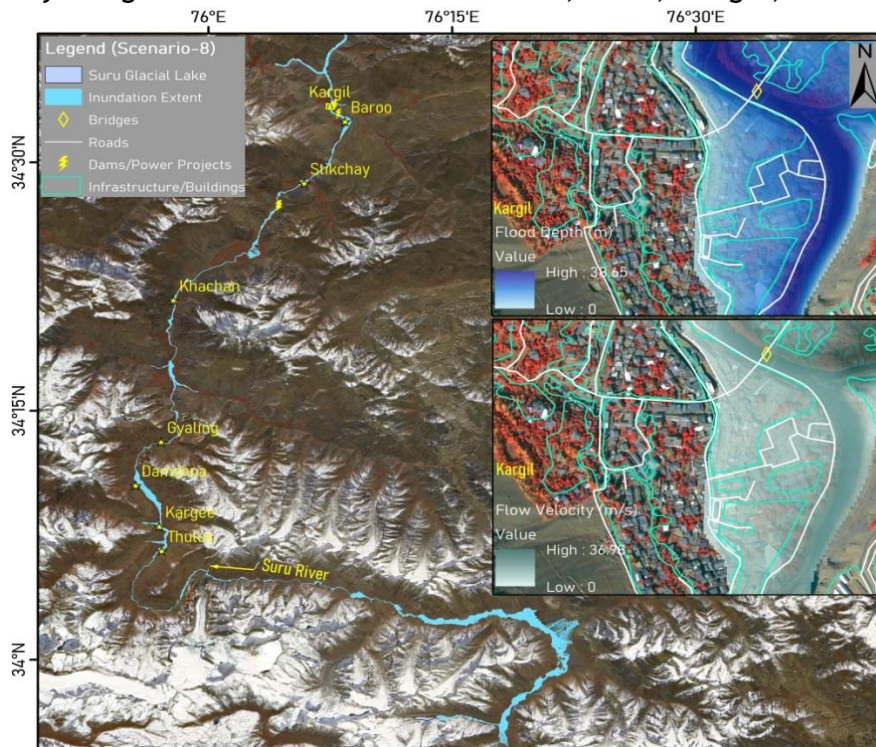


Figure 29: Map showing extent of inundation for Scenario-8

Table 15 provides number of settlements, extent of agriculture land, number of bridges and length of road network affected by scenarios 7 and 8. Table 16 provides names of settlements affected by scenarios 7 and 8.

Table 15: Infrastructure affected in GLOF Scenarios 7 and 8

Scenario	No. of Affected Settlements	Area of Agricultural Land Affected (ha)	No. of Bridges Affected	Length of Roads affected (km)	Inundated Area (ha)
Scenario-7	31	255.6	65	67.3	4,357
Scenario-8	31	254.4	65	66.7	4,345

Table 16: Details of Settlements affected in GLOF Scenarios 7 and 8

S. No.	Settlement Name	Distance from lake (km)
1	Thulus	74
2	Pranti	83.7
3	Kargee	84.9
4	Namsuru*	85
5	Khechoor	85.95
6	Youljok	88.12
7	Damshna	90.68
8	Gyaling*	96
9	Lalong	107
10	Sankoo*	107.5
11	Thas gam	108
12	Narambi	109.48
13	Nakpo Chu*	109.8
14	Faroona*	119.15
15	Khachan	120
16	Tambis	126.96
17	Kanoor	128.36

S. No.	Settlement Name	Distance from lake (km)
18	Zambakha	129.3
19	Sarchay*	131.2
20	Chutuk	134
21	Chey chey Thang	134.52
22	Lhungjhuk	137.6
23	Stikchay	138
24	Zamistang	143.48
25	Baroo	147.43
26	Kargil	149
27	Poyen	150
28	Shilikche	152.86
29	Hardas	155.06
30	Hunduman*	156.92
31	Chanigound	158.06

Note: * indicate few buildings, which are affected close to the river channel near the mentioned settlement.

Figure 30 shows close view of partly affected settlements and other infrastructure at Thulus (Left) and Kargil (Right) in both scenarios 7 and 8. The pink coloured flood inundation extent is the additional extent due to PMP over the inundation extent of scenarios 1 and 2 at the respective locations.

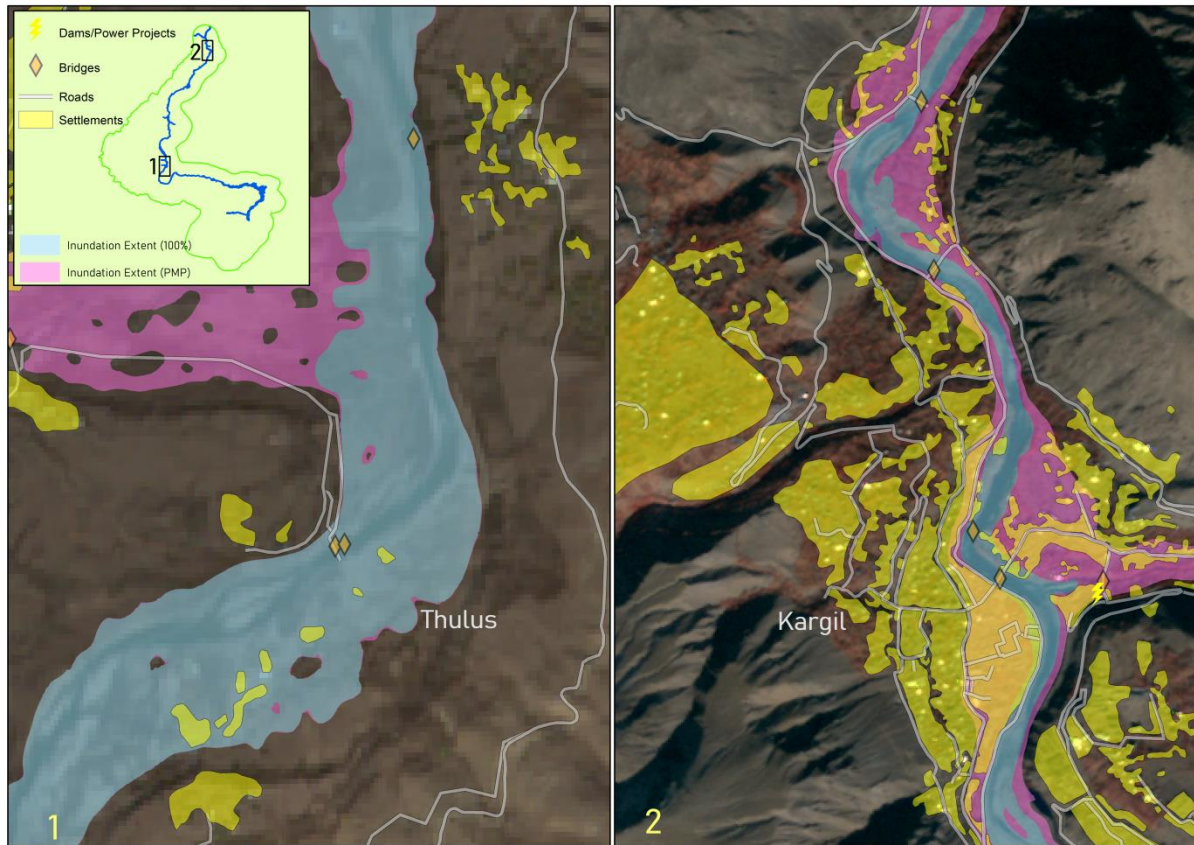


Figure 30: Map showing Close View of part of flood inundation for Scenarios - 7 and 8

5.2. GLOF Risk Assessment

The GLOF risk maps are generated for all the 8 scenarios as per procedure described under methodology section. The risk due to GLOF is categorised in Low, Moderate and High zones. An important point to note in the GAPHAZ (2017) technical document is that extreme scenarios like scenarios 7 and 8 are not assessed separately for hazard due to their extremely low frequency of occurrence. The inundation extents of these scenarios exceeding the maximum inundation extents of the other scenarios (1 and 2) are marked as zones of residual hazard. Therefore, the zones of residual risk are considered as the additional inundation zones caused due to PMP, and the risk for scenarios 7 and 8 are not assessed separately.

The results of GLOF scenarios of 1 and 2 (100% of lake volume release) and 7 and 8 (100% of lake volume release with PMP) are discussed here and results of other scenarios are provided in annexure 2. The additional risk due to PMP in scenarios 7 and 8 are shown as residual risk in the risk maps of scenarios 1 and 2 respectively.

5.2.1. GLOF Scenarios 1&7 (100% release& PMP)

The GLOF risk map for scenarios 1 and 7 are shown in figure 31. The GLOF risk map for scenario 1 consists of three categories of risk zones namely high, moderate and low whereas scenario 7 includes all three categories of scenario 1 and residual risk zone (residual risk is due to PMP). The total area under GLOF scenarios 1 and 7 are 3,260 ha and 4,357 ha respectively. The area under high, moderate and low risk zones of GLOF

scenario 1 are 647 ha, 1,775 ha and 837 ha respectively. The additional area under risk due to PMP is the residual risk zone extent of 1,097 ha. The area under the high risk zone will be most affected area with no time (less than 2 hours) for warning in case of GLOF event occurrence. Table 17 gives details of flood inundation area, number of settlements, agricultural land, number of bridges and length of road network affected exclusively under various categories of GLOF risk zones. As already mentioned in the previous section all the settlements are partly affected. The total number of settlements, agricultural land, bridges, and road length affected in scenario 1 are 13, 41.1 ha, 54 and 13.1 km respectively. Figures 32 and 33 show close view of affected infrastructure (settlements, bridges, road network, etc) and agriculture land by GLOF inundation extent near Kargil respectively. Annexure 3 provides close view of GLOF risk maps at important locations along the Suru river reach.

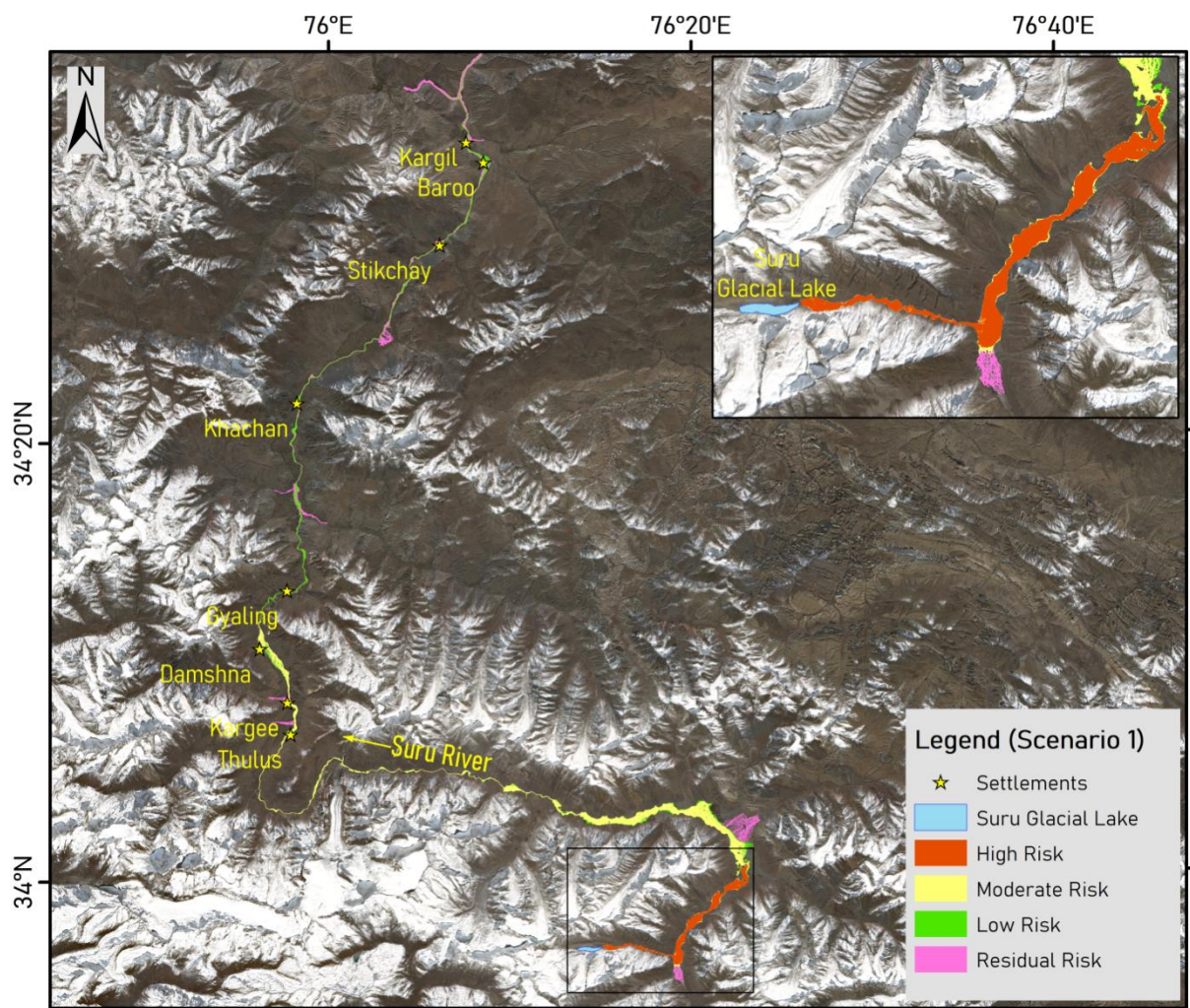


Figure 31: GLOF Risk Map for the Study Area (Scenario-1 and 7)

Table 17: Zone wise details of Infrastructure affected in GLOF Scenarios 1 and 7

Scenario	Risk Zone	Flood Inundated Area (ha)	No. of Settlements	Agricultural Land (ha)	No. of Bridges	Length of Road (km)
7	1	High	647	0	0	2.2
	Moderate	1,775	5	18.3	18	4
	Low	837	8	22.8	36	6.9
	Residual	1,097	18	214.5	11	54.2
Total		4,357	31	255.6	65	67.3

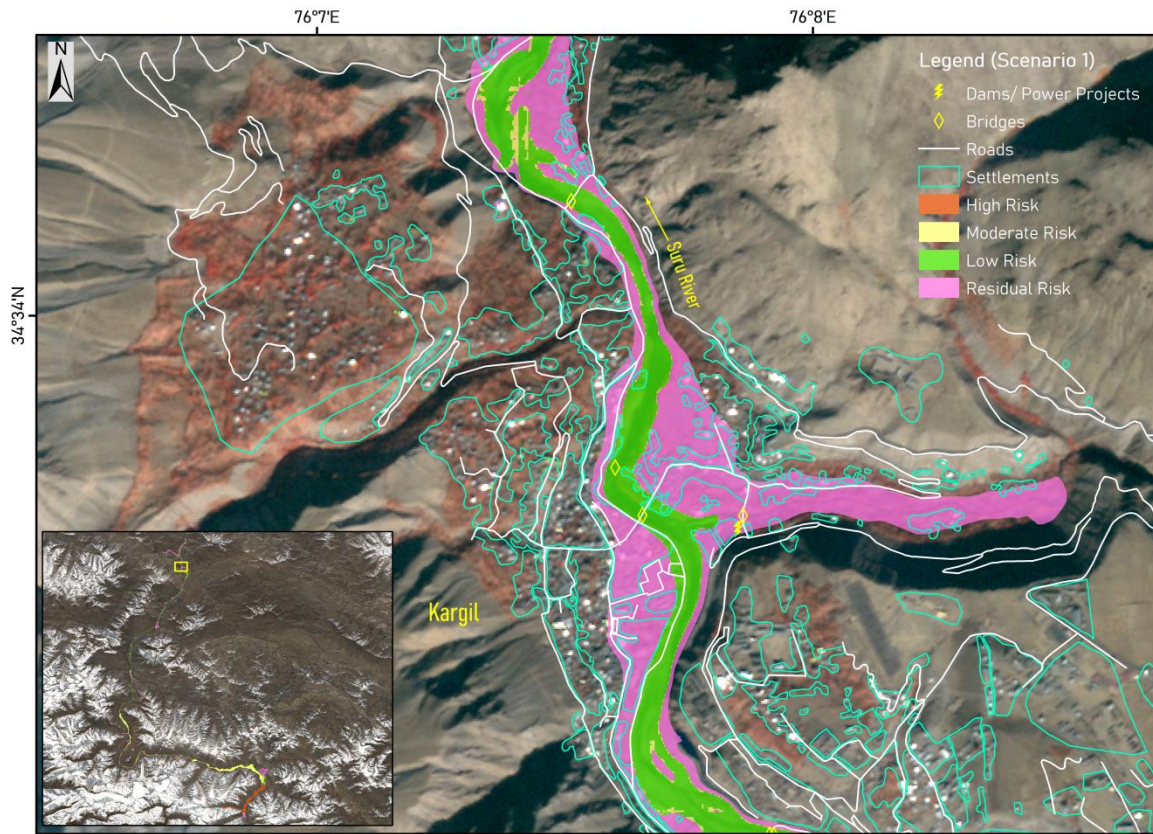


Figure 32: GLOF Risk Map showing Affected Infrastructure near Kargil (Scenario-1 and 7)

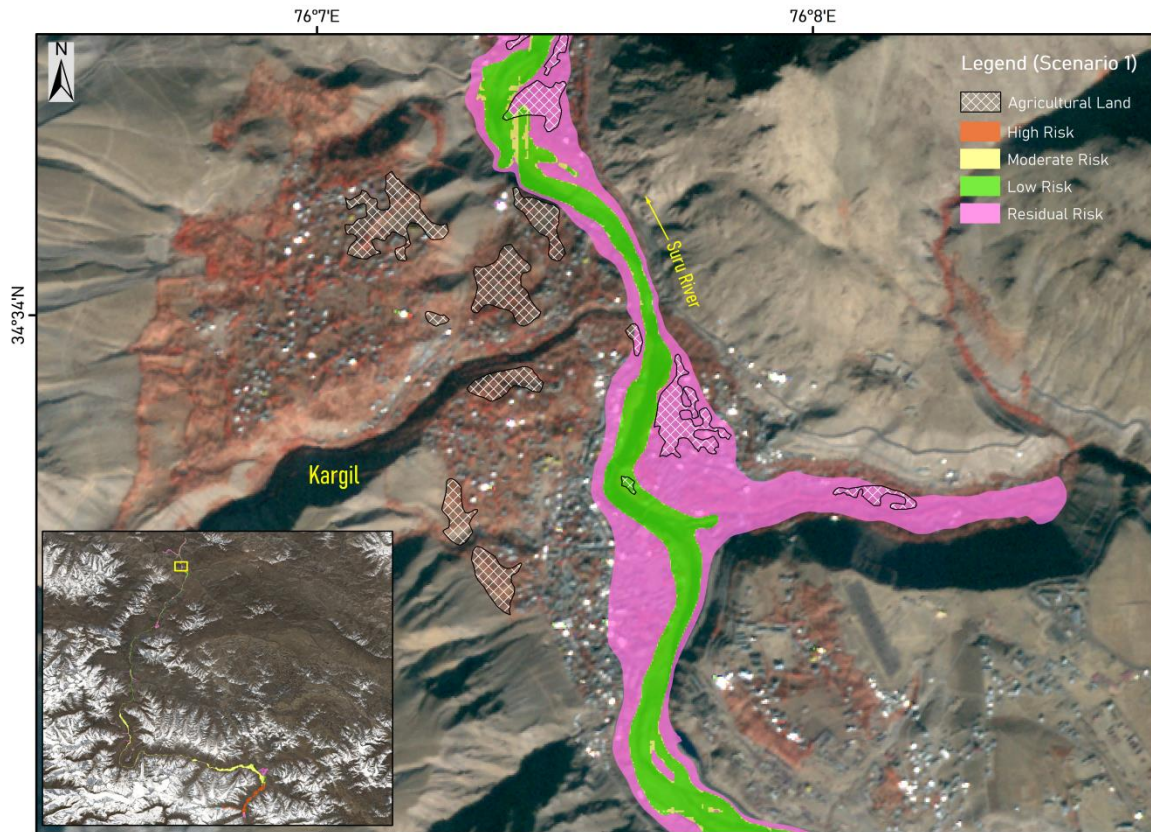


Figure 33: GLOF Risk Map showing Affected Agricultural Land near Kargil(Scenario-1 and 7)

5.2.2. GLOF Scenarios 2&8 (100% release & PMP)

The GLOF risk map for scenarios 2 and 8 are shown in Figure 34. The GLOF risk map for scenario 2 consists of three categories of risk zones namely high, moderate and low whereas scenario 8 includes all three categories of scenario 2 and residual risk zone (residual risk is due to PMP). The total area under GLOF scenarios 2 and 8 are 3,244 ha and 4,345 ha respectively. The area under high, moderate and low risk zones of GLOF scenario 2 are 655 ha, 1,749 ha and 840 ha respectively. The additional area under risk due to PMP is the residual risk zone extent of 1,101 ha. The area under the high risk zone will be most affected area with no time (less than 2 hours) for warning in case of GLOF event occurrence. Table 18 gives details of flood inundation area, number of settlements, agricultural land, number of bridges and length of road network affected exclusively under various categories of GLOF risk zones. As already mentioned in the previous section all the settlements are partly affected. The total number of settlements, agricultural land, bridges, and road length affected in scenario 2 are 13, 40.6 ha, 54 and 12.7 km respectively. Figures 35 and 36 show close view of affected infrastructure (settlements, bridges, road network, etc) and agriculture land by GLOF inundation extent near Kargil respectively.

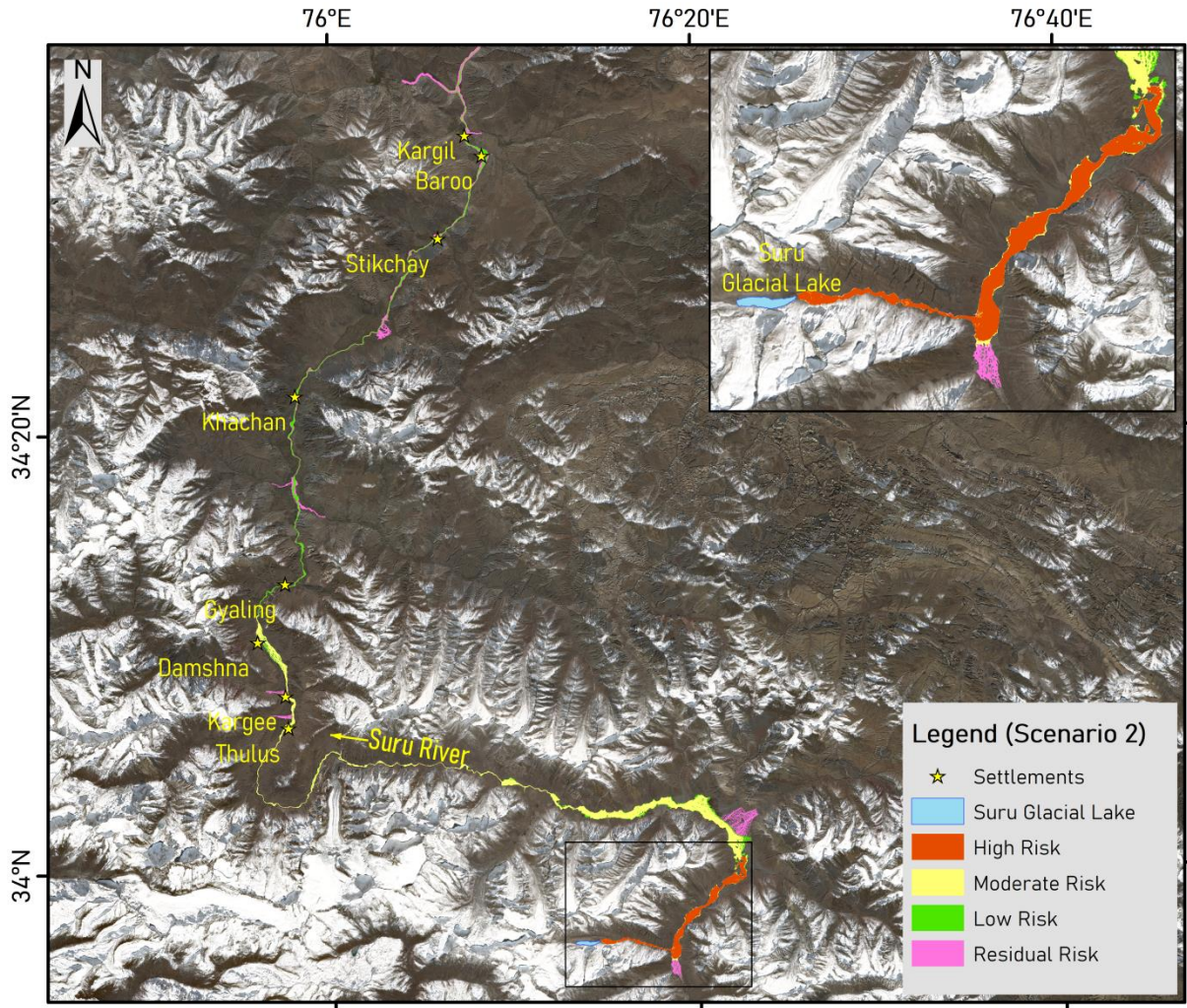


Figure 34: GLOF Risk Map for the Study Area (Scenario-2 and 8)

Table 18: Zone wise details of Infrastructure affected in GLOF Scenarios 2 and 8

Scenario	Risk Zone	Flood Inundated Area (ha)	No. of Settlements	Agricultural Land (ha)	No. of Bridges	Length of Roads (km)
8	High	655	0	0	0	2.1
	Moderate	1,749	5	18.1	17	3.9
	Low	840	8	22.5	37	6.7
	Residual	1,101	18	213.8	11	54
Total		4,345	31	254.4	65	66.7

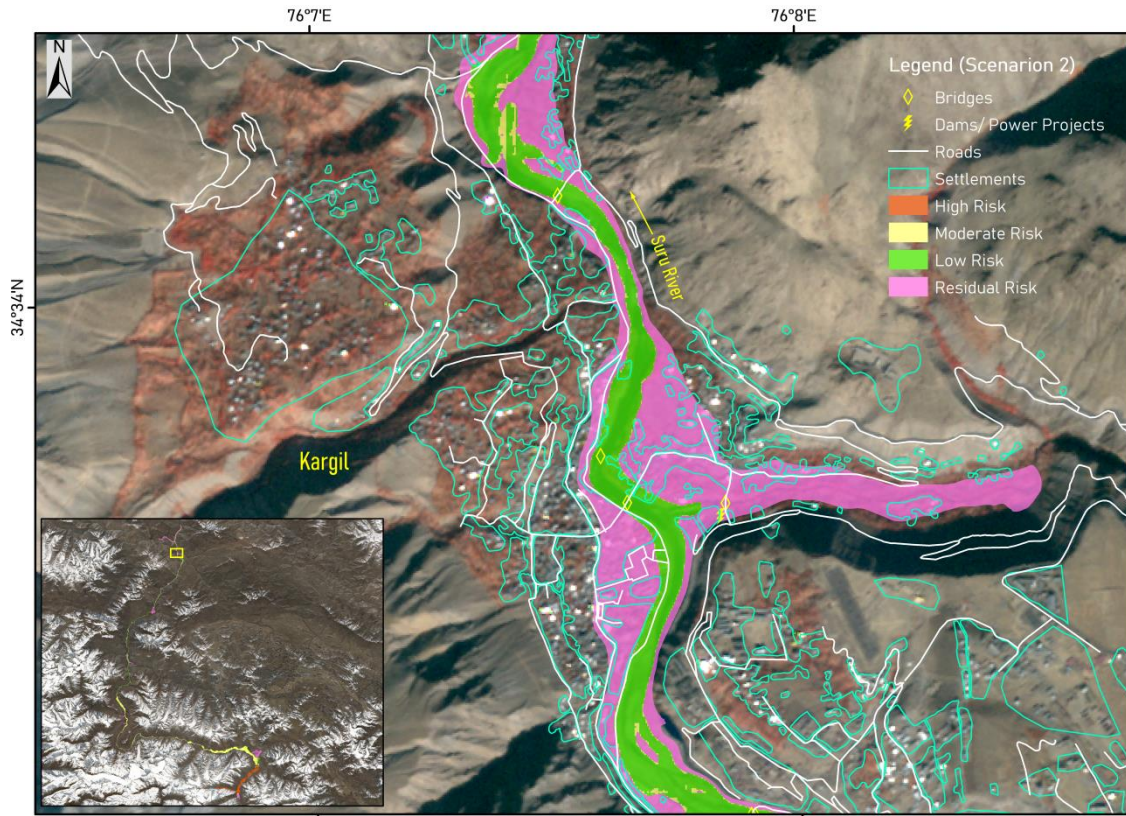


Figure 35: GLOF Risk Map showing Affected Infrastructure near Kargil (Scenario-2 and 8)

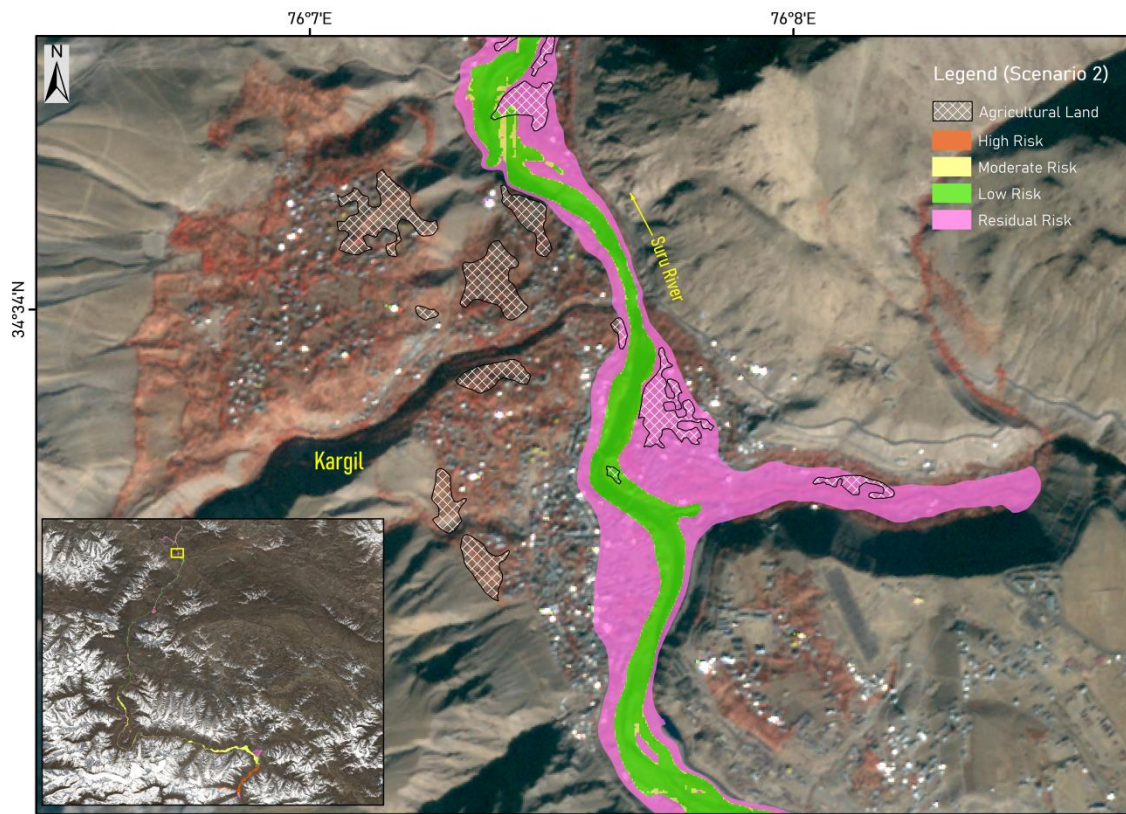


Figure 36: GLOF Risk Map showing Affected Agricultural Land near Kargil (Scenario-2 and 8)

5.3. Limitations

The limitations of this study are listed below:

1. Due to the lack of Suru glacial lake bathymetric information, the volume of the glacial lake was estimated using Huggel's formula, which may lead to different peak discharges and different flood inundation extents than the actual values.
2. Errors in the Digital Terrain Model, especially in the channel regions will affect the hydrodynamics of the flood wave. Although the major errors were corrected manually using cross sections in HEC-RAS, but few minor terrain errors may have still been neglected due to practical reasons.
3. Manning's n values adopted in the study are based on landcover data.
4. The moraine geometry was estimated using remotely sensed data, mainly from the Digital Terrain Model. Also, the condition of the moraine dam was assumed to be poor, which may not represent the actual case.
5. Dam breach parameters are estimated using Froehlich's regression equations rather than in-situ geotechnical observation-based data. There are uncertainties associated with regression-based dam breach parameters as described by Wahl (2004) and Sattar et al. (2021) with equations (xxii) and (xxiii):

$$LL = P \times (10^{-e-2Se}) \quad \text{..(xxii)}$$

$$UL = P \times (10^{-e+2Se}) \quad \text{..(xxiii)}$$

where, LL and UL are the lower and upper uncertainty limits of dam breach parameters respectively, P is the predicted dam breach parameter, e and 2Se are the mean prediction error and width of the uncertainty band respectively. For average breach width, e and 2Se are 0.01 and ± 0.39 , for breach formation time, e and 2Se are -0.22 and ± 0.64 , and for peak discharge, e and 2Se are -0.04 and ± 0.32 respectively.

6. The dam break modelling in HEC-RAS does not include estimation of water surface profiles along with sediment transport modelling.

6. Conclusions

National Remote Sensing Centre (NRSC), Hyderabad is carrying out hydrological studies using satellite data and geo-spatial techniques under National Hydrology Project. As part of this project, a detailed glacial lake inventory, prioritization of glacial lakes, Glacial Lake Outburst Flood (GLOF) inundation simulation and GLOF risk assessment for selected lakes are taken up for entire catchment of Indian Himalayan Rivers covering Indus, Ganga, and Brahmaputra River basins. Suru lake is one of the five prioritized glacial lakes identified in Indus river basin.

The Suru Glacial Lake is located at an elevation of 4,355 m a.m.s.l. in the Union Territory of Ladakh, India. A high resolution Digital Terrain Model of Tandem-X with a spatial resolution of 5 m was used in the study to simulate GLOF inundations of various scenarios. A series of 2D hydrodynamic dam-breach simulations in HEC-RAS software are developed for 8 different failure modes (overtopping and piping), different volumes of water released in case of a failure of the lake moraine (100%, 75%, and 50%), and under different weather conditions (clear-weather and Probable Maximum Precipitation). The worst-case scenario (scenario 7) was the one with a 100% discharge of the lake water under overtopping failure due to PMP occurrence over the catchment area of glacial lake. The GLOF peak hydrograph of 5,005 cumecs propagated from the moraine dam to the nearest settlement of Thulus in 7 hr46 minutes where it was estimated as 923 cumecs. The simulated GLOF peak of flood hydrographs for 100%, 75% and 50% of lake water releases scenarios (scenario 1, 3 and 5) yielded 871cumecs, 576 cumecs and 338 cumecs near settlement Thulus for overtopping failure. GLOF hazard maps are prepared by integrating flood depth and flood velocity for different scenarios.

High resolution satellite images (spatial resolution of 0.5 m) are used for mapping of settlements, agriculture lands, road network, road bridges, hydropower projects and other public utilities along the river reach for identifying the elements of exposure due to the various Suru lake GLOF scenarios. The total number of settlements, agricultural land, bridges, and road length inundated in the worst-case scenario (scenario 7) are 31, 255.6 ha, 65 and 67.3 km respectively. All the 31 settlements are partially flooded by the GLOF inundation extent.

GLOF risk maps are prepared by integrating flood hazard (flood depth X flood velocity) and flood wave arrival time, which was classified, into zones of high, medium, and low risk. The combination of flood hazard and flood wave arrival time for flood risk mapping presents a unique approach to flood risk assessment. Zones of high risk are defined as those regions where flood severity was either medium or high, and the flood wave arrival time was within 2 hours since the start of the breach. For this GLOF scenario there is no settlement affected in the high risk zone while Thulus village and nearby areas fall under the medium risk zone, and as we move further downstream, the risk reduces to low near Gyaling at distance of 96 km from lake for scenarios 1 & 2 and 7 & 8. The medium risk zone extends for a distance of 90 km along the river reach from lake covering the settlements of Thulus, Pranti, Kargee, Namsuru, and Damshna.

References

1. A. B. Shrestha, M. Eriksson, P. Mool, P. Ghimire, B. Mishra & N. R. Khanal (2010) Glacial lake outburst flood risk assessment of Sun Koshi basin, Nepal, *Geomatics, Natural Hazards and Risk*, 1:2, 157-169, DOI: 10.1080/19475701003668968
2. A. K. Sharma, S. K. Singh, A. V. Kulkarni, Ajai (2013). "Glacier Inventory in Indus, Ganga and Brahmaputra Basins of the Himalaya". *Natl. Acad. Sci. Lett.* (September-October 2013) 36(5):497-505. DOI 10.1007/s40009-013-0167-6
3. AEMI (2014). Australian Emergency Management Handbook Series, Technical Flood Risk Management Guideline: Flood Hazard, Australian Emergency Management Institute, Australian Government Attorney General's Department, Melbourne, Australia.
4. Aggarwal, S., Rai, S. C., Thakur, P. K., & Emmer, A. (2017). Inventory and recently increasing GLOF susceptibility of glacial lakes in Sikkim, Eastern Himalaya. *Geomorphology*, 295, 39-54. <https://doi.org/10.1016/j.geomorph.2017.06.014>
5. Ahmed, R.; Rawat, M.; Wani, G.F.; Ahmad, S.T.; Ahmed, P.; Jain, S.K.; Meraj, G.; Mir, R.A.; Rather, A.F.; Farooq, M. Glacial Lake Outburst Flood Hazard and Risk Assessment of Gangabal Lake in the Upper Jhelum Basin of Kashmir Himalaya Using Geospatial Technology and Hydrodynamic Modeling. *Remote Sens.* 2022, 14, 5957. <https://doi.org/10.3390/rs14235957>
6. Ahmed, R.; Wani, G.F.; Ahmad, S.T.; Mir, R.A.; Almazroui, M.; Jain, S.K.; Ahmed, P. Spatiotemporal dynamics of glacial lakes (1990-2018) in the Kashmir Himalayas, India using Remote Sensing and GIS. *Discov. Water* 2021, 1, 7.
7. Ahmed, Rayees, et al. "Glacial lake outburst flood hazard and risk assessment of Gangabal Lake in the Upper Jhelum Basin of Kashmir Himalaya using geospatial technology and hydrodynamic modeling." *Remote Sensing* 14.23 (2022): 5957.
8. Alean, J., 1985. Ice avalanches: some empirical information about their formation and reach. *J. Glaciol.* 31 (109), 324-333.
9. Allen, S. K., Zhang, G., Wang, W., Yao, T., & Bolch, T. (2019). Potentially dangerous glacial lakes across the Tibetan Plateau revealed using a large-scale automated assessment approach. *Science Bulletin*, 64(7), 435-445. <https://doi.org/10.1016/J.SCIB.2019.03.011>
10. Anaconda, P.I., Mackintosh, A., Norton, K., 2015. Reconstruction of a glacial lake outburst flood (GLOF) in the Engaño Valley, Chilean Patagonia: Lessons for GLOF risk management. *Sci. Total Environ.* 527, 1-11
11. Ankit Gupta, Ruhi Maheshwari, Nibedita Guru, Sweta, B. Simhadri Rao, P. Venkat Raju & V. Venkateshwar Rao (2021): Quantitative prioritization of potentially critical glacial Lakes in the Indus River basin using satellite derived parameters, *Geocarto International*, DOI:10.1080/10106049.2021.1975831
12. Ashim Sattar, Ajanta Goswami, Anil V. Kulkarni (2019). Hydrodynamic moraine-breach modeling and outburst flood routing - A hazard assessment of the South

- Lhonak lake, Sikkim. *Science of the Total Environment*, Vol. 668, pp. 362-378. <https://doi.org/10.1016/j.scitotenv.2019.02.388>
13. Ashim Sattar, Ajanta Goswami, Anil.V. Kulkarni, Adam Emmer, Umesh K. Haritashya, Simon Allen, Holger Frey, Christian Huggel, Future Glacial Lake Outburst Flood (GLOF) hazard of the South Lhonak Lake, Sikkim Himalaya, *Geomorphology*, Volume 388, 2021, 107783, ISSN 0169-555X, <https://doi.org/10.1016/j.geomorph.2021.107783>.
 14. Ataie-Ashthiani, B., Yavari-Ramshe, S., 2011. Numerical simulation of wave generated by landslide incidents in dam reservoirs. *Landslides* 8, 417-432.
 15. B. Simhadri Rao, Sweta, Ruhi Maheshwari, P. Venkat Raju, V. Venkateshwar Rao, Saksham Joshi, E Arivoli and Pamir Roy (2023). "Glacial Lake Atlas of Indian Himalayan River Basins". National Remote Sensing Centre, ISRO, Hyderabad, India, pp. 1-211.
 16. B. Wessel, "TanDEM-X Ground Segment - DEM Products Specification Document", EOC, DLR, Oberpfaffenhofen, Germany, Public Document TD-GS-PS-0021, Issue 3.2, 2018. [Online]. Available: <https://tandemx-science.dlr.de/>
 17. Barnard, P.L.; Owen, A.L.; Sharma, M.C.; Finkel, R.C. Natural and human-induced landsliding in the Garhwal Himalaya of northern India. *Geomorphology* 2001, 40, 21-35.
 18. Begam, S., Sen, D. & Dey, S. Moraine dam breach and glacial lake outburst flood generation by physical and numerical models. *J. Hydrol.* 563, 694-710 (2018)
 19. Bhambri, R. et al. Ice-dams, outburst floods, and movement heterogeneity of glaciers, Karakoram. *Glob. Planet. Change* 180, 100-116 (2019).
 20. Biscarini, C., 2010. Computational fluid dynamics modelling of landslide generated water waves. *Landslides* 7, 117-124.
 21. Brighenti S, Hotaling S, Finn DS, Fountain AG, Hayashi M, Herbst D, Millar CI (2021) Rock glaciers and related cold rocky landforms: overlooked climate refugia for mountain biodiversity. *Glob Change Biol* 27(8):1504-1517
 22. Caroline Taylor, Tom R. Robinson, Stuart Dunning, J. Rachel Carr & Matthew Westoby (2023). Glacial lake outburst floods threaten millions globally. *Nature Communications*, 14:487. <https://doi.org/10.1038/s41467-023-36033-x>
 23. Carrivick, J. L., & Tweed, F. S. (2016). A global assessment of the societal impacts of glacier outburst floods. *Global and Planetary Change*, 144, 1-16. <https://doi.org/10.1016/j.gloplacha.2016.07.001>
 24. Chow, V.T., 1959, Open Channel Hydraulics, McGraw-Hill Book Company, NY.
 25. Chowdhury, A.; Kroczeck, T.; De, S.K.; Vilímek, V.; Sharma, M.C.; Debnath, M. Glacial Lake Evolution (1962-2018) and Outburst Susceptibility of Gurudongmar Lake Complex in the Tista Basin, Sikkim Himalaya (India). *Water* 2021, 13, 3565. <https://doi.org/10.3390/w13243565>
 26. Clague, J.J., Evans, S.C., 2000. A review of catastrophic drainage of moraine-dammed lakes in British Columbia. *Quat. Sci. Rev.* 19 (17-18), 1763-1783.

27. Cogley, J. G. (2016). Glacier shrinkage across High Mountain Asia. *Annals of Glaciology*, 57(71), 41-49. <https://doi.org/10.3189/2016AoG71A040>
28. Cogley, J.G., Hock, R., Rasmussen, L.A., Arendt, A.A., Bauder, A., Braithwaite, R.J., Jansson, P., Kaser, G., Möller, M., Nicholson L., Zemp, M. (2011). “Glossary of Glacier Mass Balance and Related Terms”, IHP-VII Technical Documents in Hydrology No. 86, IACS Contribution No. 2, UNESCO-IHP, Paris.
29. Compendium of Task Force Report on NDMA Guidelines Management of Glacial Lake Outburst Floods (GLOFs) A Publication of the National Disaster Management Authority, Government of India. October 2020, New Delhi.
30. Cook, K. L., Andermann, C., Gimbert, F., Adhikari, B. R. & Hovius, N. Glacial lake outburst floods as drivers of fluvial erosion in the Himalaya. *Science* 362, 53-57 (2018).
31. CWC, Guidelines for Mapping Flood Risks Associated with Dams (CWC, 2018)
32. D.M. Hershfield, Method for estimating probable maximum precipitation, *J. Am. Waterworks Assoc.* 57 (1965) 965-972.
33. Das S, Kar NS, Bandyopadhyay S (2015) Glacial lake outburst flood at Kedarnath, Indian Himalaya: a study using digital elevation models and satellite images. *Nat Hazards*. doi:10.1007/s11069-015-1629-6
34. Dasallas, L.; Kim, Y.; An, H. Case Study of HEC-RAS 1D-2D Coupling Simulation: 2002 Baeksan Flood Event in Korea. *Water* 2019, 11, 2048.
35. Dubey, S., & Goyal, M. K. (2020). Glacial Lake Outburst Flood Hazard, Downstream Impact, and Risk Over the Indian Himalayas. *Water Resources Research*, 56, e2019WR026533. <https://doi.org/10.1029/2019WR026533>
36. Emmer, A. & Cochachin, A. The causes and mechanisms of moraine-dammed lake failures in the cordillera blanca, North American Cordillera, and Himalayas. *Acta Univ. Carol., Geogr.* 48, 5-15 (2013).
37. Escuder-Bueno, I., Castillo-Rodriguez, J. T., Zechner, S., Jobstl, C., Perales-Momparler, S., Petaccia, G., 2012. “A quantitative flood risk analysis methodology for urban areas with integration of social research data”. *Nat. Hazards Earth Syst. Sci.*, 12, pp. 2843-2863
38. Faeh, R., Mueller, R., Rousselot, P., Veprek, R., Vetsch, D., Volz, C., Vonwiller, L., Farshi, D., 2012. BASEMENT – Basic Simulation Environment for Computation of Environmental Flow and Natural Hazard Simulation. VAW Mitteilung, ETH Zurich
39. Falappi, S., Gallati, M., 2007. SPH simulation of water waves generated by granular landslides. *Proceedings, 32nd Congress of International Association of Hydrological Resources, Venice, Italy* 933, pp. 1-10.
40. Farinotti, D., Round, V., Huss, M., Compagno, L. & Zekollari, H. Large hydropower and water-storage potential in future glacier-free basins. *Nature* 575, 341-344 (2019).
41. Fread, D.L., 1982. DAMBRK: The NWS Dam-break Flood Forecasting Model. U.S. National Weather Service, Hydrologic Research Laboratory, Silver Spring, MD.

42. Froehlich, D.C., 1995a. Peak Outflow from Breached Embankment Dam. *J. Water Resour. Plan.Manag.*121 (1), 90-97.
43. Froehlich, D.C., 1995b. “Embankment Dam Breach Parameters Revisited,” *Water Resources Engineering, Proceedings of the 1995 ASCE Conference on Water Resources Engineering, San Antonio, Texas, August 14-18, 1995*, p. 887-891. American Society of Civil Engineers, Reston, VA
44. GAPHAZ 2017: Assessment of Glacier and Permafrost Hazards in Mountain Regions - Technical Guidance Document. Prepared by Allen, S., Frey, H., Huggel, C. et al. Standing Group on Glacier and Permafrost Hazards in Mountains (GAPHAZ) of the International Association of Cryospheric Sciences (IACS) and the International Permafrost Association (IPA). Zurich, Switzerland / Lima, Peru, 72 pp.
45. Gilany, N.; Iqbal, J. Geospatial analysis and simulation of glacial lake outburst flood hazard in Shyok Basin of Pakistan. *Environ. Earth Sci.* 2020, 79, 139.
46. Graham W. J., 1999. “A Procedure for Estimating Loss of Life Caused by Dam Failure”. DSO-99-06.pp 35-39.
47. Guha-Sapir D, Below R, Hoyois P (2014) EM-DAT: International Disaster Database. UniversitéCatholique de Louvain, Brussels, Belgium.www.emdat.be. Accessed 20 Nov 2014
48. Guoqing Zhang, Tandong Yao, HongjieXie, Weicai Wang, Wei Yang (2015). “An inventory of glacial lakes in the Third Pole region and their changes in response to global warming”. *Global and Planetary Change*, Vol. 131, pp. 148-157. <http://dx.doi.org/10.1016/j.gloplacha.2015.05.013>
49. GuoxiongZheng, Simon Keith Allen, AnmingBao, Juan Antonio Ballesteros-Cánovas, Matthias Hus, Guoqing Zhang, Junli Li, Ye Yuan, Liangliang Jiang, Tao Yu, Wenfeng Chen and Markus Stoffel (2021). “Increasing risk of glacial lake outburst floods from future Third Pole deglaciation”. *Nature Climate Change*, Vol. 11, pp. 411-417.
50. Gupta, A., Guru, N., Maheshwari, R., Sweta, Rao, B.S. (2019). “Inventory of Glacial Lakes in Gilgit Subbasin of Indus Basin using high resolution satellite imagery”. *Journal of Indian Cartographer*, vol. 38, pp. 212-219. <https://incaindia.org/cartographic-volume/>
51. Guru, N, Gupta, A., Sweta, Maheshwari, R., Rao, B.S., Raju, P.V., Rao, V.V. (2019). “Identification of potential lakes susceptible to GLOF in Jhelum Subbasin of Indus Basin”. In: Naik GM et al., (Eds.), *Hydraulics, Water Resources, Coastal and Environmental Engineering*, Ch 155, pp. 1452-1462, BS Publications, Hyderabad, India.
52. Haerberli W, Huggel C, Paul F, Zemp M. (2013). “Glacial responses to climate change”. In: Shroder JF, editor. *Treatise on geomorphology*, vol. 13, pp. 152-75.
53. Haerberli, W. et al. New lakes in deglaciating high-mountain regions – opportunities and risks. *Climatic Change* 139, 201-214 (2016).
54. HEC-RAS Technical Document-39 (2014). “Using HEC-RAS for Dam Break Studies”, USACE, Hydrologic Engineering Center.

55. Heller, V., Hager, W.H., Minor, H.-E., 2008a. Scale effects in subaerial landslide generated impulse waves. *Exp. Fluids* 44, 691-703.
56. Hewitt, K. & Liu, J. Ice-dammed lakes and outburst floods, Karakoram Himalaya: historical perspectives on emerging threats. *Phys. Geogr.* 31, 528-551 (2010).
57. Huggel, C., Kääh, A., Haerberli, W., Teysseire, P., Paul, F. (2002). "Remote sensing based assessment of hazards from glacier lake outbursts: a case study in the Swiss Alps". *Canadian Geotechnical Journal*, vol. 39(2), pp. 316-330. <https://doi.org/10.1139/t01-099>
58. Huili Chen, Jiaheng Zhao, Qihua Liang, Sudan Bikash Maharjan, Sharad Prasad Joshi (2021). Assessing the potential impact of glacial lake outburst floods on individual objects using a high-performance hydrodynamic model and open-source data. *Science of Total Environment*. Vol. 806. <https://doi.org/10.1016/j.scitotenv.2021.151289>
59. Huizinga, J., Moel, H. de, Szewczyk, W. (2017). Global flood depth-damage functions. Methodology and the database with guidelines. EUR 28552 EN. doi: 10.2760/16510
60. Huss M, Bookhagen B, Huggel C, Jacobsen D, Bradley RS, Clague JJ, Winder M (2017) Toward mountains without permanent snow and ice. *Earths Future* 5(5):418-435
61. Hussain A, Nasab N, Bano D, Karim D, Anwar W, Hussain K, Uddin N (2020) Glacier lake outburst flood modeling of Khurdopin glacier lake using HEC-RAS and GIS. In: Селевые потоки: катастрофы, риск, прогноз, защита. pp 208-220
62. ICIMOD (2011). "Glacial lakes and glacial lake outburst floods in Nepal. Kathmandu: ICIMOD.
63. ICIMOD.(2022). Land cover of HKH region [Data set].ICIMOD. <https://doi.org/10.26066/RDS.1972511>
64. IPCC, 2014. Climate Change 2014: Impacts, Adaptation, and Vulnerability. Part A: Global and Sectoral Aspects. In: Field, C.B., Barros, V.R., Dokken, D.J., Mach, K.J., Mastrandrea, M.D., Bilir, T.E., Chatterjee, M., Ebi, K.L., Estrada, Y.O., Genova, R.C., Girma, B., Kissel, E.S., Levy, A.N., MacCracken, S., Mastrandrea, P.R., White, L.L. (Eds.), Contribution of Working Group II to the Fifth Assessment Report of the Intergovernmental Panel on Climate Change. Cambridge University Press, Cambridge, United Kingdom and New York, NY, USA (1132 pp.).
65. Ives, J. D., Shrestha, R. B., & Mool, P. K. (2010). Formation of glacial lakes in the Hindu Kush-Himalayas and GLOF risk assessment. ICIMOD Kathmandu.
66. Kang, S.C., Xu, Y.W., You, Q.L., Flügel, W., Pepin, N., Yao, T., 2010. Review of climate and cryospheric change in the Tibetan Plateau. *Environ. Res. Lett.* 5, 015101.
67. Kaushik, S., Rafiq, M., Joshi, P. K., & Singh, T. (2020). Examining the glacial lake dynamics in a warming climate and GLOF modelling in parts of Chandra basin, Himachal Pradesh, India. *Science of the Total Environment*, 714, 136455. <https://doi.org/10.1016/J.SCITOTENV.2019.136455>

68. King, O., Dehecq, A., Quincey, D., and Carrivick, J. (2018). Contrasting Geometric and Dynamic Evolution of lake and Land-Terminating Glaciers in the central Himalaya. *Glob. Planet. Change* 167, 46-60. doi:10.1016/j.gloplacha.2018.05.006
69. Klimeš J, Novotný J, Novotná I, de Urries BJ, Vilímek V, Emmer A, Frey H (2016) Landslides in moraines as triggers of glacial lake outburst floods: example from Palcacocha Lake (Cordillera Blanca, Peru). *Landslides* 13(6):1461-1477
70. Kougkoulos I, Cook SJ, Edwards LA, Clarke LJ, Symeonakis E, Dortch JM, Nesbitt K (2018) Modelling glacial lake outburst flood impacts in the Bolivian Andes. *Nat Hazards* 94(3):1415-1438
71. Kraaijenbrink PDA, Bierkens MFP, Lutz AF, Immerzeel WW (2017). "Impact of a global temperature rise of 1.5 degrees Celsius on Asia's glaciers". *Nature*. 549(7671):257-60. <https://doi.org/10.1038/nature23878>
72. L'Heureux, J.S., Glimsdal, S., Longva, O., Hansen, L., Harbitz, C.B., 2011. The 1888 shoreline landslide and tsunami in Trondheimsfjorden, central Norway. *Mar. Geophys. Res.* 32, 313-329.
73. Li, Y., A. Ahuja, and J. E. Padgett. 2012. "Review of methods to assess, design for, and mitigate multiple hazards." *J. Perform. Constr. Facil.* 26 (1): 104-117. [https://doi.org/10.1061/\(ASCE\)CF.1943-5509.0000279](https://doi.org/10.1061/(ASCE)CF.1943-5509.0000279).
74. Linsbauer, A., Frey, H., Haerberli, W., Machguth, H., Azam, M. F., & Allen, S. (2016). Modelling glacier-bed overdeepenings and possible future lakes for the glaciers in the Himalaya–Karakoram region. *Annals of Glaciology*, 57(71), 119-130.
75. M.J. Westoby, N.F. Glasser, J. Brasington, M.J. Hambrey, D.J. Quincey, J.M. Reynolds (2014). "Modelling outburst floods from moraine-dammed glacial lakes". *Earth-Science Reviews*, Vol. 134, pp. 137-159. <http://dx.doi.org/10.1016/j.earscirev.2014.03.009>
76. MacDonald, Thomas C., and Langridge-Monopolis, J, 1984. Breaching characteristics of dam failures. *ASCE Journal of Hydraulic Engineering*, Vol. 110, No. 5, May 1984, pages 567 - 586
77. Majeed, U., Rashid, I., Sattar, A., Allen, S., Stoffel, M., Nüsser, M., Schmidt, S., 2021. Recession of Gya Glacier and the 2014 glacial lake outburst flood in the Trans-Himalayan region of Ladakh, India. *Sci. Total Environ.* 756, 144008
78. Manish Rawat, Rayees Ahmed, Sanjay Kumar Jain, Anil Kumar Lohani, Gopinadh Rongali, Kailash Chandra Tiwari (2022). Glacier-glacial lake changes and modeling glacial lake outburst flood in Upper Ganga Basin, India. *Modeling Earth Systems and Environment*. <https://doi.org/10.1007/s40808-022-01512-5>
79. Martha TR, Roy P, Govindharaj KB, Kumar KV, Diwakar PG, Dadhwal VK (2014) Landslides triggered by the June 2013 extreme rainfall event in parts of Uttarakhand state. *India Landslides*. doi:10.1007/s10346-014-0540-7
80. Maurer, J. M., Schaefer, J. M., Rupper, S., & Corley, A. (2019). Acceleration of ice loss across the Himalayas over the past 40 years. *Science Advances*, 5(6), eaav7266. <https://doi.org/10.1126/sciadv.aav7266>

81. Mohanty L., Maiti S., (2021). Probability of glacial lake outburst flooding in the Himalaya. *Resources, Environment and Sustainability*, Vol. 5, 100031. <https://doi.org/10.1016/j.resenv.2021.100031>
82. Mool PK (2005) Monitoring of glaciers and glacial lakes from 1970 s to 2000 in Poiqu Basin, Tibet Autonomous Region, PR China. Unpublished report prepared by ICIMOD, Kathmandu, Nepal, and CAREERI, Gansu, China
83. Morris, M.W., Hanson, G., Hassan, M., 2008. Improving the accuracy of breach modelling: why are we not progressing faster? *J. Flood Risk Manag.* 1, 150-161.
84. Nie, Y. et al. An inventory of historical glacial lake outburst floods in the Himalayas based on remote sensing observations and geomorphological analysis. *Geomorphology* 308, 91-106 (2018).
85. Otto, J.C., 2019. Proglacial Lakes in High Mountain Environments. *Geomorphology of Proglacial Systems, Geography of the Physical Environment* 231-247. https://doi.org/10.1007/978-3-319-94184-4_14.
86. Owen, L.A.; Sharma, M.C.; Bigwood, R. Landscape modification and geomorphological consequences of the 20th October 1991 earthquake and the July-August 1992 monsoon in the Garhwal Himalaya. *Zeitschrift für Geomorphol.* 1996, 103, 359-372.
87. Pandey, P., Banerjee, D., Ali, S.N. et al. Simulation and risk assessment of a possible glacial lake outburst flood (GLOF) in the Bhilangna Valley, central Himalaya, India. *J Earth Syst Sci* 131, 184 (2022). <https://doi.org/10.1007/s12040-022-01940-y>
88. Peduzzi, P., 2010. Landslides and vegetation cover in the 2005 North Pakistan earthquake: a GIS and statistical quantitative approach. *Nat. Hazards Earth Syst. Sci.* 10 (4), 623-640.
89. Prakash, C., & Nagarajan, R. (2017). Outburst susceptibility assessment of moraine-dammed lakes in Western Himalaya using an analytic hierarchy process. *Earth Surface Processes and Landforms*, 42(14), 2306-2321. <https://doi.org/10.1002/ESP.4185>
90. Pratap, B., Dobhal, D.P., Bhambri, R., Mehta, M., Tewari, V.C. (2016). "Four decades of glacier mass balance observations in the Indian Himalaya". *Regional Environmental Change*, vol. 16(3), pp. 643-658. <https://doi.org/10.1007/s10113-015-0791-4>
91. Psomiadis, E.; Tomanis, L.; Kavvadias, A.; Soulis, K.X.; Charizopoulos, N.; Michas, S. Potential Dam Breach Analysis and FloodWave Risk Assessment Using HEC-RAS and Remote Sensing Data: A Multicriteria Approach. *Water* 2021, 13, 364. <https://doi.org/10.3390/w13030364>
92. Raj, K. B. G., Remya, S. N., & Kumar, K. V. (2013). Remote sensing-based hazard assessment of glacial lakes in Sikkim Himalaya. *Current Science*, 359-364.
93. Rawat M., Ahmed R., Jain S. K., Lohani A. K., Rongali G., Tiwari K. C., (2022). Glacier-glacial lake changes and modeling glacial lake outburst flood in Upper

- Ganga Basin, India. *Modeling Earth Systems and Environment*.
<https://doi.org/10.1007/s40808-022-01512-5>
94. Rawat, Manish, et al. "Glacial lake outburst flood risk assessment using remote sensing and hydrodynamic modeling: a case study of Satluj basin, Western Himalayas, India." *Environmental Science and Pollution Research* 30.14 (2023): 41591-41608.
 95. Rounce, D. R., McKinney, D.C., Lala, J.M., Byers, A. C. & Watson, C. S. A new remote hazard and risk assessment framework for glacial lakes in the Nepal Himalaya. *Hydrol. Earth Syst. Sci.* 20, 3455-3475 (2016).
 96. S. K. Allen | P. Rastner | M. Arora | C. Huggel | M. Stoffel (2015). Lake outburst and debris flow disaster at Kedarnath, June 2013: hydrometeorological triggering and topographic predisposition. *Landslides* (2016) 13:1479-1491 DOI 10.1007/s10346-015-0584-3
 97. Saint-Venant BD. 1871. Theory of unsteady flow, with application to river floods and to propagation of tides in river channels. *French Acad Sci.* 73:148-154, 237-240.
 98. Sakai, A., & Fujita, K. (2017). Contrasting glacier responses to recent climate change in high-mountain Asia. *Scientific Reports*, 7(1), 13,717.
<https://doi.org/10.1038/s41598-017-14256-5>
 99. Sati SP, Gahalaut VK (2013) The fury of the floods in the north-west Himalayan region: the Kedarnath tragedy. *Geomatics, Nat Hazards Risk* 4:193-201
 100. Sattar, A., Allen, S., Mergili, M., Haerberli, W., Frey, H., Kulkarni, A. V., et al. (2023). Modeling potential glacial lake outburst flood process chains and effects from artificial lake-level lowering at Gepang Gath Lake, Indian Himalaya. *Journal of Geophysical Research: Earth Surface*, 128, e2022JF006826.
<https://doi.org/10.1029/2022JF006826>
 101. Sattar, A., Goswami, A., & Kulkarni, A. V. (2019). Hydrodynamic moraine-breach modeling and outburst flood routing—A hazard assessment of the South Lhonak lake, Sikkim. *Science of the Total Environment*, 668, 362-378.
<https://doi.org/10.1016/j.scitotenv.2019.02.388>
 102. Schmidt, S.; Nüsser, M.; Baghel, R.; Dame, J. Cryosphere hazards in Ladakh: The 2014 Gya glacial lake outburst flood and its implications for risk assessment. *Nat. Hazards* 2020, 104, 2071-2095
 103. Singh, V.P., 1996. *Dam Breach Modelling Technology*. Kluwer Academic Publishers, Dordrecht, Boston, London (242 pp.).
 104. Soil Conservation Service (1971). *National Engineering Handbook, Section 4: Hydrology*. USDA, Springfield, VA.
 105. Sonam Rinzin, Guoqing Zhang, Ashim Sattar, Sonam Wangchuk, Simon K. Allen, Stuart Dunning, MengerPeng, GLOF hazard, exposure, vulnerability, and risk assessment of potentially dangerous glacial lakes in the Bhutan Himalaya, *Journal of Hydrology*, Volume 619, 2023, 129311, ISSN 0022-1694,
<https://doi.org/10.1016/j.jhydrol.2023.129311>.

106. Song, C., Sheng, Y., Wang, J., Ke, L., Madson, A., Nie, Y., 2017. Heterogeneous glacial lake changes and links of lake expansions to the rapid thinning of adjacent glacier termini in the Himalayas. *Geomorphology* 280, 30-38.
107. Sunwi Maskey, Rijan Bhakta Kayastha, Rakesh Kayastha (2020). "Glacial Lakes Outburst Floods (GLOFs) modelling of Thulagi and Lower Barun Glacial Lakes of Nepalese Himalaya". *Progress in Disaster Science*, pp. 100-106. <http://dx.doi.org/10.1016/j.pdisas.2020.100106>
108. Tawde, S. A., Kulkarni, A. V., & Bala, G. (2017). An estimate of glacier mass balance for the Chandra basin, western Himalaya, for the period 1984-2012. *Annals of Glaciology*, 58(75pt2), 99-109. <https://doi.org/10.1017/aog.2017.18>
109. Teng, J.; Jakeman, A.J.; Vaze, J.; Croke, B.F.W.; Dutta, D.; Kim, S. Flood inundation modelling: A review of methods, recent advances and uncertainty analysis. *Environ. Model. Softw.* 2017, 90, 201-216.
110. Tsutaki, S., Fujita, K., Nuimura, T., Sakai, A., Sugiyama, S., Komori, J., et al. (2019). Contrasting Thinning Patterns between lake- and Land-Terminating Glaciers in the Bhutanese Himalaya. *The Cryosphere* 13 (10), 2733-2750. doi:10.5194/tc-13-2733-2019
111. V. Te Chow, A general formula for hydrologic frequency analysis, *Eos, Trans. Am. Geophys. Union* 32 (1951) 231-237, doi:10.1029/TR032i002p00231.
112. Veh, G., Korup, O., Walz, A., 2020. Hazard from himalayan glacier lake outburst floods. *Proc. Natl. Acad. Sci.* 117 (2), 907-912.
113. Wahl, T.L., 1998. Prediction of Embankment Dam Breach Parameters - A Literature Review and Needs Assessment. U.S. Dept. of the Interior, Bureau of Reclamation, Dam Safety Report DSO-98-004, Denver, CO.
114. Wahl, T.L., 2004. Uncertainty of predictions for Embankment Dam breach Parameters. *J. Hydraul. Eng.* 130, 389-397
115. Walder, J.S., Watts, P., Sorensen, O.E., Janssen, K., 2003. Tsunamis generated by subaerial mass flows. *J. Geophys. Res. Solid Earth* 108 (B5).
116. Wang, W., Gao, Y., Anaconda, P.I., Lei, Y., Xiang, Y., Zhang, G., Li, S., Lu, A., 2018. Integrated hazard assessment of Cirenmaco glacial lake in Zhangzangbo valley, Central Himalayas. *Geomorphology* 306, 292-305
117. Wang, W., Yao, T., Gao, Y., Yang, X., Kattel, D.B., 2011. A first-order method to identify potentially dangerous glacial lakes in a region of the southeastern Tibetan Plateau. *Mt. Res. Dev.* 31 (2), 122-130
118. Washakh, R.M.A.; Chen, N.; Wang, T.; Almas, S.; Ahmad, S.R.; Rahman, M. GLOF Risk Assessment Model in the Himalayas: A Case Study of a Hydropower Project in the Upper Arun River. *Water* 2019, 11, 1839. <https://doi.org/10.3390/w11091839>
119. Wei, G., Kirby, J.T., Grilli, S.T., Subramanya, R., 1995. A fully nonlinear Boussinesq model for free surface waves, part 1: highly nonlinear unsteady waves. *J. Fluid Mech.* 294, 71-92.

120. Westoby, M.J., Glasser, N.F., Brasington, J., Hambrey, M.J., Quincey, D.J., Reynolds, J.M., 2014. Modelling outburst floods from moraine-dammed glacial lakes. *Earth Sci. Rev.* 134, 137-159.
121. Worni, R., Huggel, C., & Stoffel, M. (2013). Glacial lakes in the Indian Himalayas – From an area-wide glacial lake inventory to on-site and modeling based risk assessment of critical glacial lakes. *Science of the Total Environment*, 468-469, S71-S84. <https://doi.org/10.1016/J.SCITOTENV.2012.11.043>
122. Worni, R., Huggel, C., J. Clague J., Schaub Y., & Stoffel, M. (2014). Coupling glacial lake impact, dam breach, and flood processes: A modeling perspective, *Geomorphology* 224, <http://dx.doi.org/10.1016/j.geomorph.2014.06.031>
123. Worni, R., Huggel, C., Stoffel, M., 2012. Glacial lakes in the Indian Himalayas— from an area-wide glacial lake inventory to on-site and modeling based risk assessment of critical glacial lakes. *Sci. Total Environ.* 468, S71-S84.
124. WRL, 2014. Water Resources Laboratory. “Flood Hazard Technical Report”, University of New South Wales, Australia.
125. Xu, Y. and Zhang, L. M., 2009. Breaching parameters for earth and rockfill dams. *ASCE Journal of Geotechnical and Geoenvironmental Engineering*, Volume 135, No. 12, pages 1957-1970, December 2009.
126. Yong Nie, QiaoLiua, Jida Wang, Yili Zhang, Yongwei Sheng, Shiyin Liu (2018). “An inventory of historical glacial lake outburst floods in the Himalayas based on remote sensing observations and geomorphological analysis”. *Geomorphology*, Vol. 308, pp. 91-106. <https://doi.org/10.1016/j.geomorph.2018.02.002>

Annexure 1: Results of GLOF Scenarios of 3 to 6

1. GLOF Scenarios 3&4 (75% release)

The GLOF scenarios 3 and 4 are simulated for 75% of lake volume release (10.81 MCM) in two failure modes (scenario 3 for overtopping and scenario 4 for piping). Figure 37 shows GLOF hydrograph downstream of the lake for scenario 3 (overtopping failure mode). The flood hydrograph reached its peak of 2,652 cumecs in 1 hour 2minutes after the initiation of breach in the lake. Figure 38 shows GLOF hydrographs downstream of the lake at various locations on the river reach for scenario 3. The peak of the flood hydrograph is attenuated from 2,652 cumecs to 305 cumecs over river reach length of 149 km at Kargil.

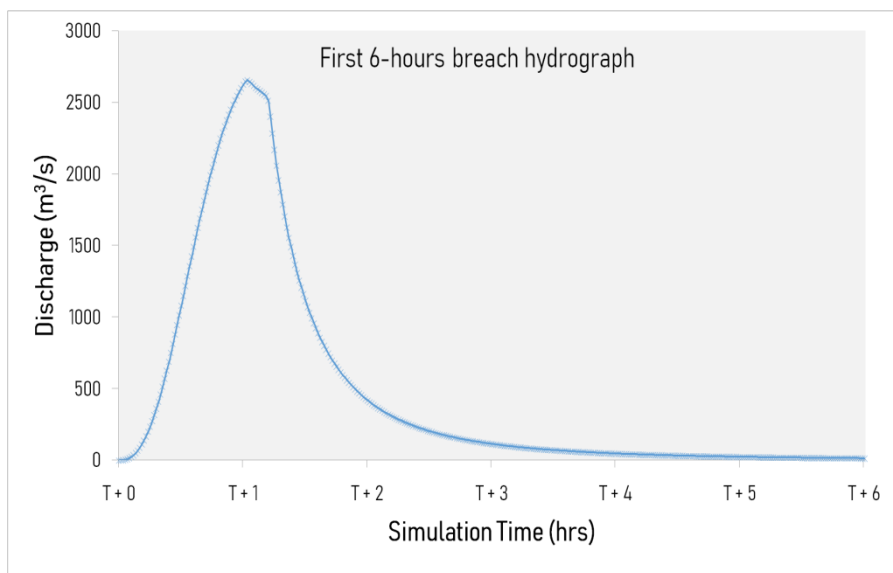


Figure 37: GLOF hydrograph for Scenario-3 (75% volume discharge - Overtopping failure)

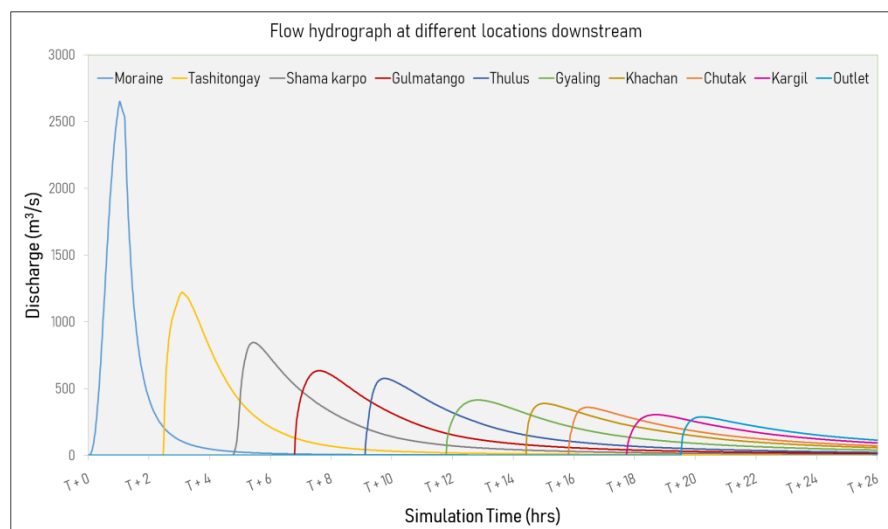


Figure 38: GLOF hydrographs at Different Downstream Locations for scenario-3

Figure 39 shows GLOF hydrograph downstream of the lake for scenario 4 (piping failure mode). The flood hydrograph reached its peak of 2,413 cumecs in 51 minutes after the initiation of breach in the lake. Figure 40 shows GLOF hydrographs downstream of the lake at various locations on the river reach for scenario 4. The peak of the flood hydrograph is attenuated from 2,413 cumecs to 294 cumecs over river reach length of 149 km at Kargil.

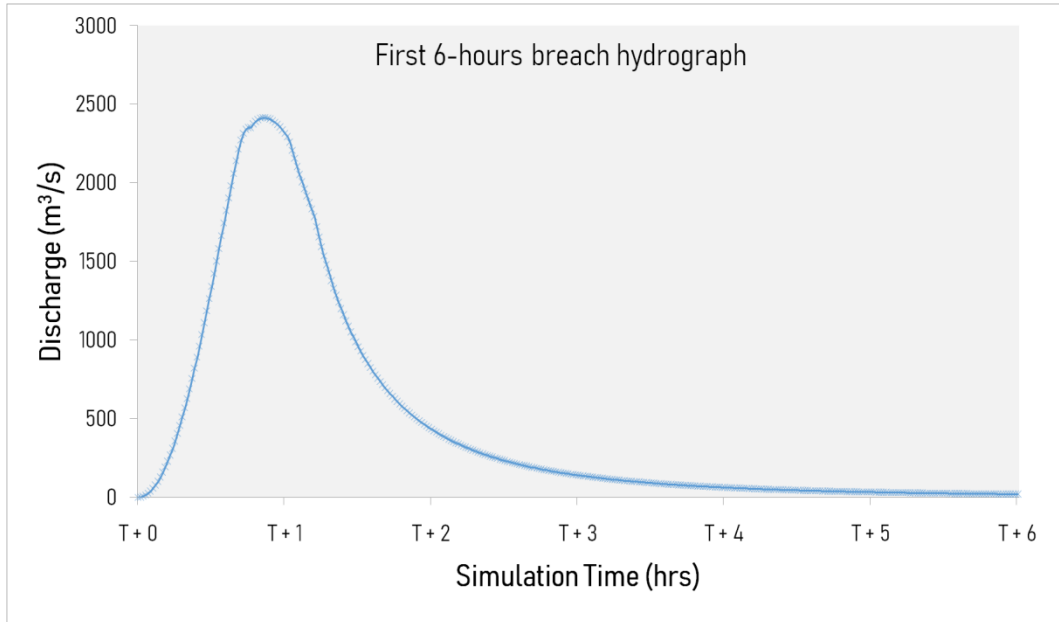


Figure 39: GLOF hydrograph for Scenario-4 (75% volume discharge - Piping failure)

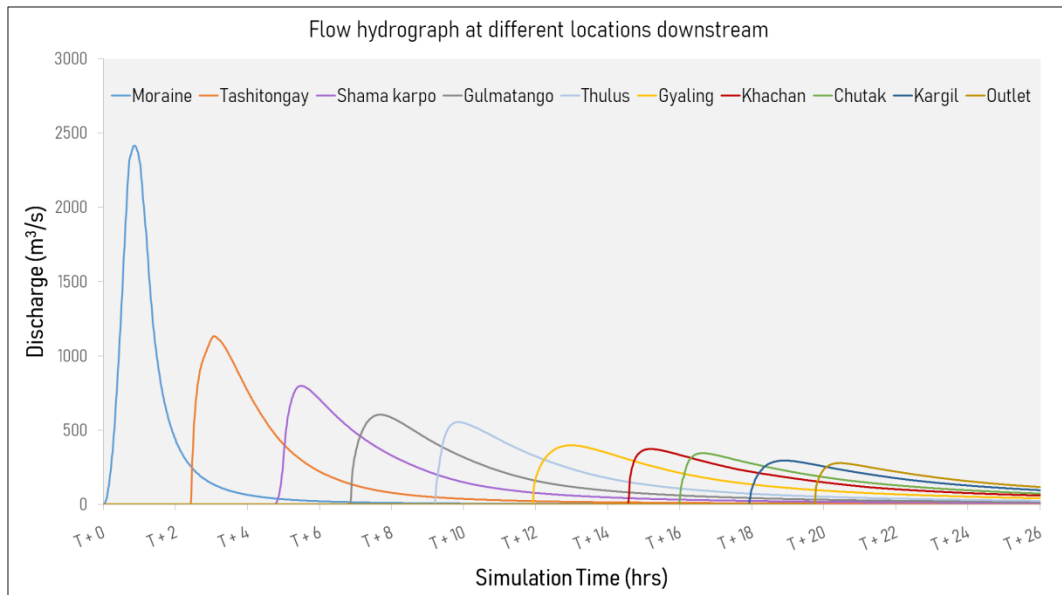


Figure 40: GLOF hydrographs at Different Downstream Locations for scenario-4

Table 19 describes the flood wave characteristics of GLOF scenario 3. After the breach of lake, the flood wave reaches nearest village of Thulus located at a distance of 74 km with peak discharge of 576 cumecs (maximum depth: 4.5 m; maximum velocity: 5.1 m/s) and as the flood wave traverses further downstream gets attenuated.

Table 19: Flood Wave Characteristics of GLOF Scenario 3

Location	Distance from Lake (km)	Time to peak	Peak Discharge (m ³ /s)	Max Depth (m)	Max Velocity (m/s)
Tashitongay	19	03hr 05mins	1,219	3.5	4.3
Shama karmo	33	05hr 26mins	845	2.8	1.7
Gulmatango	46	07hr 36mins	632	3.8	4.4
Thulus	74	09hr 45mins	576	4.5	5.1
Gyaling	96	12hr 50mins	413	3	3.8
Khachan	120	15hr 02mins	387	2.7	4.8
Chutuk	134	16hr 27mins	359	3.8	1.3
Kargil	149	18hr 42mins	305	3.2	2.1
Outlet	160	20hr 12mins	287	1.7	3.5

Table 20 describes the flood wave characteristics of GLOF scenario 4. After the breach of lake, the flood wave reaches nearest village of Thulus located at a distance of 74 km with peak discharge of 553 cumecs (maximum depth: 4.4 m; maximum velocity: 5.1 m/s) and as the flood wave traverses further downstream gets attenuated.

Table 20: Flood Wave Characteristics of GLOF Scenario 4

Location	Distance from Lake (km)	Time to peak	Peak Discharge (m ³ /s)	Max Depth (m)	Max Velocity (m/s)
Tashitongay	19	03hr 04mins	1,132	3.3	4.3
Shama karmo	33	05hr 29mins	796	2.1	1.7
Gulmatango	46	07hr 41mins	605	3.7	4.4
Thulus	74	09hr 51mins	553	4.4	5.1
Gyaling	96	12hr 58mins	398	3	3.7
Khachan	120	15hr 11mins	373	2.7	4.7
Chutuk	134	16hr 38mins	346	3.7	1.3
Kargil	149	18hr 54mins	294	3.2	2
Outlet	160	20hr 26mins	278	1.7	3.5

Figure 41 shows the map of flood inundation extent along with major settlements affected due to the flood for GLOF scenario 3. The inset images show flood depth and flood velocity near Kargil city along with GLOF affected settlements, roads, bridges and other infrastructure.

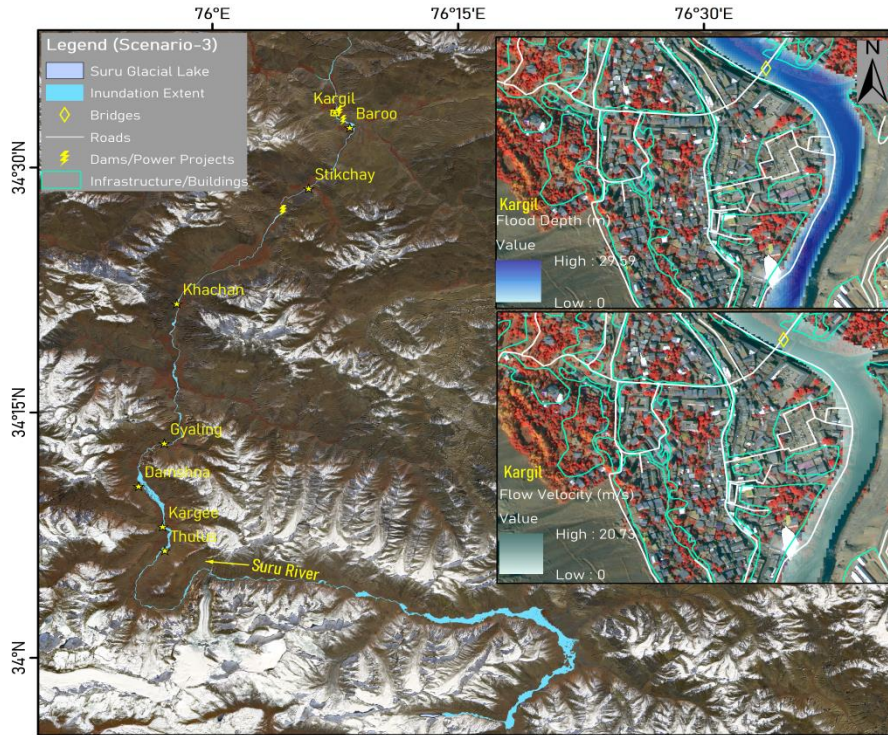


Figure 41: Map of Flood Inundation Extent for GLOF Scenario-3

Figure 42 shows the map of flood inundation extent along with major settlements affected due to the flood for GLOF scenario 4. The inset images show flood depth and flood velocity near Kargil city along with GLOF affected settlements, roads, bridges and other infrastructure.

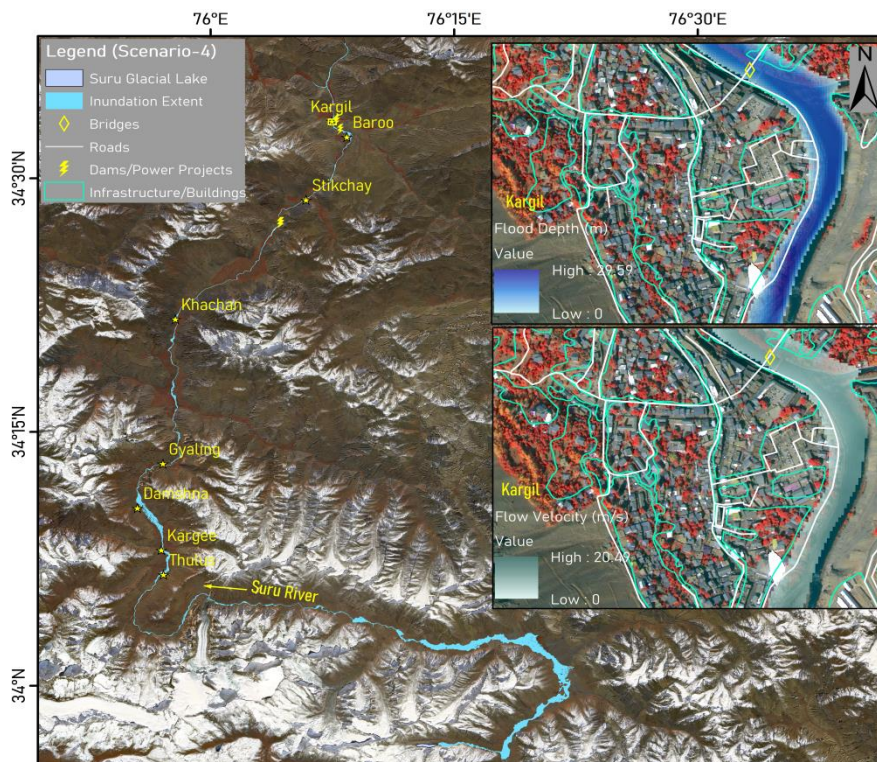


Figure 42: Map showing extent of inundation for Scenario-4

Table 21 provides number of settlements, extent of agriculture land, number of bridges and length of road network affected by scenarios 3 and 4. Table 22 provides names of settlements affected by scenarios 3 and 4. All the settlements (10) are partly affected by the GLOF inundation. The three settlements (Gyaling, Stickchay and Zamistang) affected in scenario 1 & 2 are not affected in scenario 3 & 4.

Table 21: Infrastructure affected in GLOF Scenarios 3 and 4

Scenario	No. of Affected Settlements	Area of Agricultural Land Affected (ha)	No. of Bridges Affected	Length of Roads affected (km)	Inundated Area (ha)
Scenario-3	10	29.1	54	9	2990
Scenario-4	10	28.2	54	8.4	2960

Table 22: Names of Settlements affected in GLOF Scenarios 3 and 4

S. No.	Settlement Name	Distance from lake (km)
1	Thulus	74
2	Kargee	84.9
3	Namsuru*	85
4	Damshna	90.68
5	Khachan*	120
6	Zambakha*	129.3
7	Sarchay*	131.2
8	Baroo	147.43
9	Kargil	149
10	Poyen	150

Note: * indicate few buildings, which are affected close to the river channel near the mentioned settlement.

2. GLOF Scenarios 5&6 (50% release)

The GLOF scenarios 5 and 6 are simulated for 50% of lake volume release (7.20 MCM) in two failure modes (scenario 5 for overtopping and scenario 6 for piping). Figure 43 shows GLOF hydrograph downstream of the lake for scenario 5 (overtopping failure mode). The flood hydrograph reached its peak of 1,544 cumecs in 1 hour 18 minutes after the initiation of breach in the lake. Figure 44 shows GLOF hydrographs downstream of the lake at various locations on the river reach for scenario 5. The peak of the flood hydrograph is attenuated from 1,544 cumecs to 155 cumecs over river reach length of 149 km at Kargil.

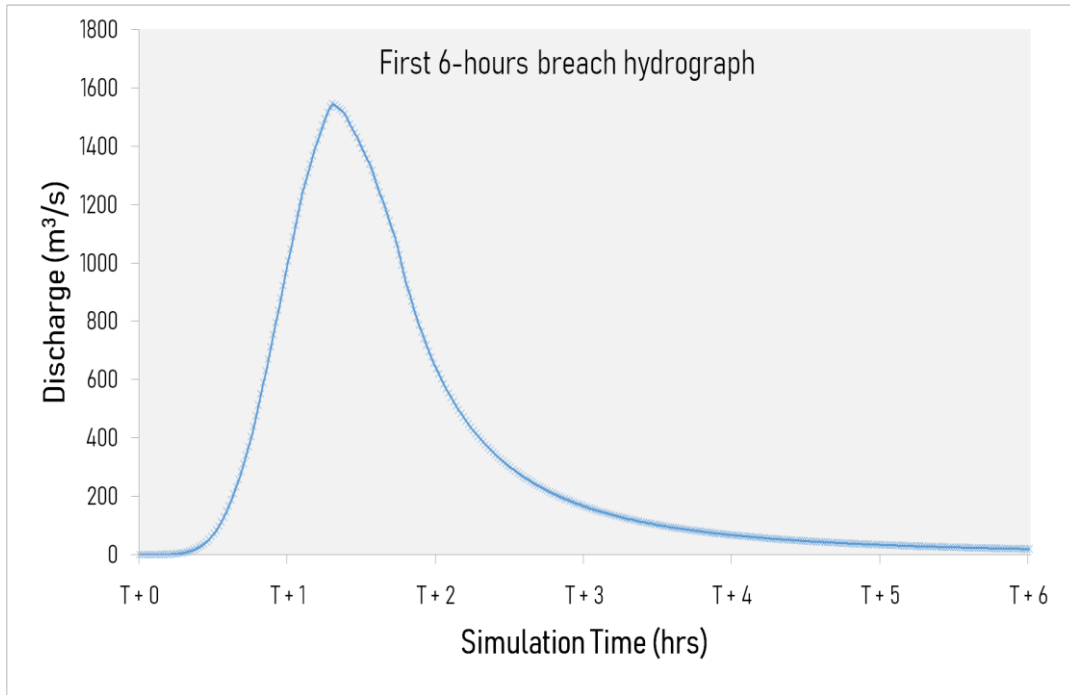


Figure 43: GLOF hydrograph for Scenario-5 (50% volume discharge - Overtopping failure)

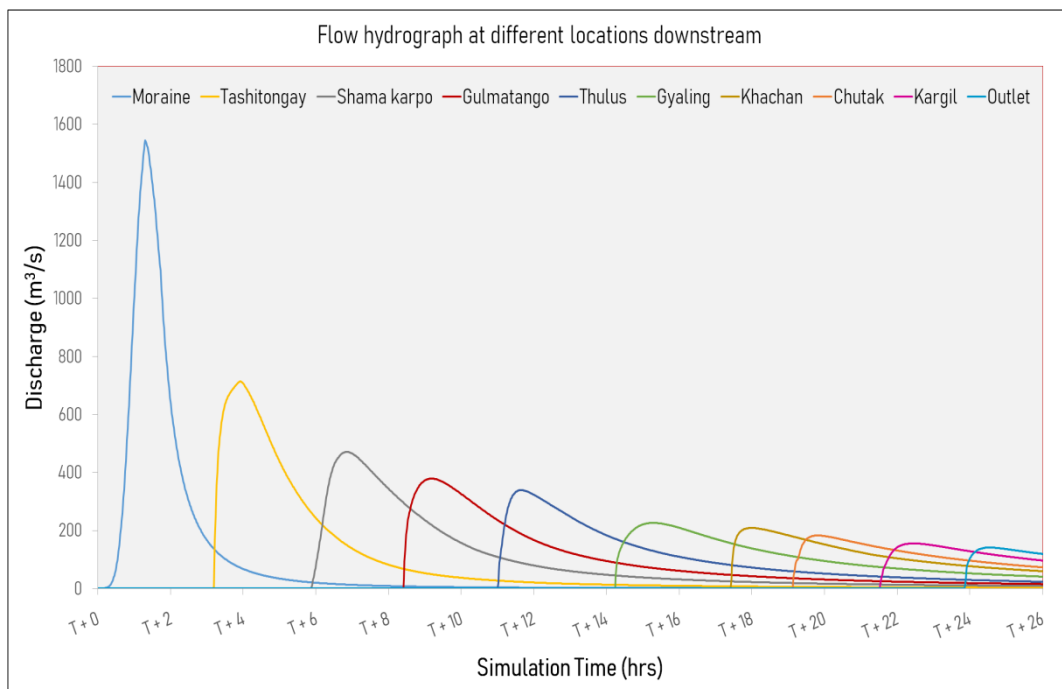


Figure 44: GLOF hydrographs at Different Downstream Locations for scenario-5

Figure 45 shows GLOF hydrograph downstream of the lake for scenario 6 (piping failure mode). The flood hydrograph reached its peak of 1,429 cumecs in 1 hour 16 minutes after the initiation of breach in the lake. Figure 46 shows GLOF hydrographs downstream of the

lake at various locations on the river reach for scenario 6. The peak of the flood hydrograph is attenuated from 1,429 cumecs to 152 cumecs over river reach length of 149 km at Kargil.

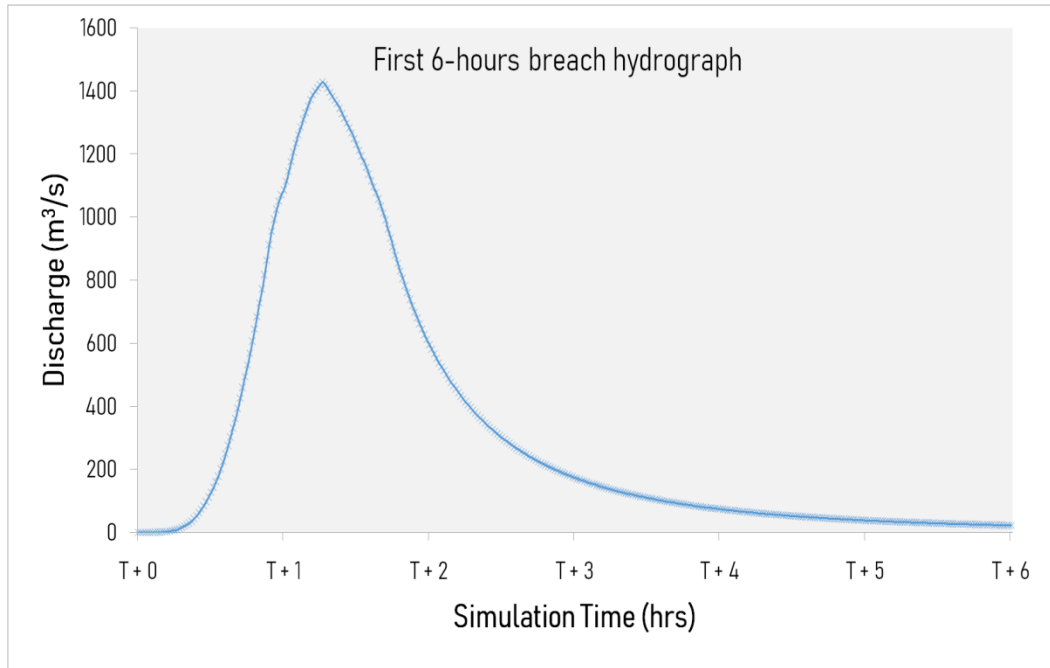


Figure 45: GLOF hydrograph for Scenario-6 (50% volume discharge - Piping failure)

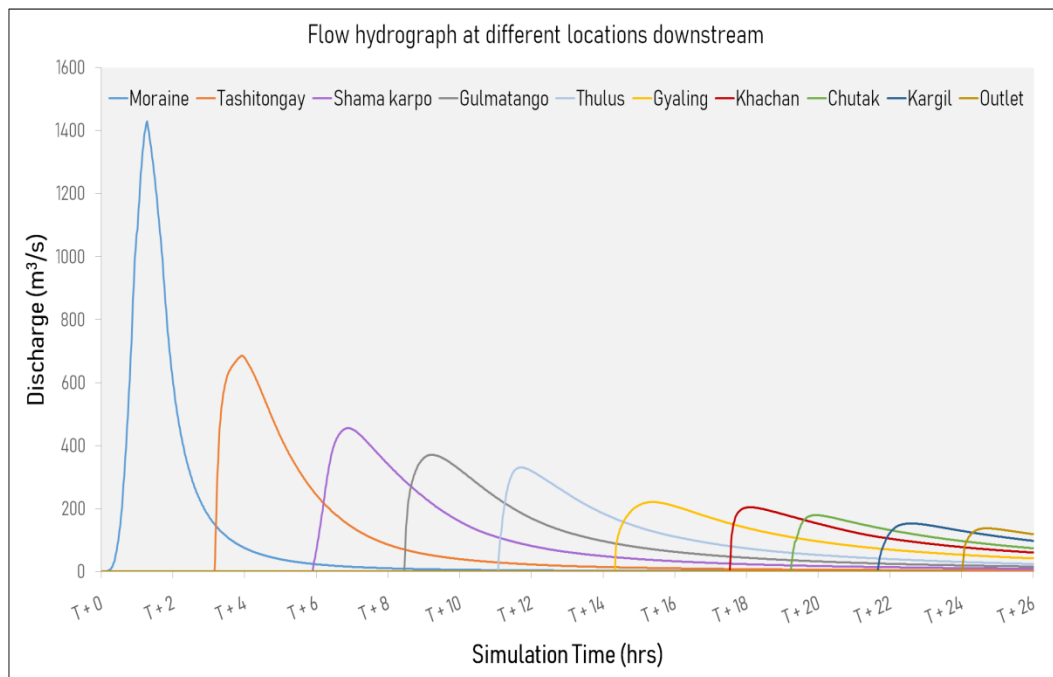


Figure 46: GLOF hydrographs at Different Downstream Locations for scenario-6

Table 23 describes the flood wave characteristics of GLOF scenario 5. After the breach of lake, the flood wave reaches nearest village of Thulus located at a distance of 74 km with peak discharge of 338 cumecs (maximum depth: 3.4 m; maximum velocity: 4.4 m/s) and as the flood wave traverses further downstream gets attenuated.

Table 23: Flood Wave Characteristics of GLOF Scenario 5

Location	Distance from Lake (km)	Time to peak	Peak Discharge (m ³ /s)	Max Depth (m)	Max Velocity (m/s)
Tashitongay	19	03hr 55mins	713	2.9	3.6
Shama karmo	33	06hr 51mins	470	1.7	1.4
Gulmatango	46	09hr 11mins	378	3	3.8
Thulus	74	11hr 38mins	338	3.4	4.4
Gyaling	96	15hr 16mins	225	2.3	2.8
Khachan	120	17hr 59mins	208	1.9	4.3
Chutuk	134	19hr 48mins	183	2.8	0.9
Kargil	149	22hr 27mins	155	2.2	1.7
Outlet	160	24hr 31mins	140	1.2	2.5

Table 24 describes the flood wave characteristics of GLOF scenario 6. After the breach of lake, the flood wave reaches nearest village of Thulus located at a distance of 74 km with peak discharge of 330 cumecs (maximum depth: 3.3 m; maximum velocity: 4.4 m/s) and as the flood wave traverses further downstream gets attenuated.

Table 24: Flood Wave Characteristics of GLOF Scenario 6

Location	Distance from Lake (km)	Time to peak	Peak Discharge (m ³ /s)	Max Depth (m)	Max Velocity (m/s)
Tashitongay	19	03hr 55mins	686	2.9	3.6
Shama karmo	33	06hr 53mins	456	1.7	1.4
Gulmatango	46	09hr 13mins	370	2.9	3.6
Thulus	74	11hr 42mins	330	3.3	4.4
Gyaling	96	15hr 22mins	220	2.3	2.7
Khachan	120	18hr 06mins	205	1.8	4.2
Chutuk	134	19hr 56mins	179	2.8	0.9
Kargil	149	22hr 34mins	152	2.2	1.7
Outlet	160	24hr 42mins	137	1.2	2.5

Figure 47 shows the map of flood inundation extent along with major settlements affected due to the flood for GLOF scenario 5. The inset images show flood depth and flood velocity near Kargil city along with GLOF affected settlements, roads, bridges and other infrastructure.

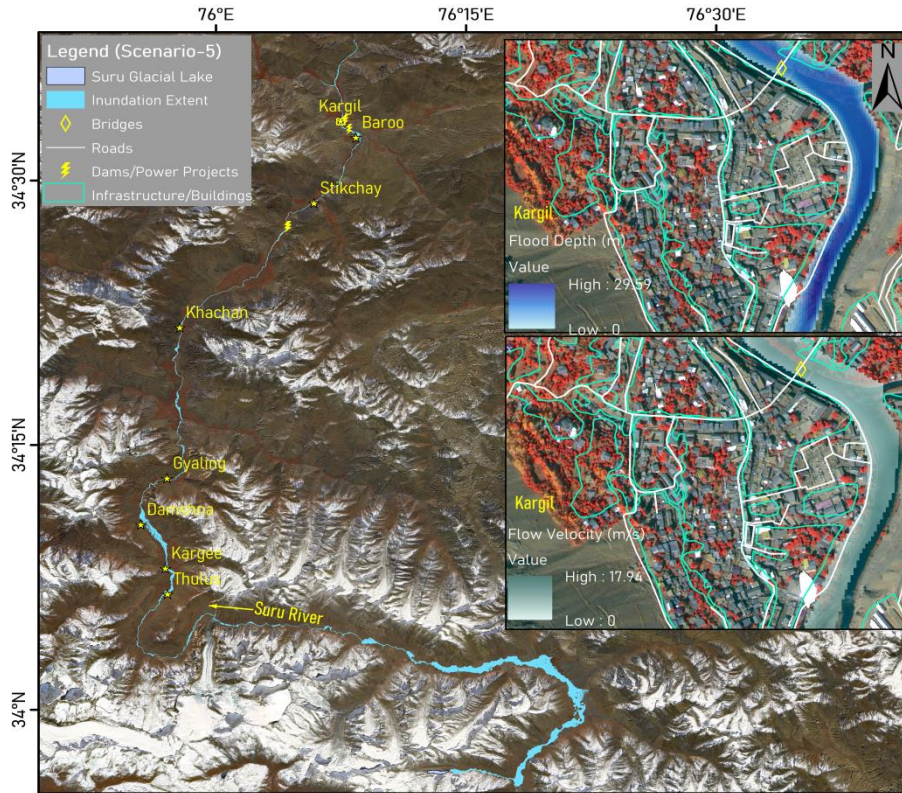


Figure 47: Map of Flood Inundation Extent for GLOF Scenario-5

Figure 48 shows the map of flood inundation extent along with major settlements affected due to the flood for GLOF scenario 6. The inset images show flood depth and flood velocity near Kargil city along with GLOF affected settlements, roads, bridges and other infrastructure.

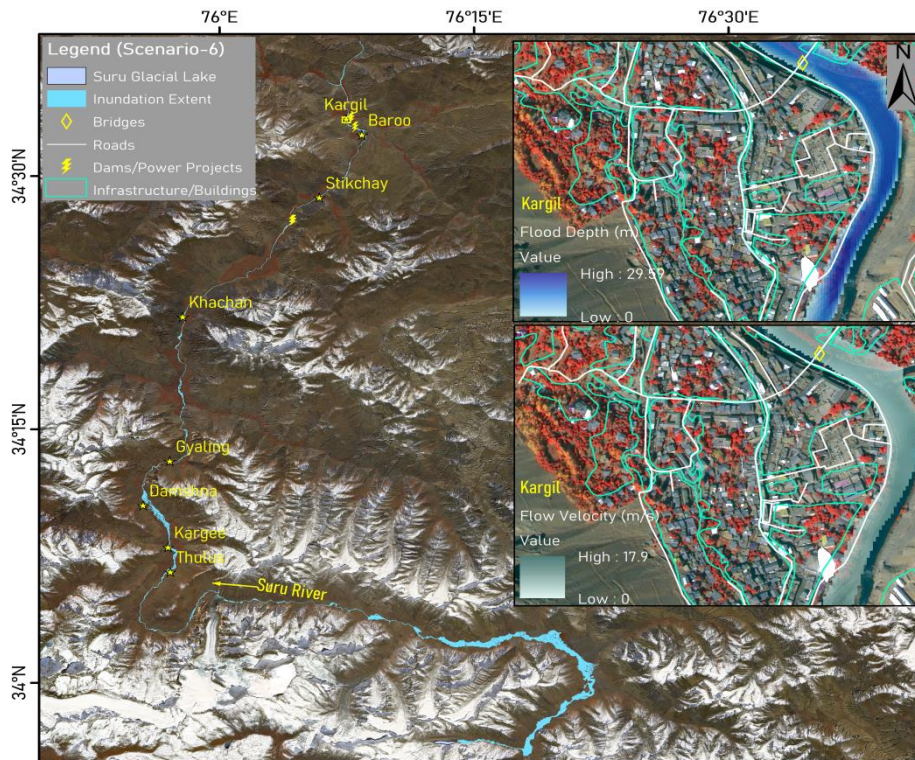


Figure 48: Map showing extent of inundation for Scenario-6

Table 25 provides number of settlements, extent of agriculture land, number of bridges and length of road network affected by scenarios 5 and 6. Table 26 provides names of settlements affected by scenarios 5 and 6. All the settlements (8) are partly affected by the GLOF inundation. The two settlements (Namsuru and sarchay) affected in scenario 3&4 are not affected in scenario 5 & 6.

Table 25: Infrastructure affected in GLOF Scenarios 5 and 6

Scenario	No. of Affected Settlements	Area of Agricultural Land Affected (ha)	No. of Bridges Affected	Length of Roads affected (km)	Inundated Area (ha)
Scenario-5	8	17.8	52	5.8	2690
Scenario-6	8	17.6	52	5.6	2674

Table 26: Names of Settlements affected in GLOF Scenarios 5 and 6

S. No.	Settlement Name	Distance from lake (km)
1	Thulus	74
2	Kargee*	84.9
3	Damshna*	90.68
4	Khachan*	120
5	Zambakha*	129.3
6	Baroo	147.43
7	Kargil	149
8	Poyen	150

Note: * indicate few buildings, which are affected close to the river channel near the mentioned settlement.

Annexure 2: Results of GLOF Risk Assessment for Scenarios of 3 to 6

The results of Suru glacial lake GLOF risk assessment for the scenarios 3 to 6 are described here.

1. GLOF Risk for Scenario 3 (75% release-Overtopping failure mode)

The GLOF risk map for scenario 3 is shown in Figure 49. The area under high, moderate and low risk zones of GLOF scenario 3 are 467 ha, 1,457 ha and 1,066 ha respectively. The area under the high risk zone will be most affected area with no time (less than 2 hours) for warning in case of GLOF event occurrence. Table 27 gives details of flood inundation area, number of settlements, agricultural land, number of bridges and length of road network affected exclusively under various categories of GLOF risk zones. As already mentioned in the previous section all the settlements are partly affected. The total number of settlements, agricultural land, bridges, and road length affected in scenario 3 are 10, 29.1 ha, 54 and 9 km respectively. Figures 50 and 51 show close view of affected infrastructure (settlements, bridges, road network, etc) and agriculture land by GLOF inundation extent near Kargil respectively.

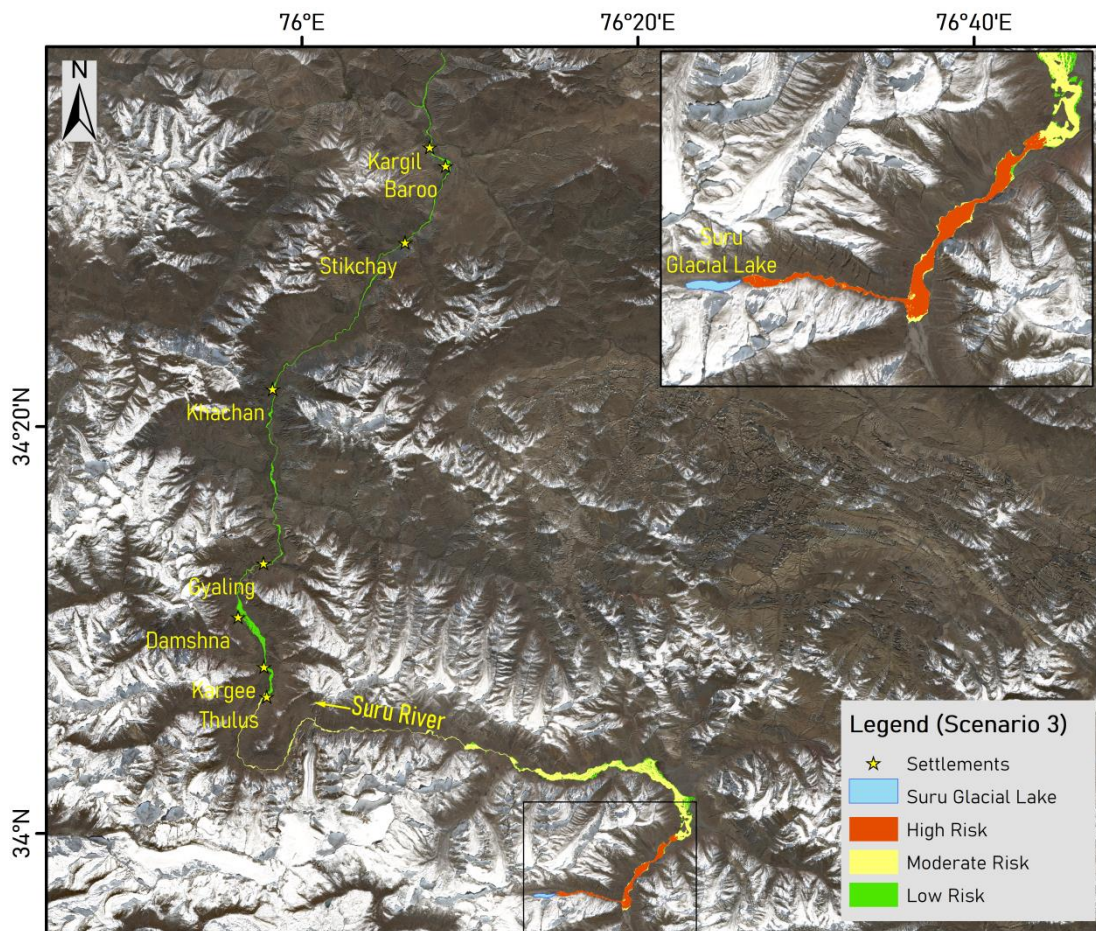


Figure 49: GLOF Risk Map for the Study Area (Scenario-3)

Table 27: Zone wise details of Infrastructure affected in GLOF Scenario 3

Scenario	Risk Zone	Flood Inundated Area (ha)	No. of Settlements	Agricultural Land (ha)	No. of Bridges	Length of Road (km)
3	High	467	0	0	0	1.1
	Moderate	1,457	0	3.7	12	2
	Low	1,066	10	25.4	42	5.9
Total		2,990	10	29.1	54	9

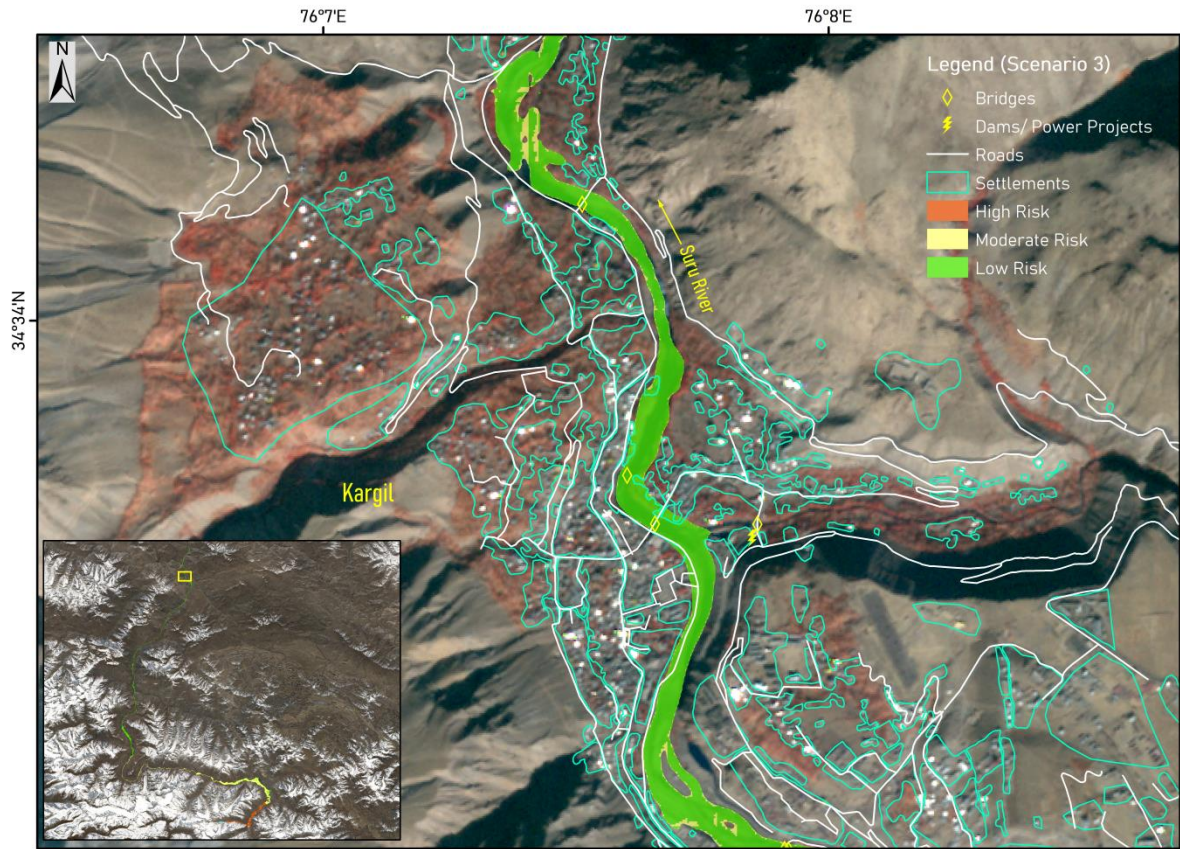


Figure 50: GLOF Risk Map showing Affected Infrastructure near Kargil (Scenario-3)

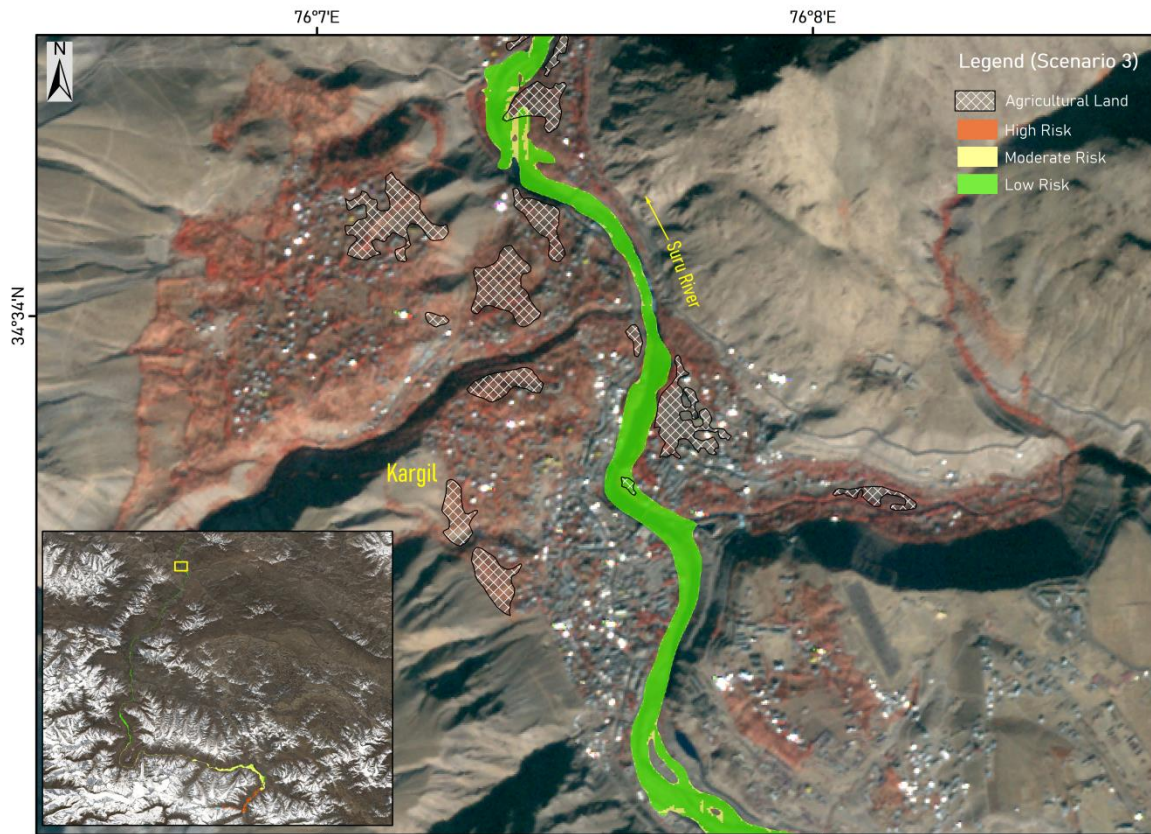


Figure 51: GLOF Risk Map showing Affected Agricultural Land near Kargil (Scenario-3)

2. GLOF Risk for Scenario 4 (75% release- Piping failure mode)

The GLOF risk map for scenario 4 is shown in Figure 52. The area under high, moderate and low risk zones of GLOF scenario 4 are 475 ha, 1,404 ha and 1,081 ha respectively. The area under the high risk zone will be most affected area with no time (less than 2 hours) for warning in case of GLOF event occurrence. Table 28 gives details of flood inundation area, number of settlements, agricultural land, number of bridges and length of road network affected exclusively under various categories of GLOF risk zones. As already mentioned in the previous section all the settlements are partly affected. The total number of settlements, agricultural land, bridges, and road length affected in scenario 4 are 10, 28.2 ha, 54 and 8.4 km respectively. Figures 53 and 54 show close view of affected infrastructure (settlements, bridges, road network, etc) and agriculture land by GLOF inundation extent near Kargil respectively.

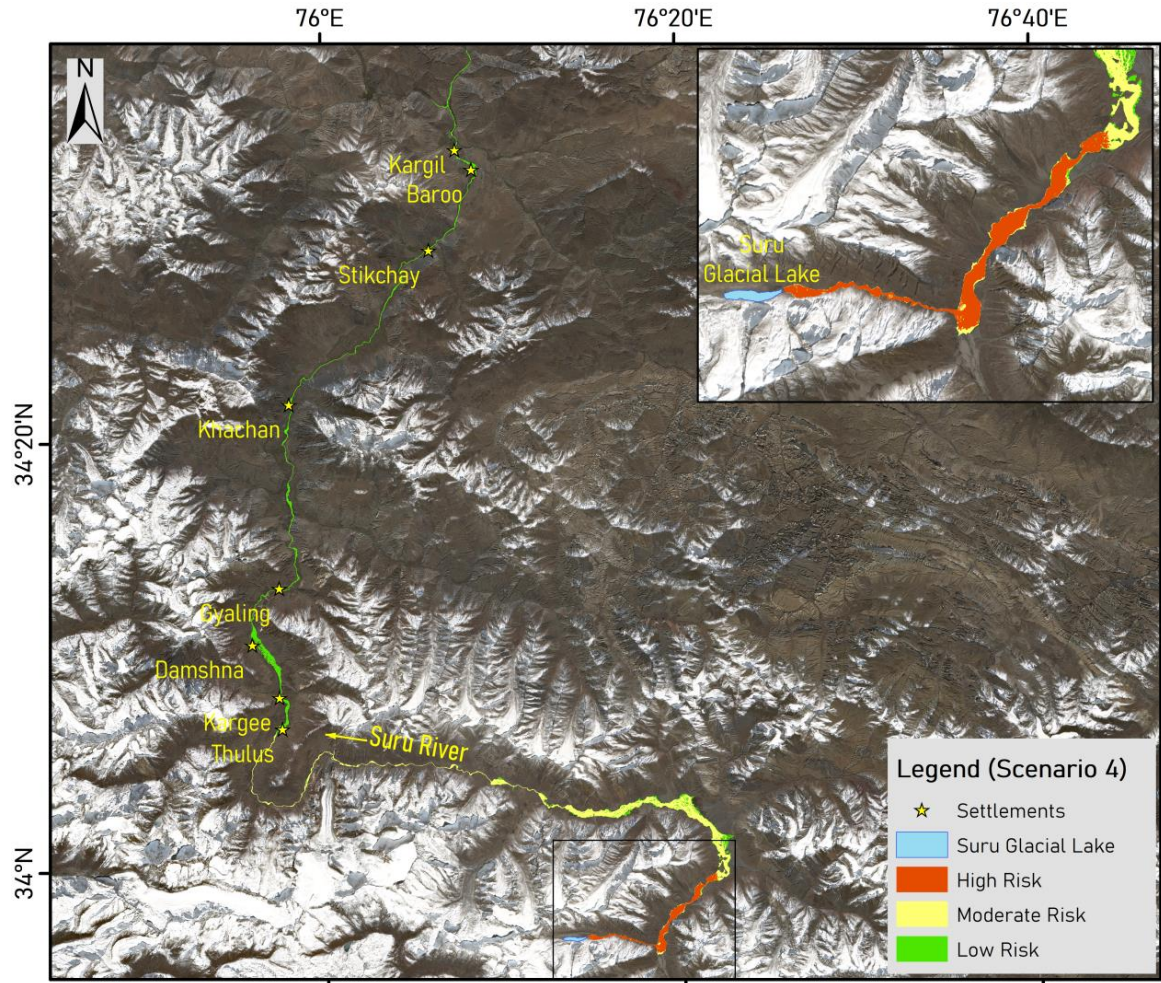


Figure 52: GLOF Risk Map for the Study Area (Scenario-4)

Table 28: Zone wise details of Infrastructure affected in GLOF Scenario 4

Scenario	Risk Zone	Flood Inundated Area (ha)	No. of Settlements	Agricultural Land (ha)	No. of Bridges	Length of Road (km)
4	High	475	0	0	0	1
	Moderate	1,404	0	2.8	12	1.7
	Low	1,081	10	25.4	42	5.7
Total		2,960	10	28.2	54	8.4

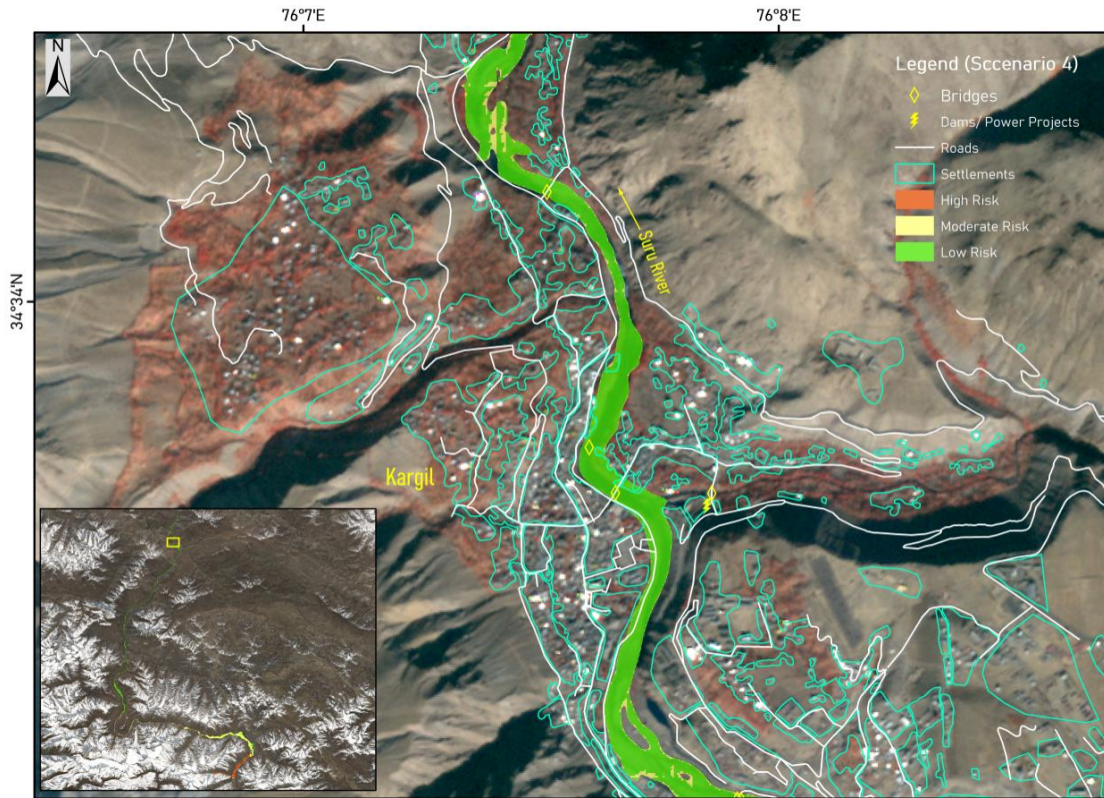


Figure 53: GLOF Risk Map showing Affected Infrastructure near Kargil (Scenario-4)

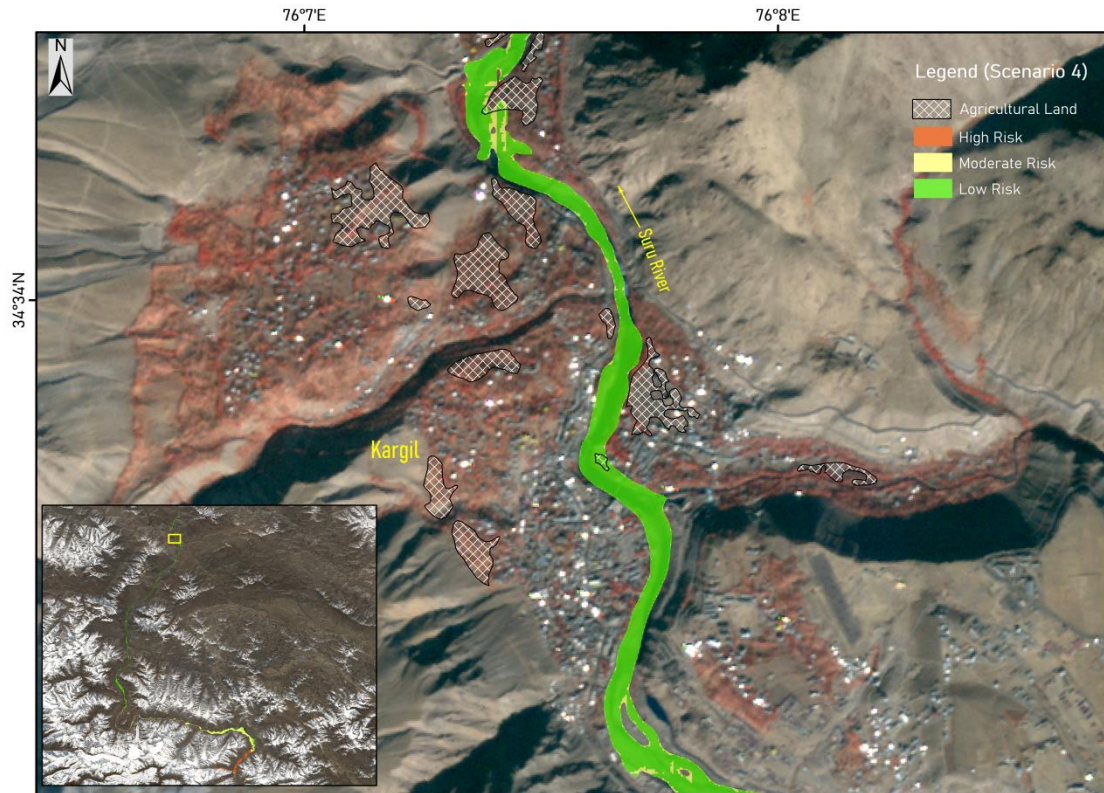


Figure 54: GLOF Risk Map showing Affected Agricultural Land near Kargil (Scenario-4)

3. GLOF Risk for Scenario 5 (50% release- Overtopping failure mode)

The GLOF risk map for scenario 5 is shown in Figure 55. The area under high, moderate and low risk zones of GLOF scenario 5 are 305 ha, 1,120 ha and 1,265 ha respectively. The area under the high risk zone will be most affected area with no time (less than 2 hours) for warning in case of GLOF event occurrence. Table 29 gives details of flood inundation area, number of settlements, agricultural land, number of bridges and length of road network affected exclusively under various categories of GLOF risk zones. As already mentioned in the previous section all the settlements are partly affected. The total number of settlements, agricultural land, bridges, and road length affected in scenario 5 are 8, 17.8 ha, 52 and 5.8 km respectively. Figures 56 and 57 show close view of affected infrastructure (settlements, bridges, road network, etc) and agriculture land by GLOF inundation extent near Kargil respectively.

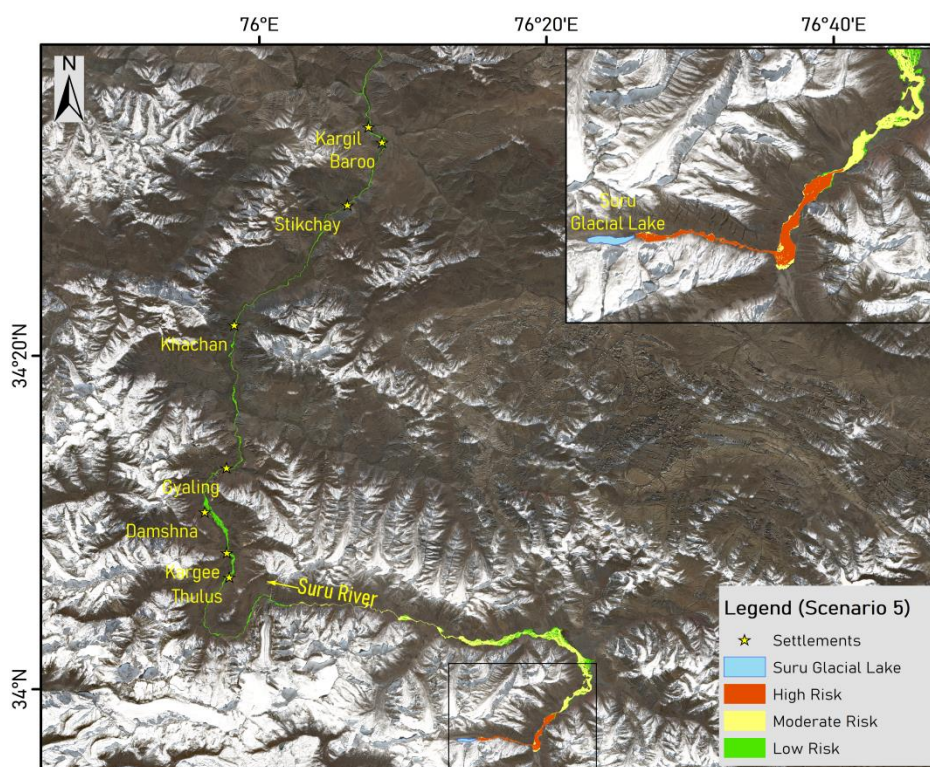


Figure 55: GLOF Risk Map for the Study Area (Scenario-5)

Table 29: Zone wise details of Infrastructure affected in GLOF Scenario 5

Scenario	Risk Zone	Flood Inundated Area (ha)	No. of Settlements	Agricultural Land (ha)	No. of Bridges	Length of Road (km)
5	High	305	0	0	0	0.1
	Moderate	1,120	0	1.2	3	1.3
	Low	1,265	8	16.6	49	4.4
Total		2,690	8	17.8	52	5.8

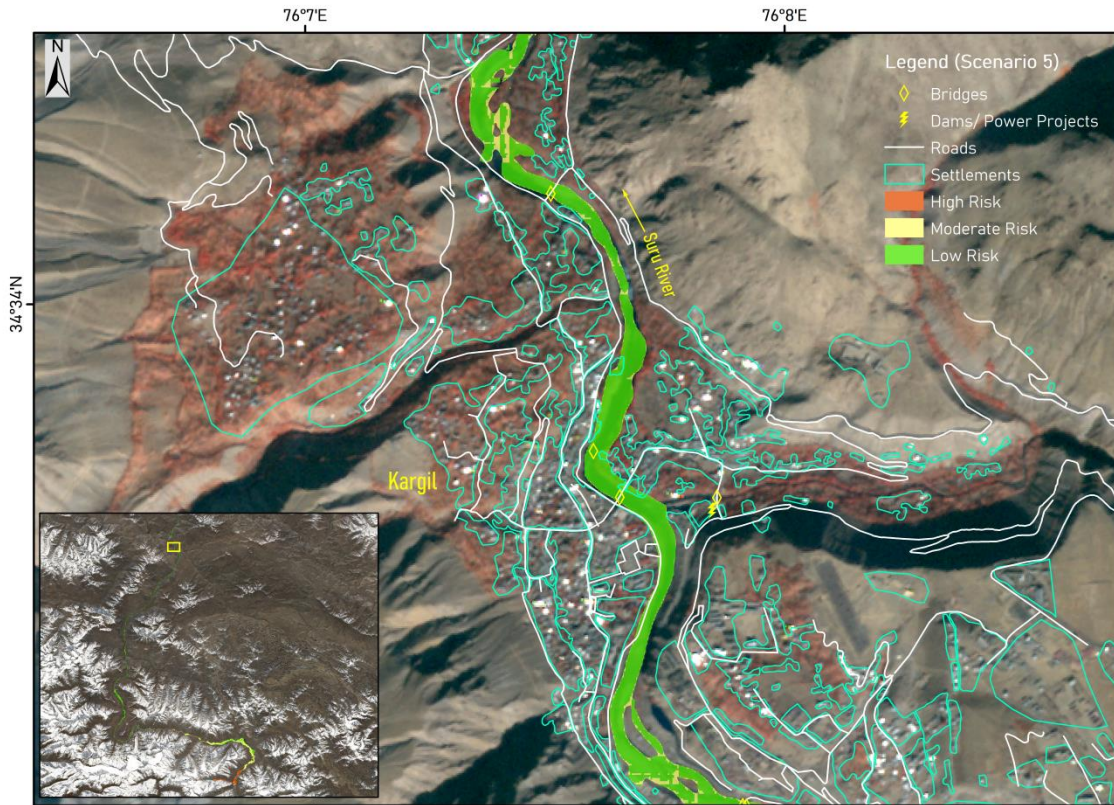


Figure 56: GLOF Risk Map showing Affected Infrastructure near Kargil (Scenario-5)

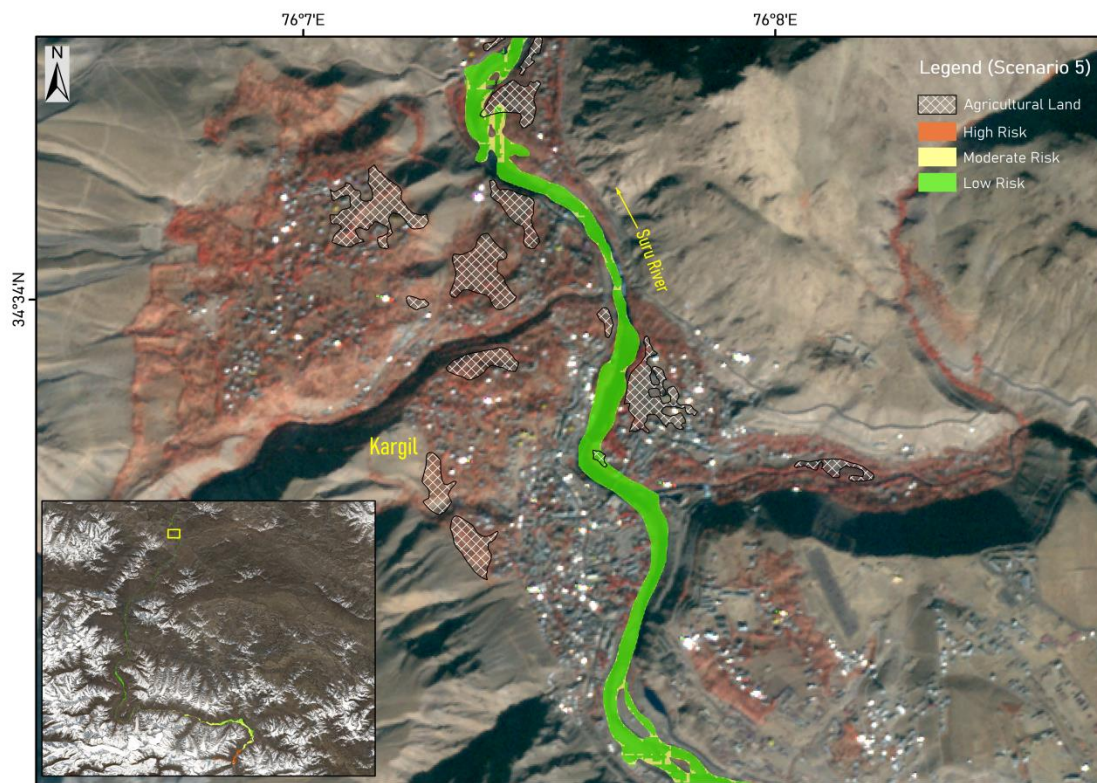


Figure 57: GLOF Risk Map showing Affected Agricultural Land near Kargil (Scenario-5)

4. GLOF Risk for Scenario 6 (50% release- Piping failure mode)

The GLOF risk map for scenario 6 is shown in Figure 58. The area under high, moderate and low risk zones of GLOF scenario 6 are 306 ha, 1,091 ha and 1,277 ha respectively. The area under the high risk zone will be most affected area with no time (less than 2 hours) for warning in case of GLOF event occurrence. Table 30 gives details of flood inundation area, number of settlements, agricultural land, number of bridges and length of road network affected exclusively under various categories of GLOF risk zones. As already mentioned in the previous section all the settlements are partly affected. The total number of settlements, agricultural land, bridges, and road length affected in scenario 6 are 8, 17.6 ha, 52 and 5.6 km respectively. Figures 59 and 60 show close view of affected infrastructure (settlements, bridges, road network, etc) and agriculture land by GLOF inundation extent near Kargil respectively.

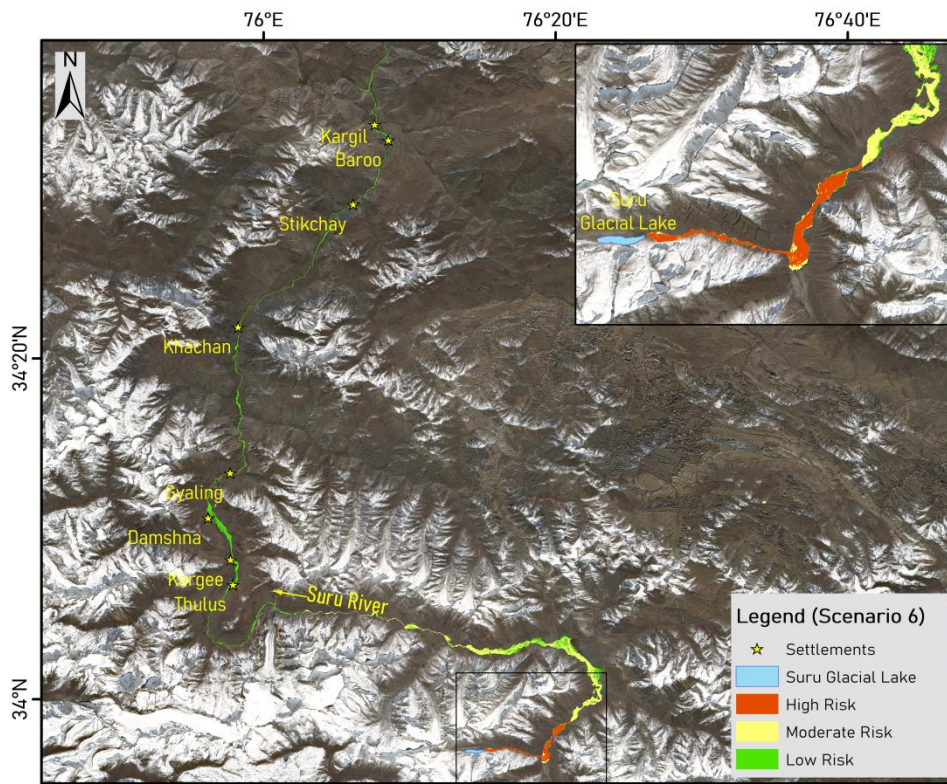


Figure 58: GLOF Risk Map for the Study Area (Scenario-6)

Table 30: Zone wise details of Infrastructure affected in GLOF Scenario 6

Scenario	Risk Zone	Flood Inundated Area (ha)	No. of Settlements	Agricultural Land (ha)	No. of Bridges	Length of Road (km)
6	High	306	0	0	0	0.3
	Moderate	1,091	0	1.2	3	1.1
	Low	1,277	8	16.4	49	4.2
Total		2,674	8	17.6	52	5.6

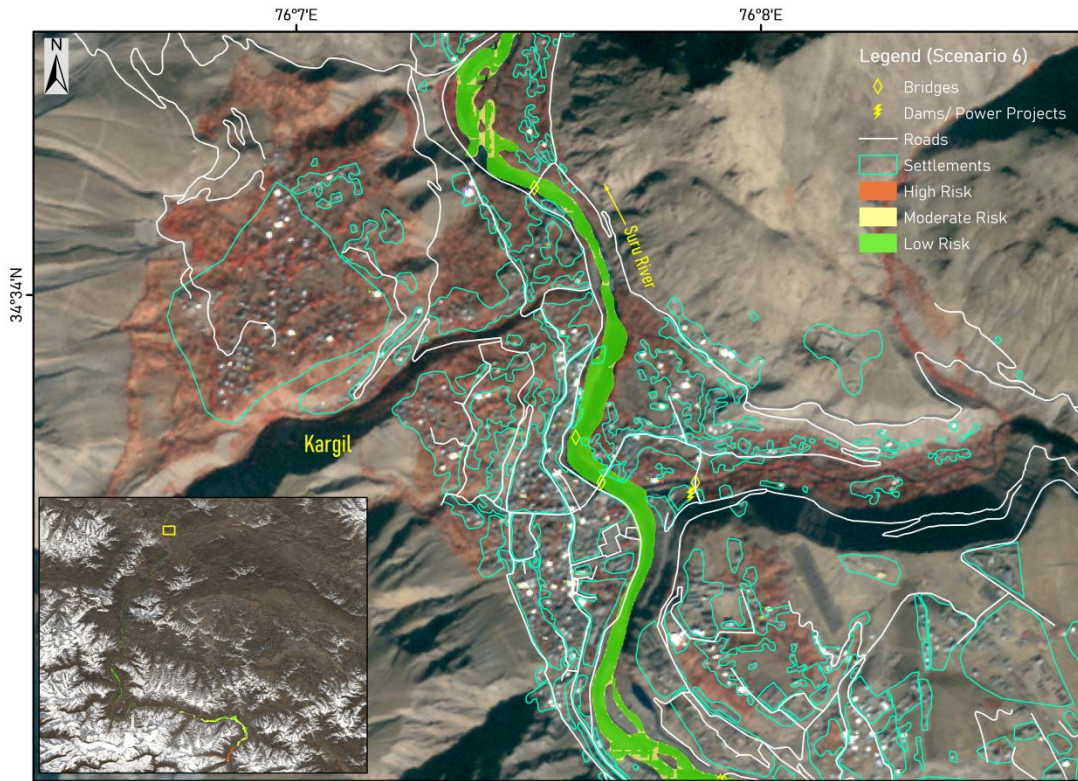


Figure 59: GLOF Risk Map showing Affected Infrastructure near Kargil (Scenario-6)

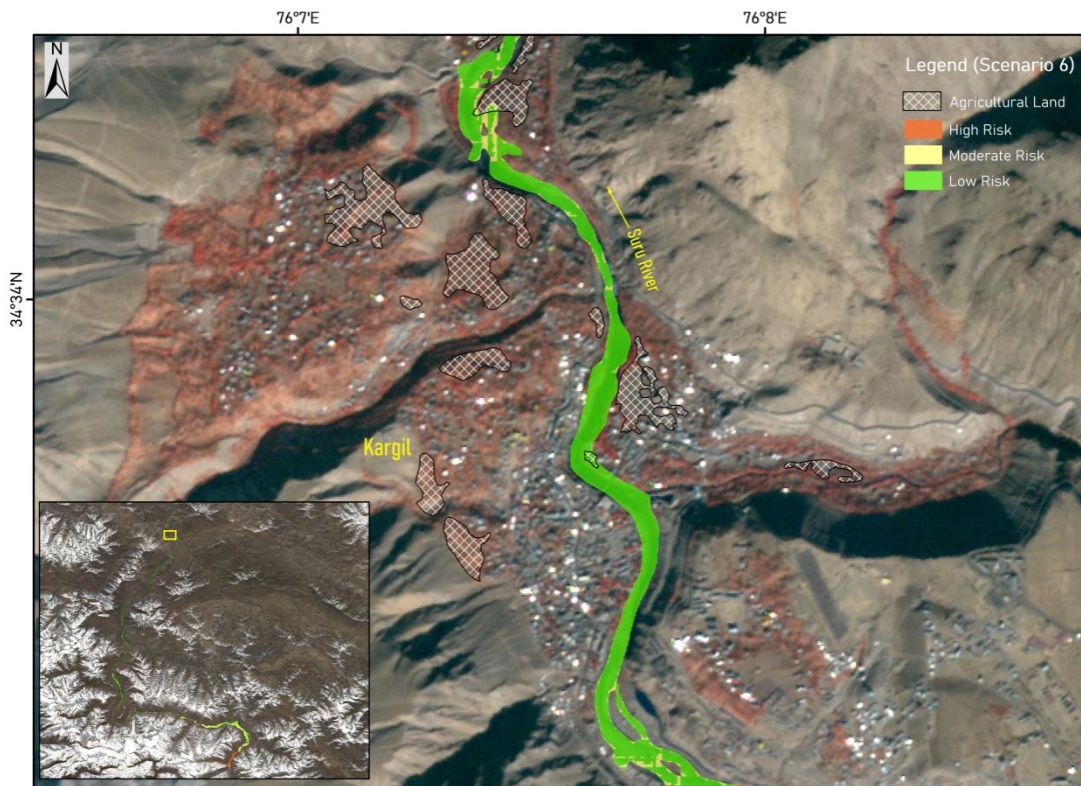
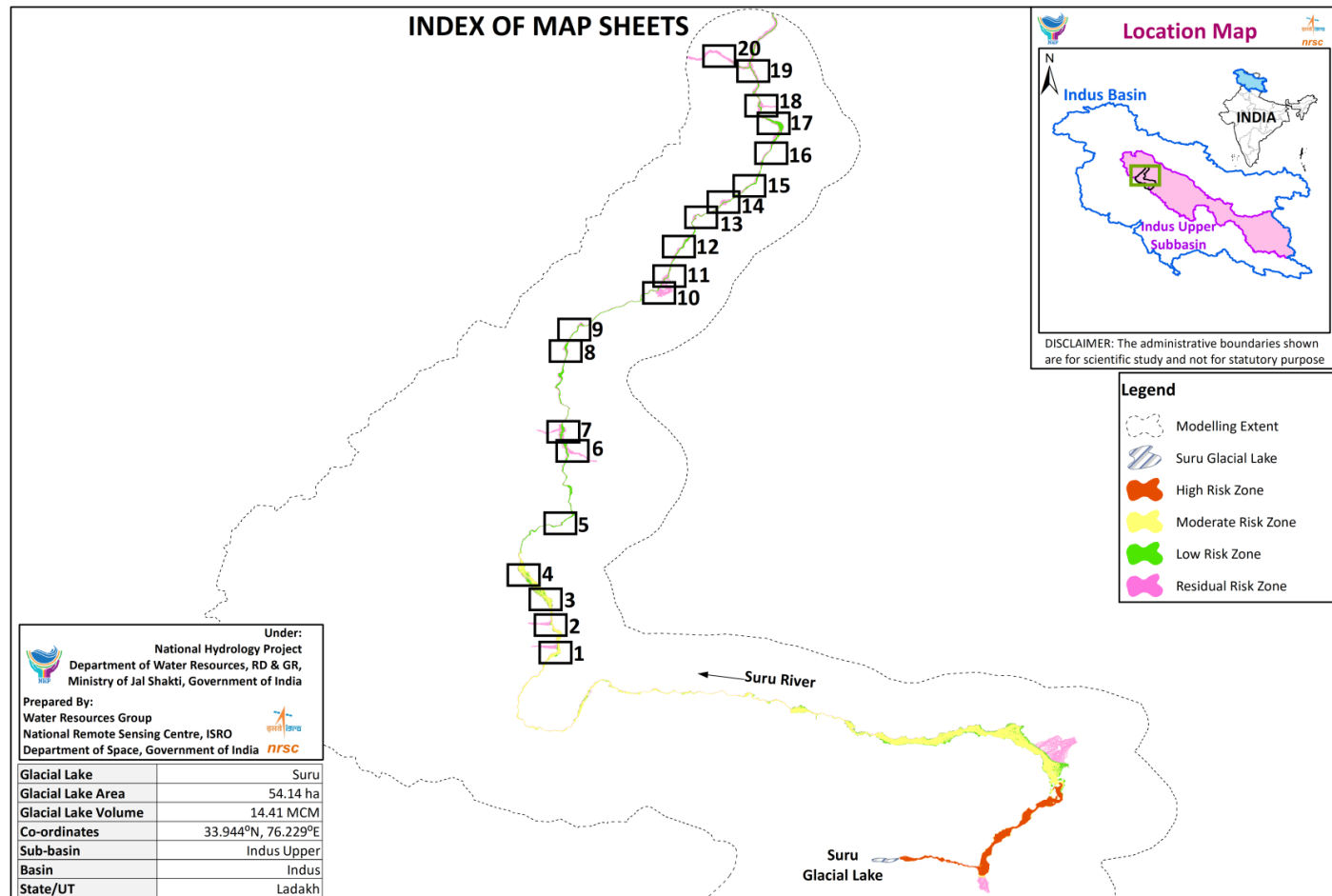
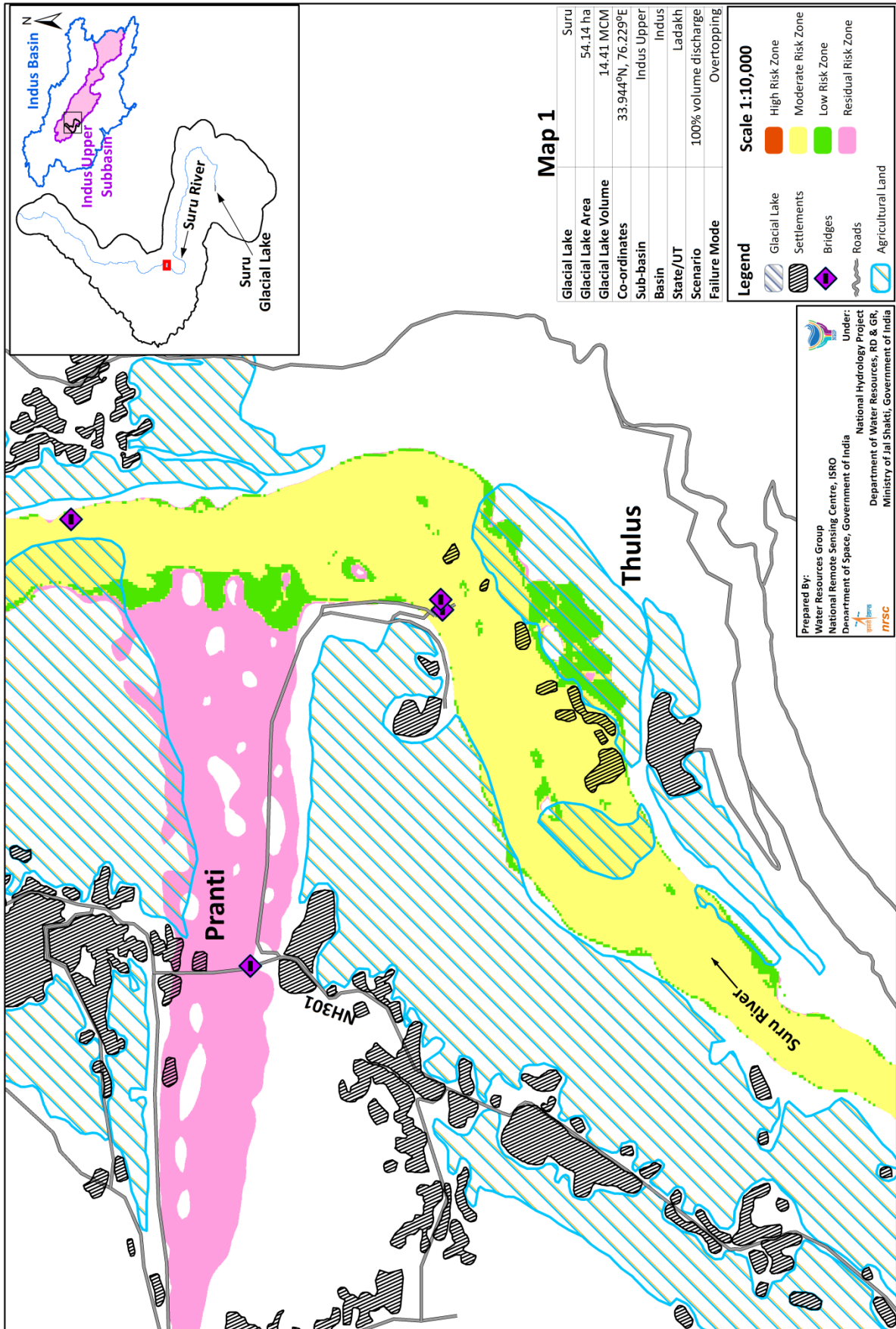


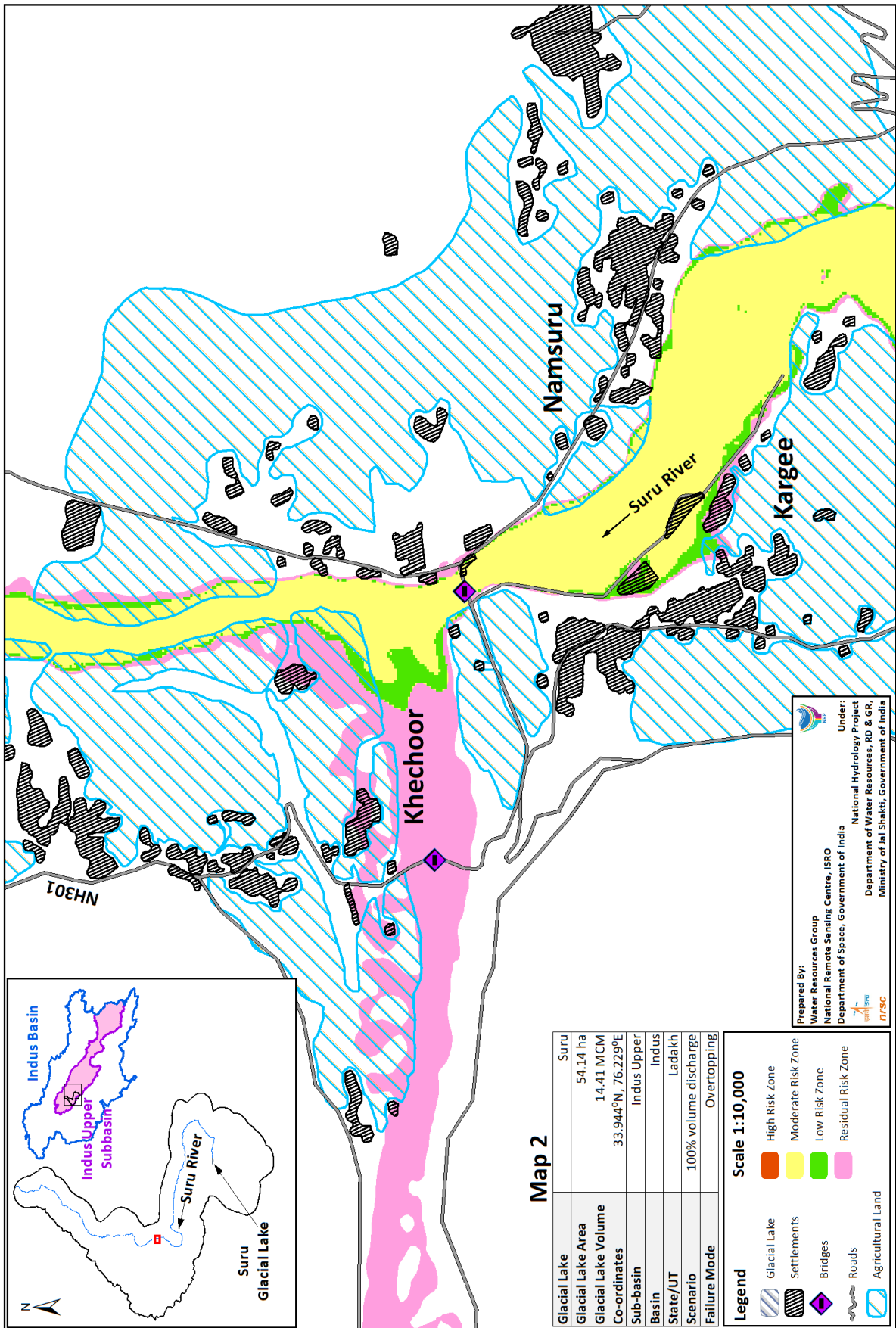
Figure 60: GLOF Risk Map showing Affected Agricultural Land near Kargil (Scenario-6)

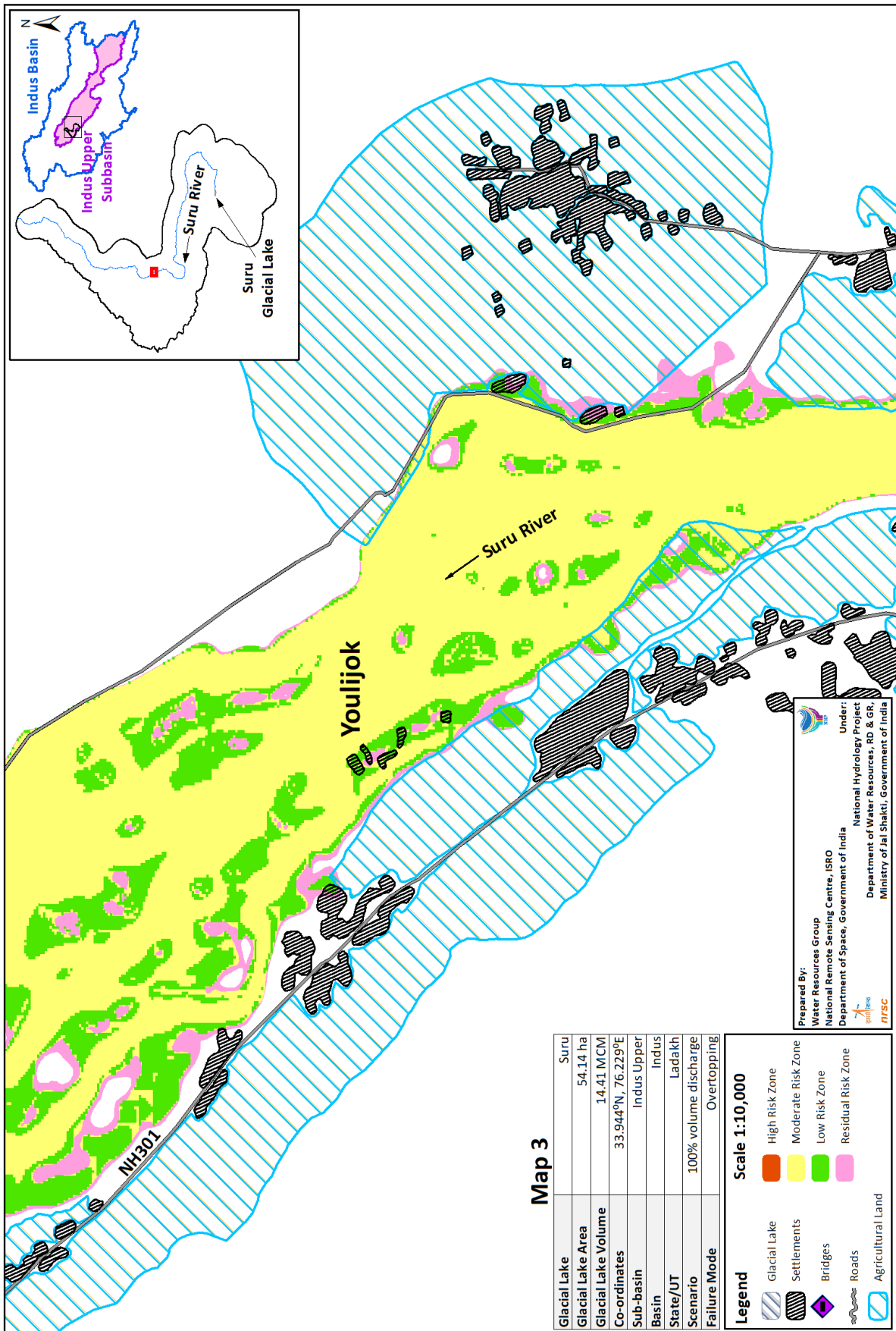
Annexure 3: GLOF Risk maps for Scenarios of 1 and 7

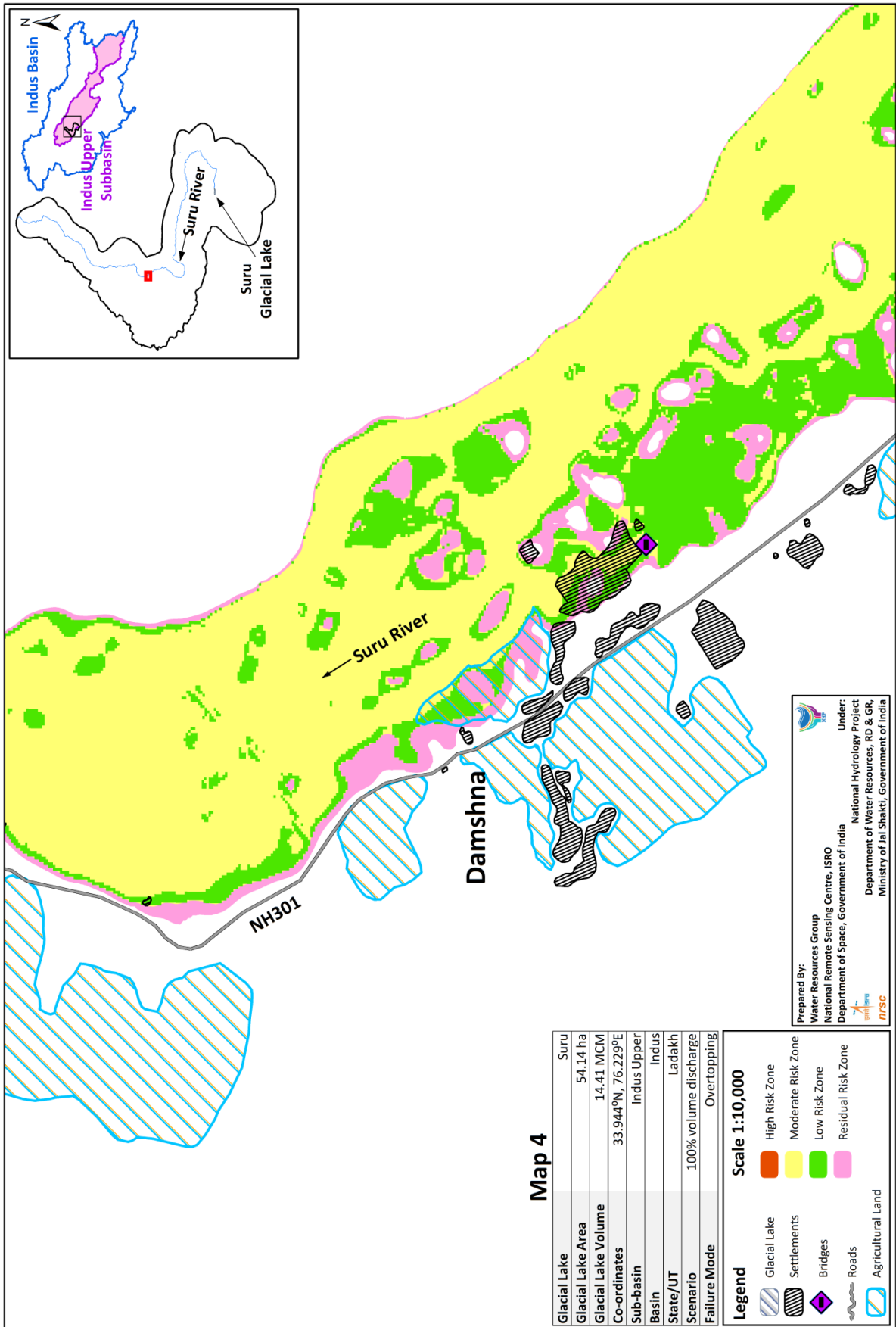
The Suru glacial lake GLOF risk zone maps of close view at important locations (20) along Suru river reach for the scenarios 1 and 7 are given here.











Map 4

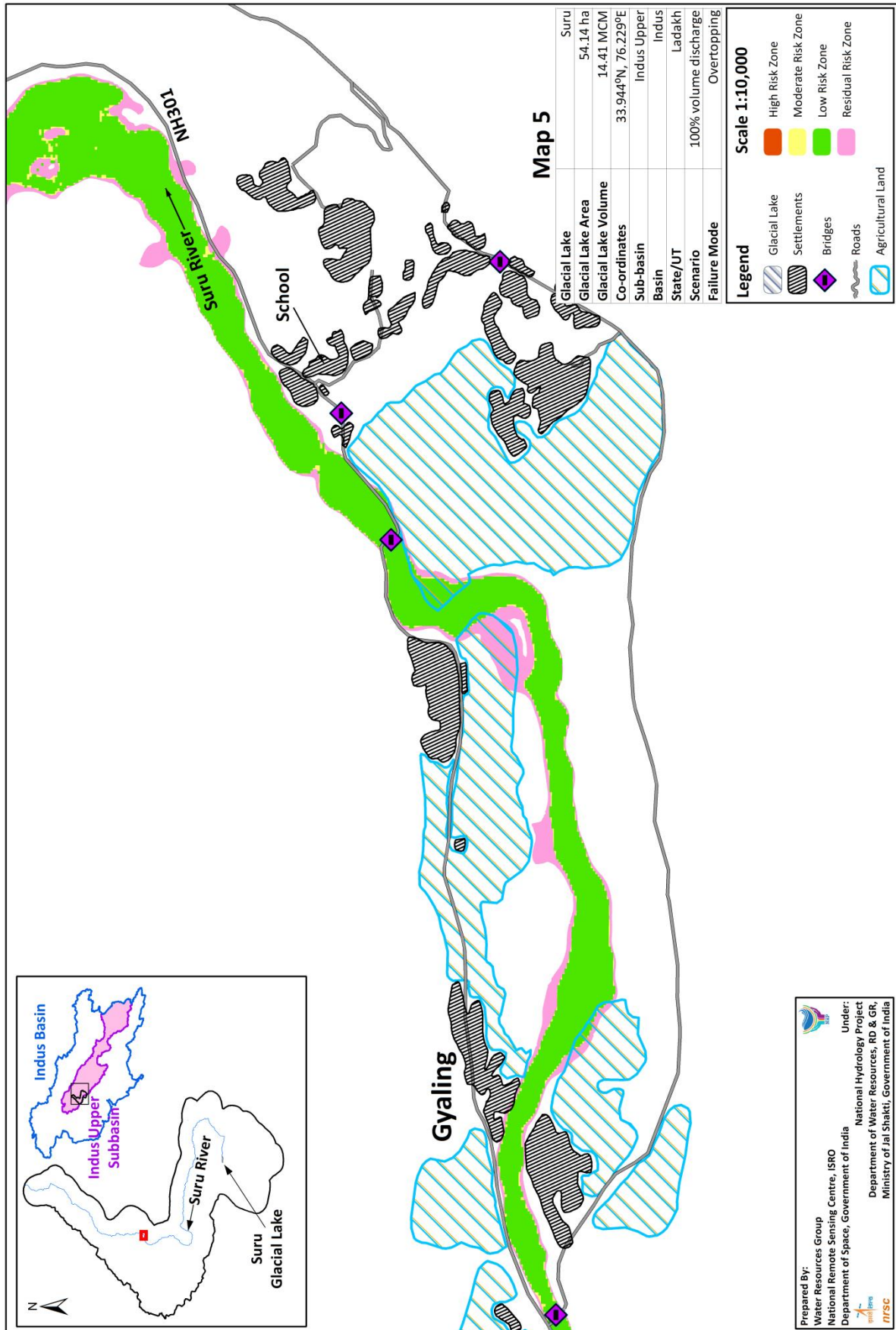
Glacial Lake	Suru
Glacial Lake Area	54.14 ha
Glacial Lake Volume	14.41 MCM
Co-ordinates	33.944°N, 76.229°E
Sub-basin	Indus Upper
Basin	Indus
State/UT	Ladakh
Scenario	100% volume discharge
Failure Mode	Overtopping

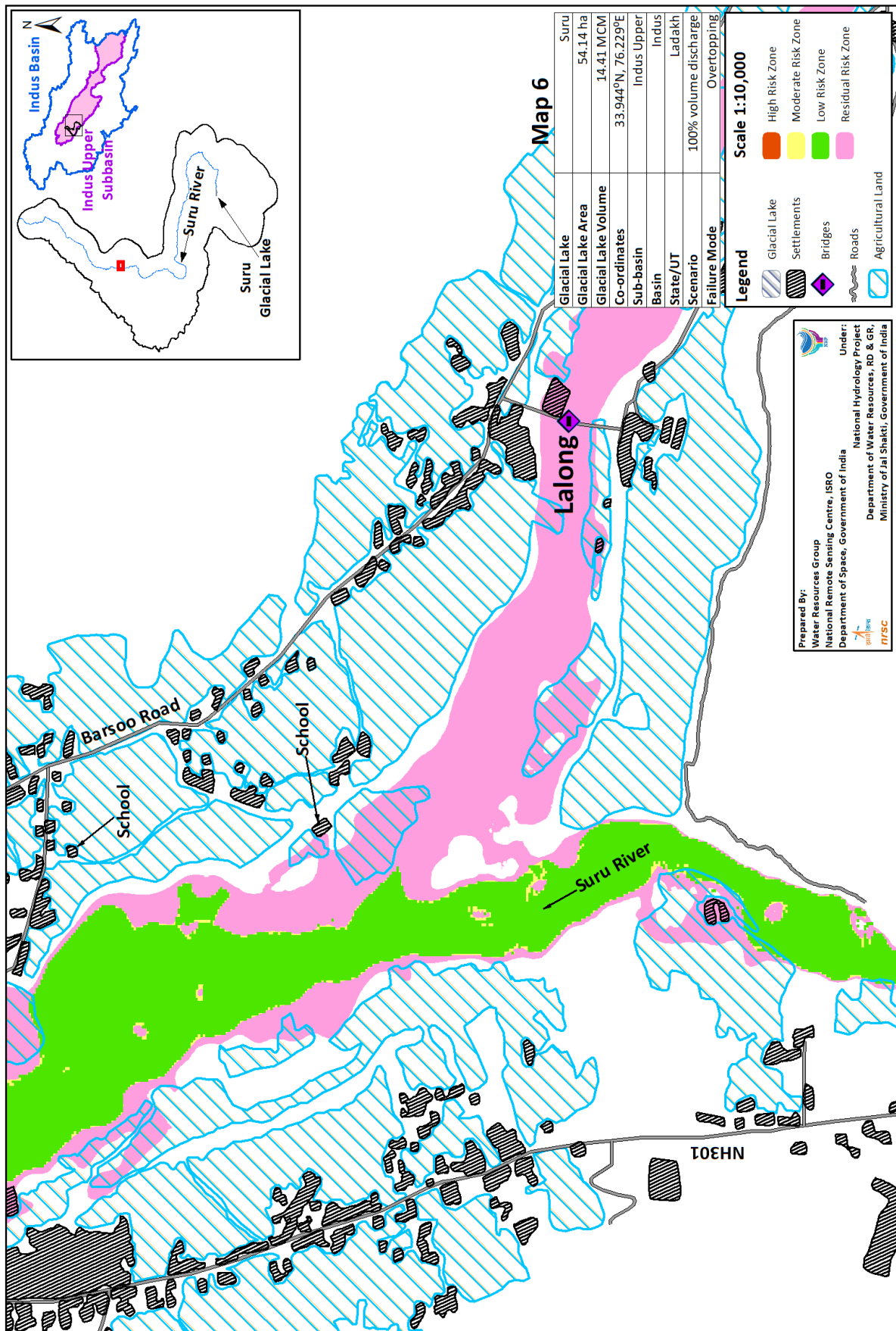
Legend
Scale 1:10,000

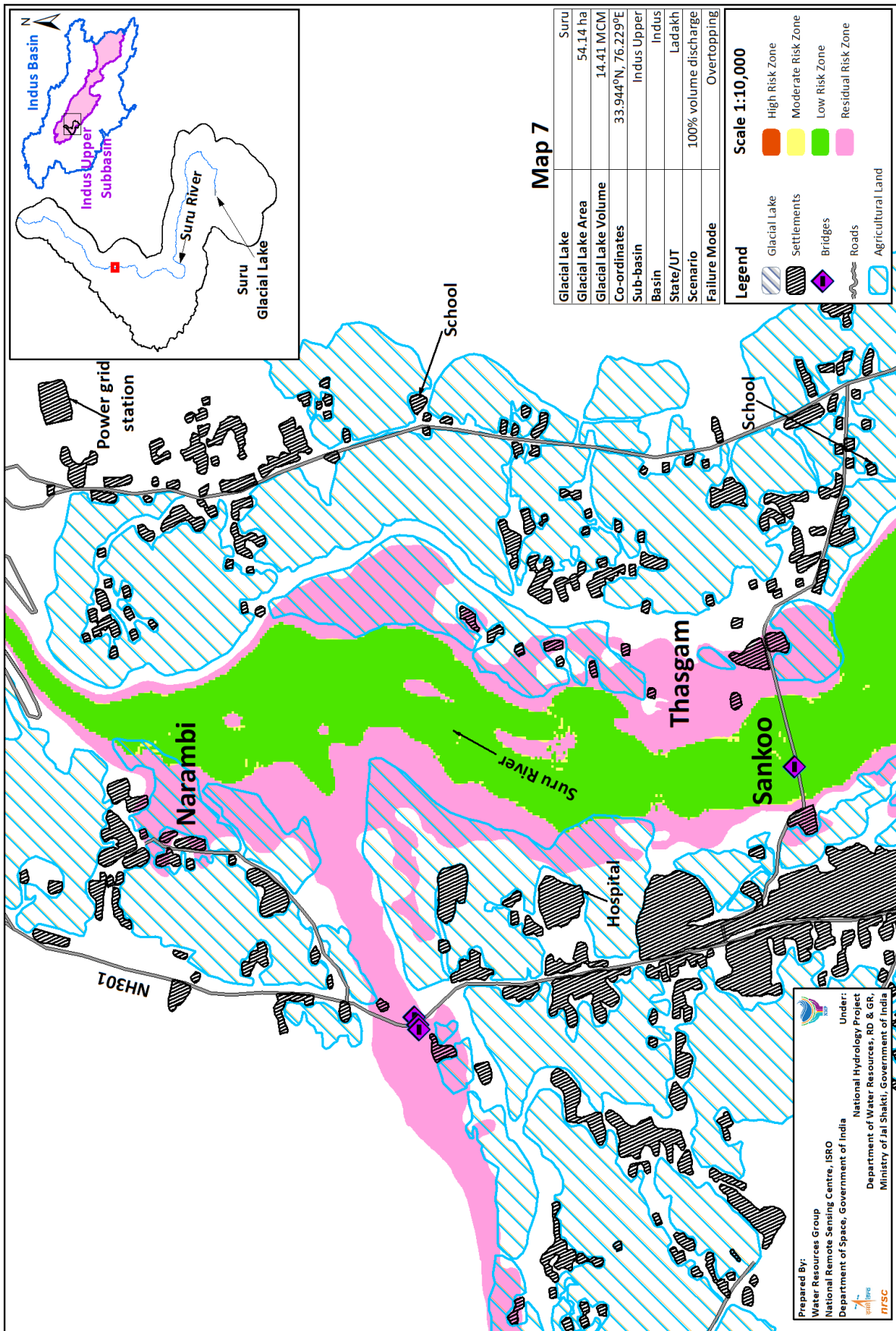
- High Risk Zone
- Moderate Risk Zone
- Low Risk Zone
- Residual Risk Zone
- Glacial Lake
- Settlements
- Bridges
- Roads
- Agricultural Land

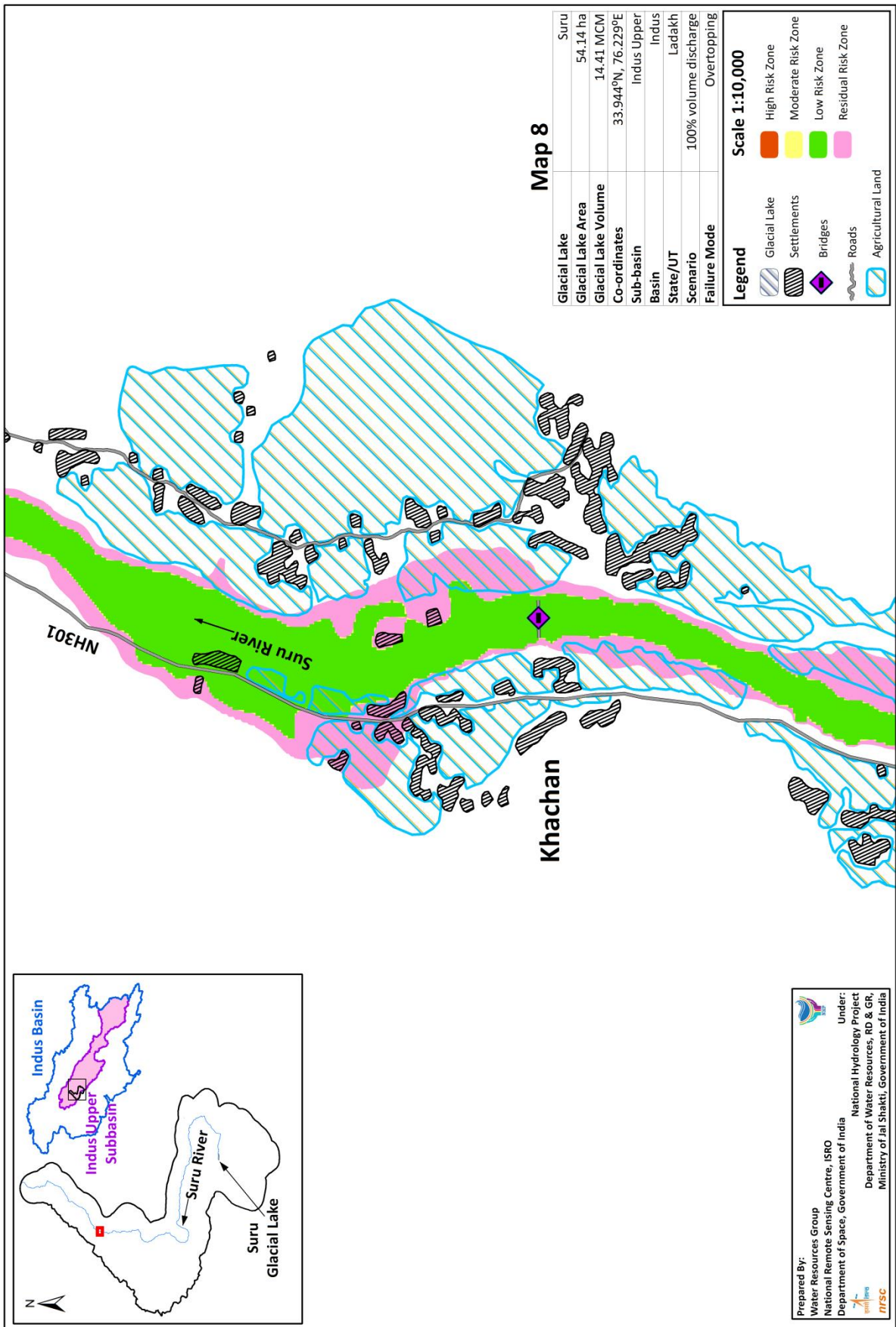
Prepared By:
Water Resources Group
National Remote Sensing Centre, ISRO
Department of Space, Government of India

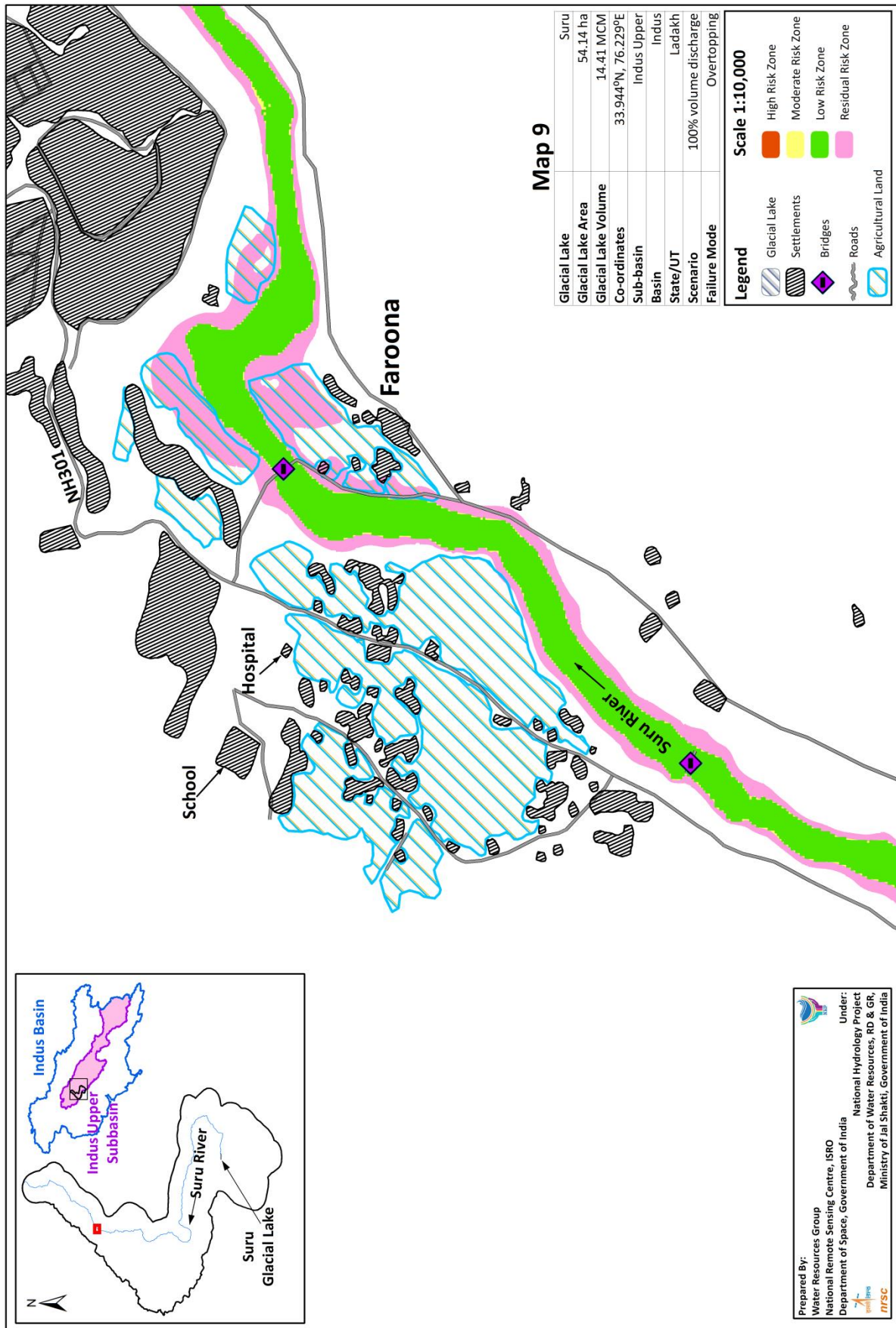
Under:
National Hydrology Project
Department of Water Resources, RD & GR,
Ministry of Jal Shakti, Government of India

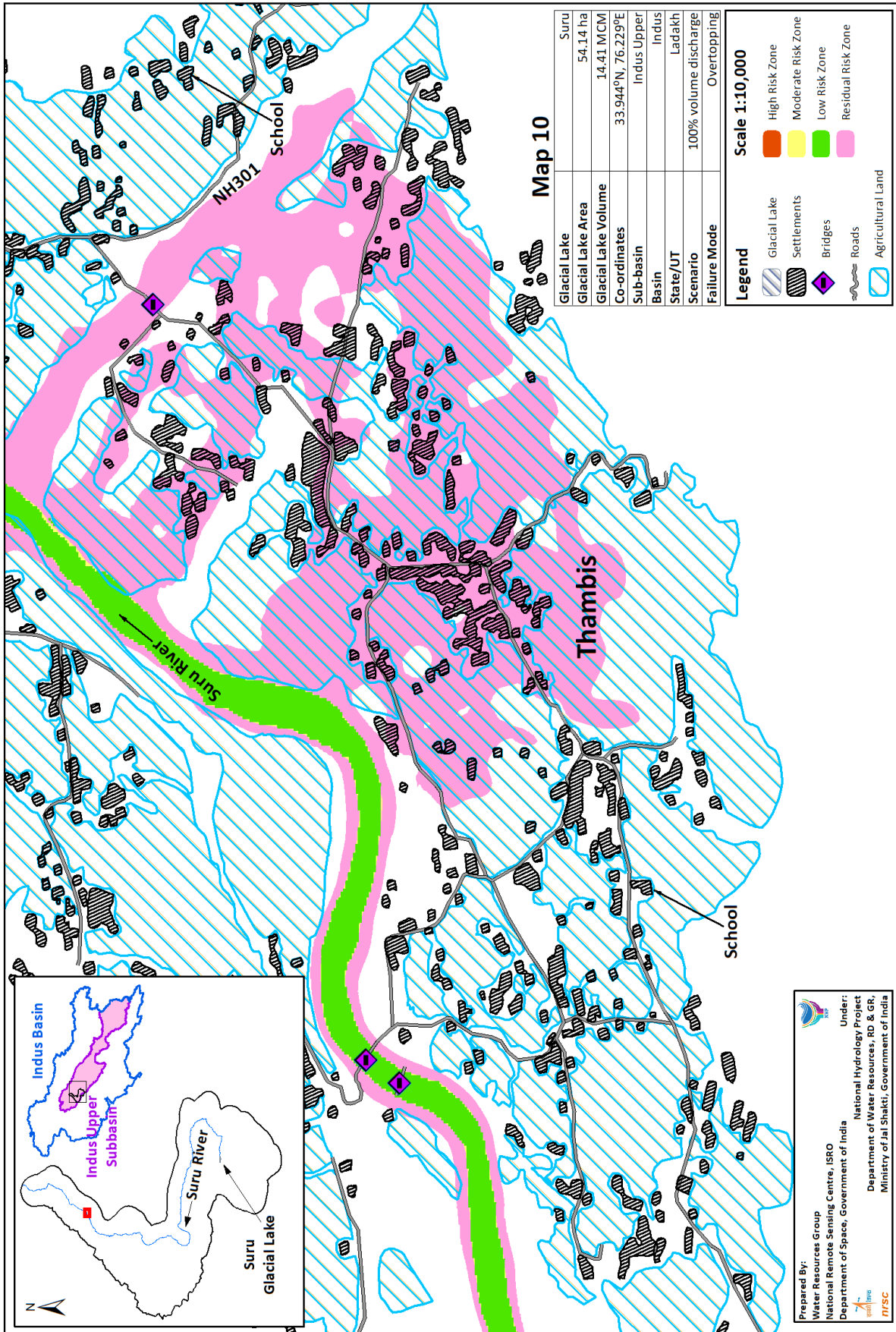


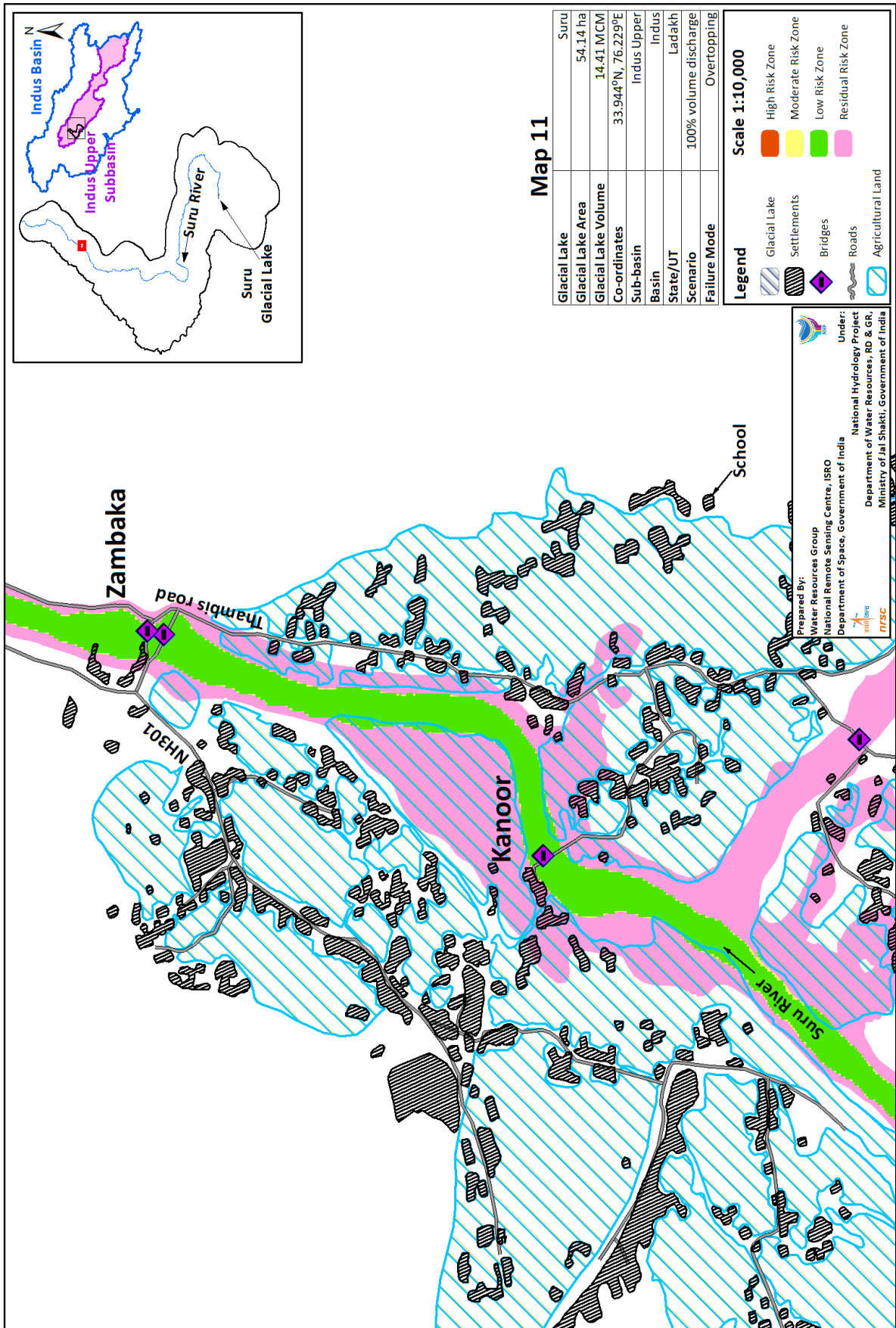


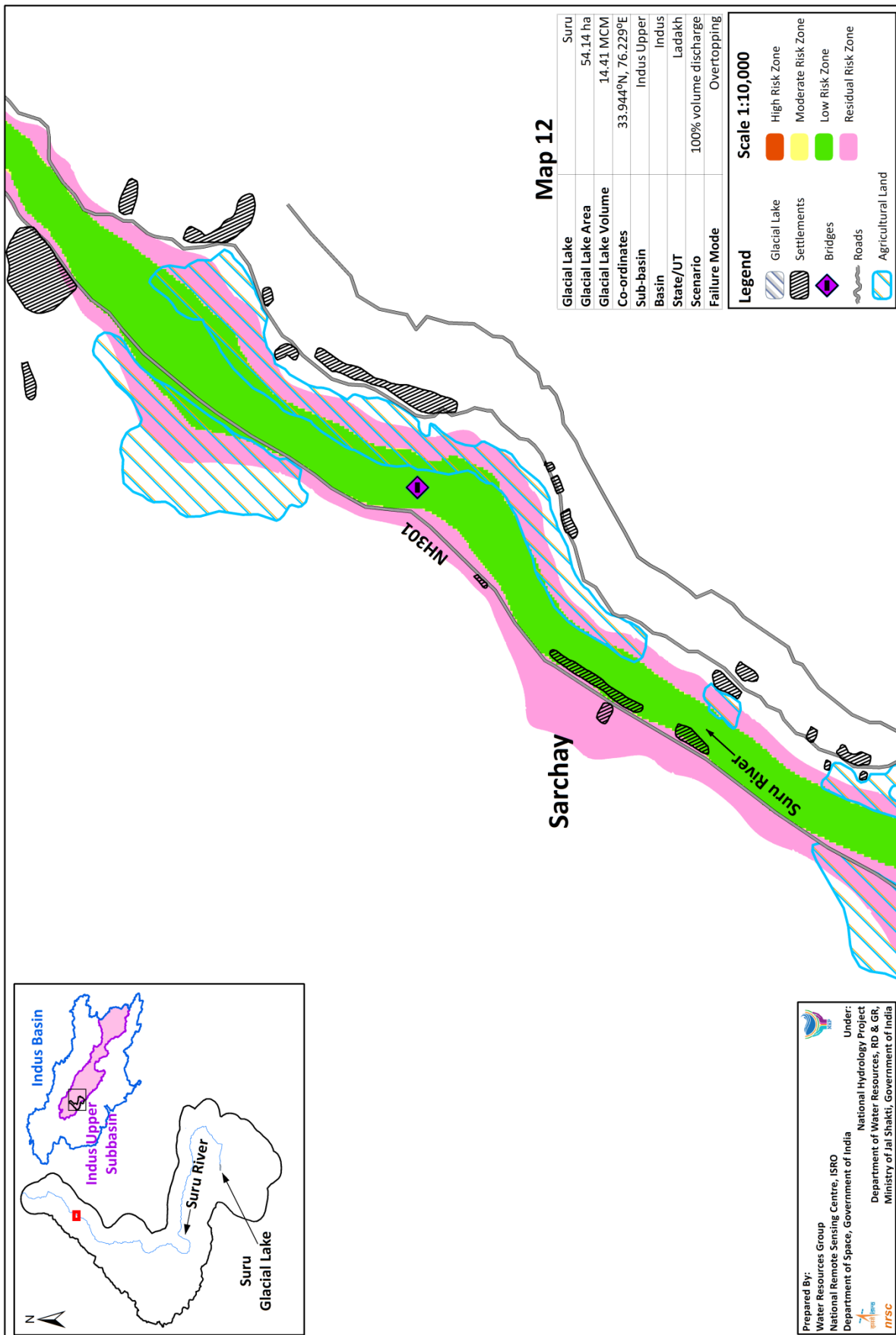


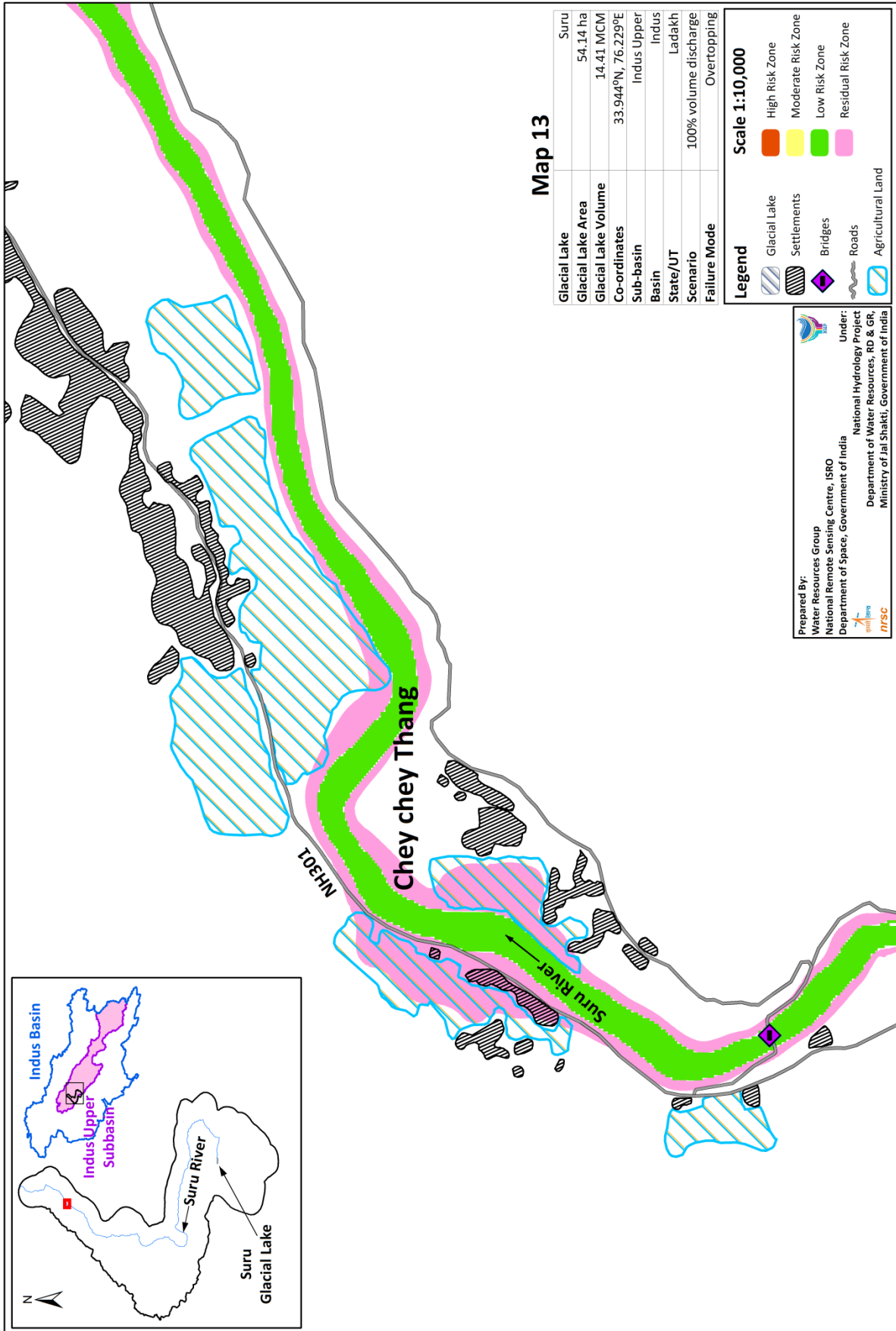


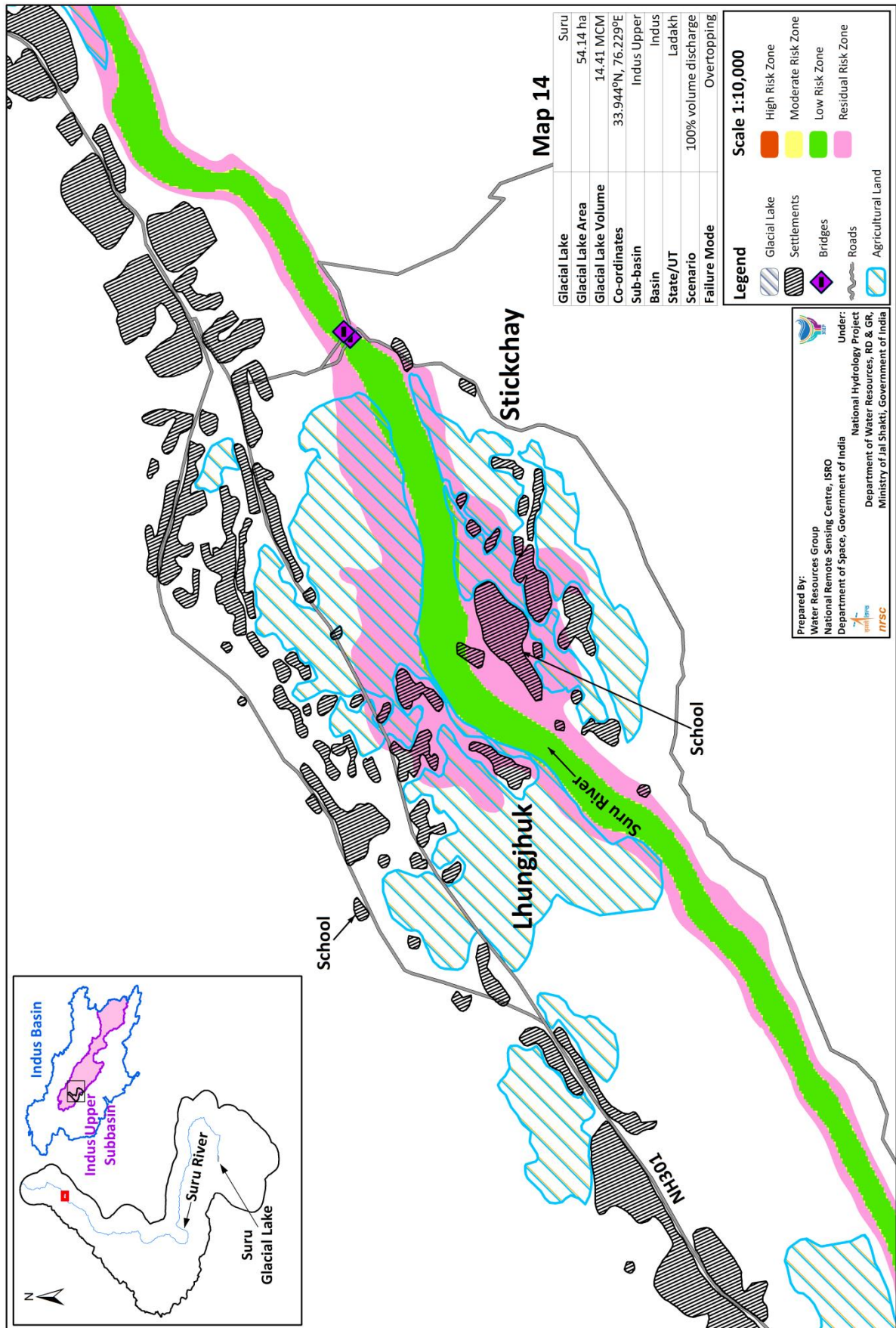


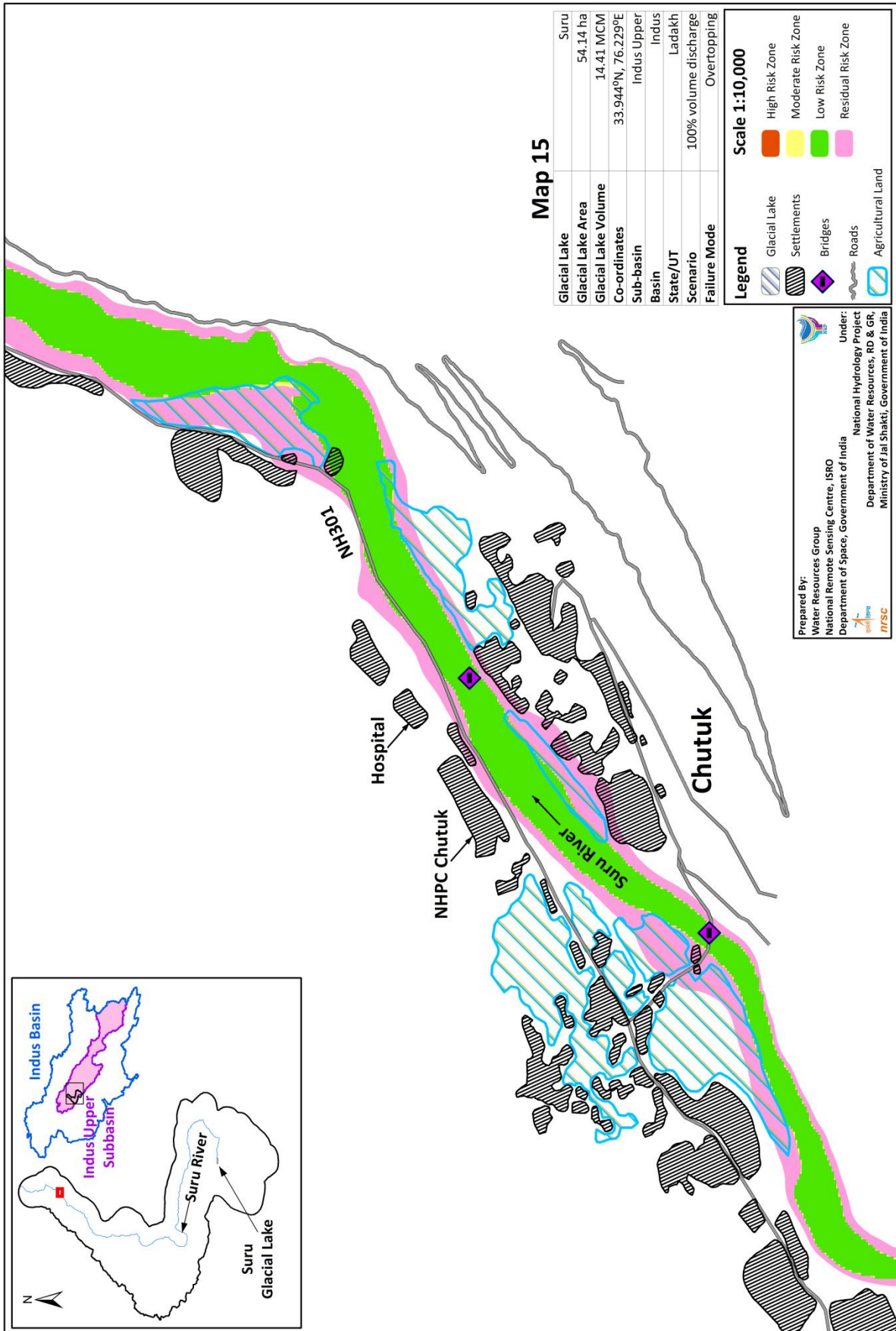


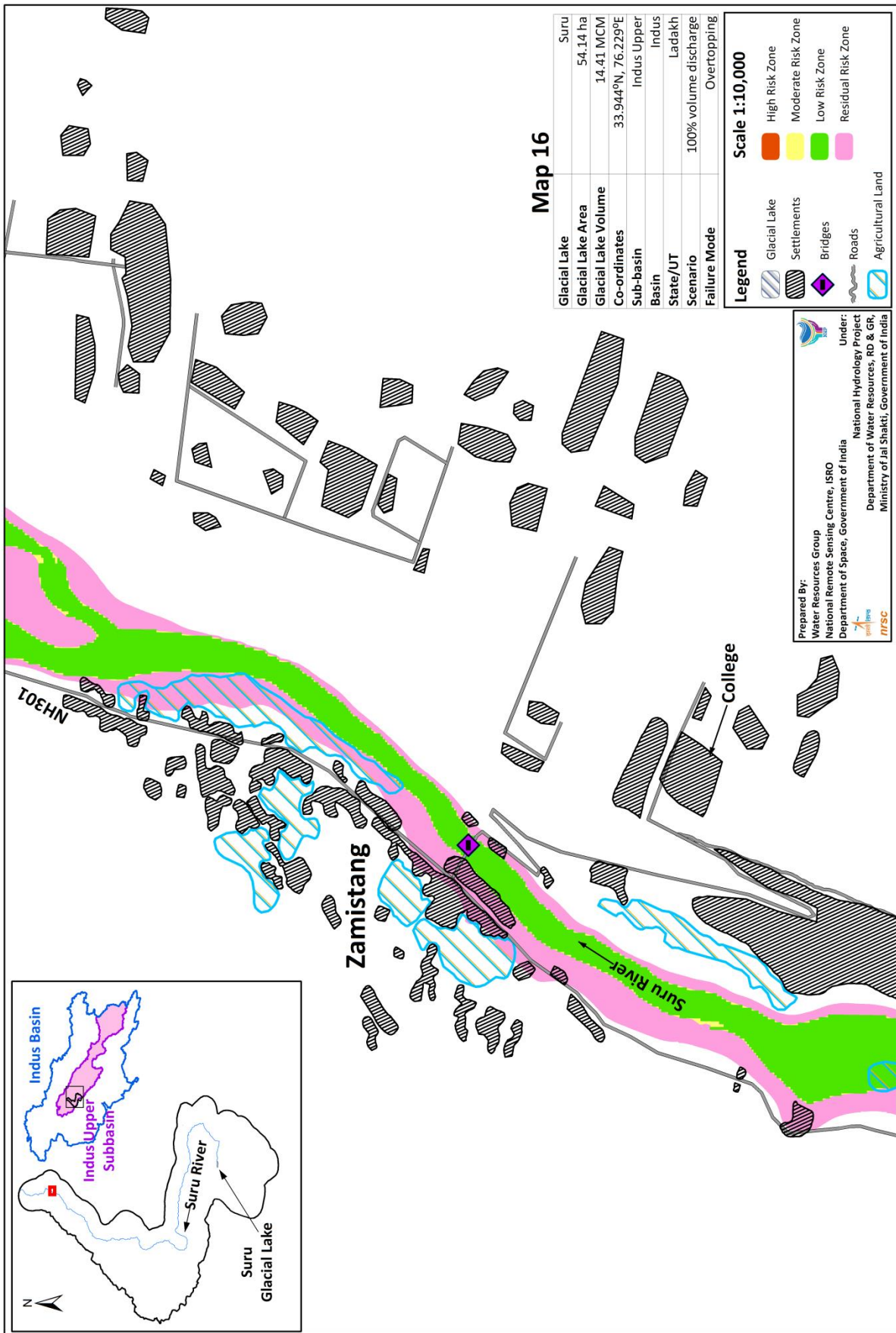


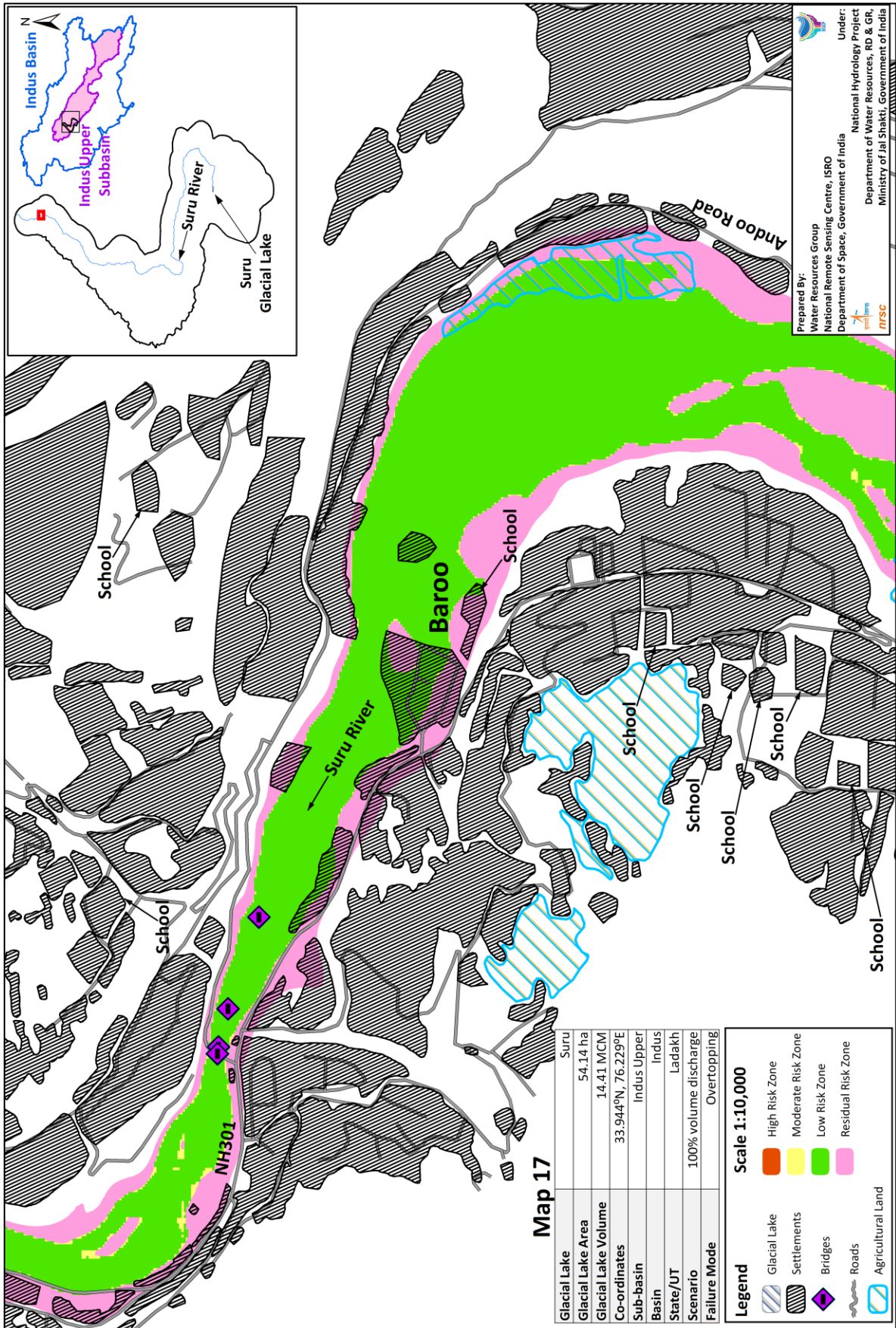


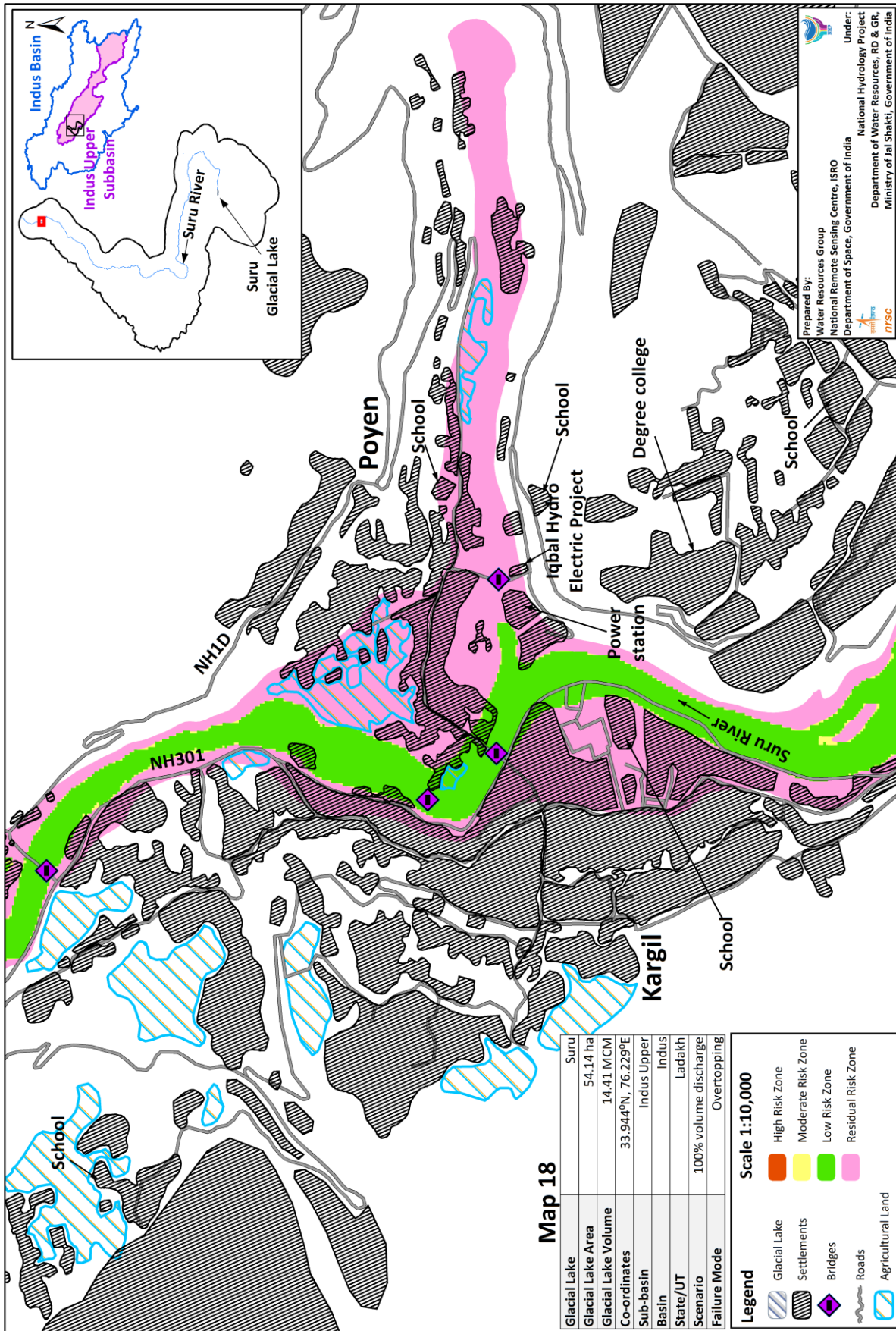


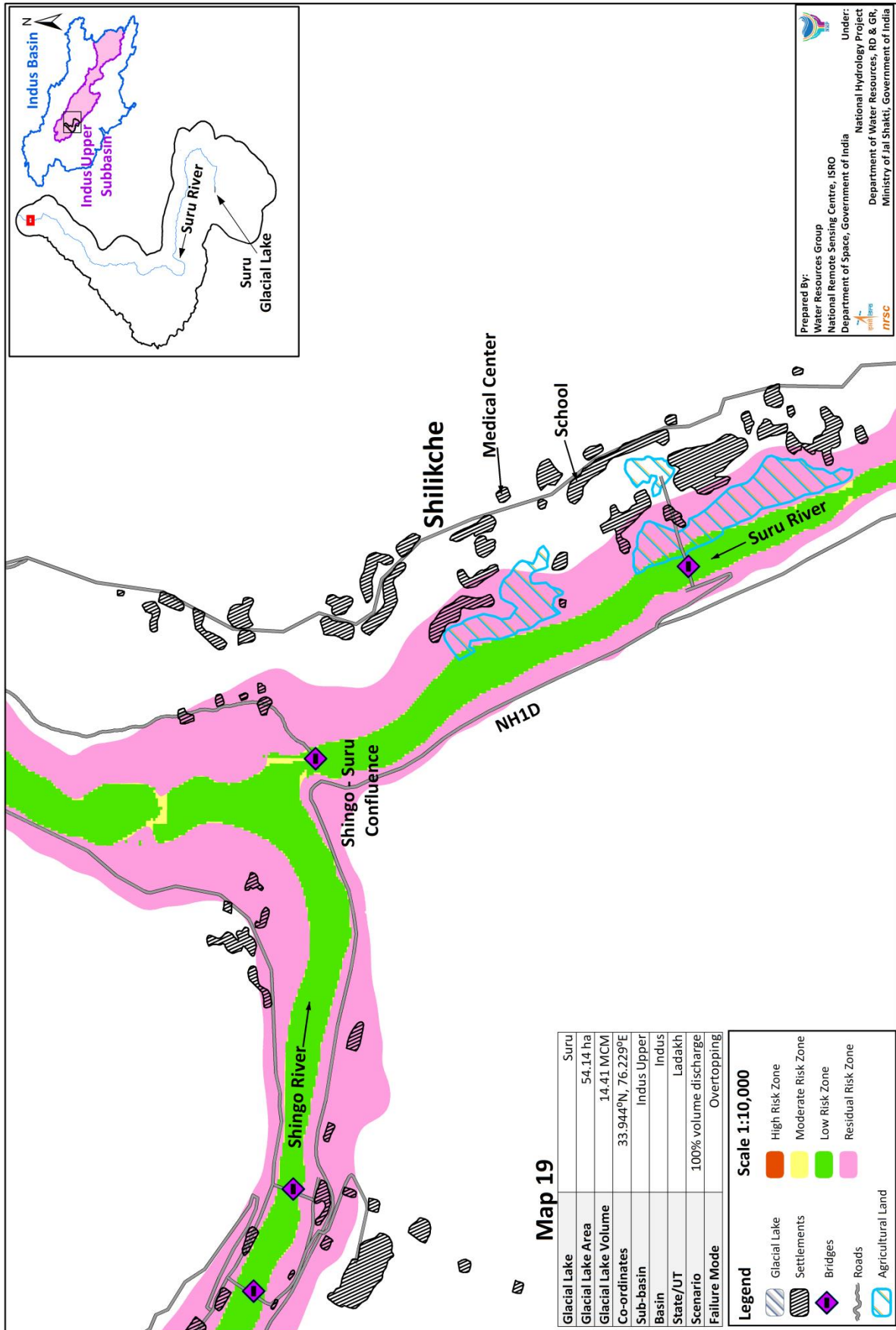


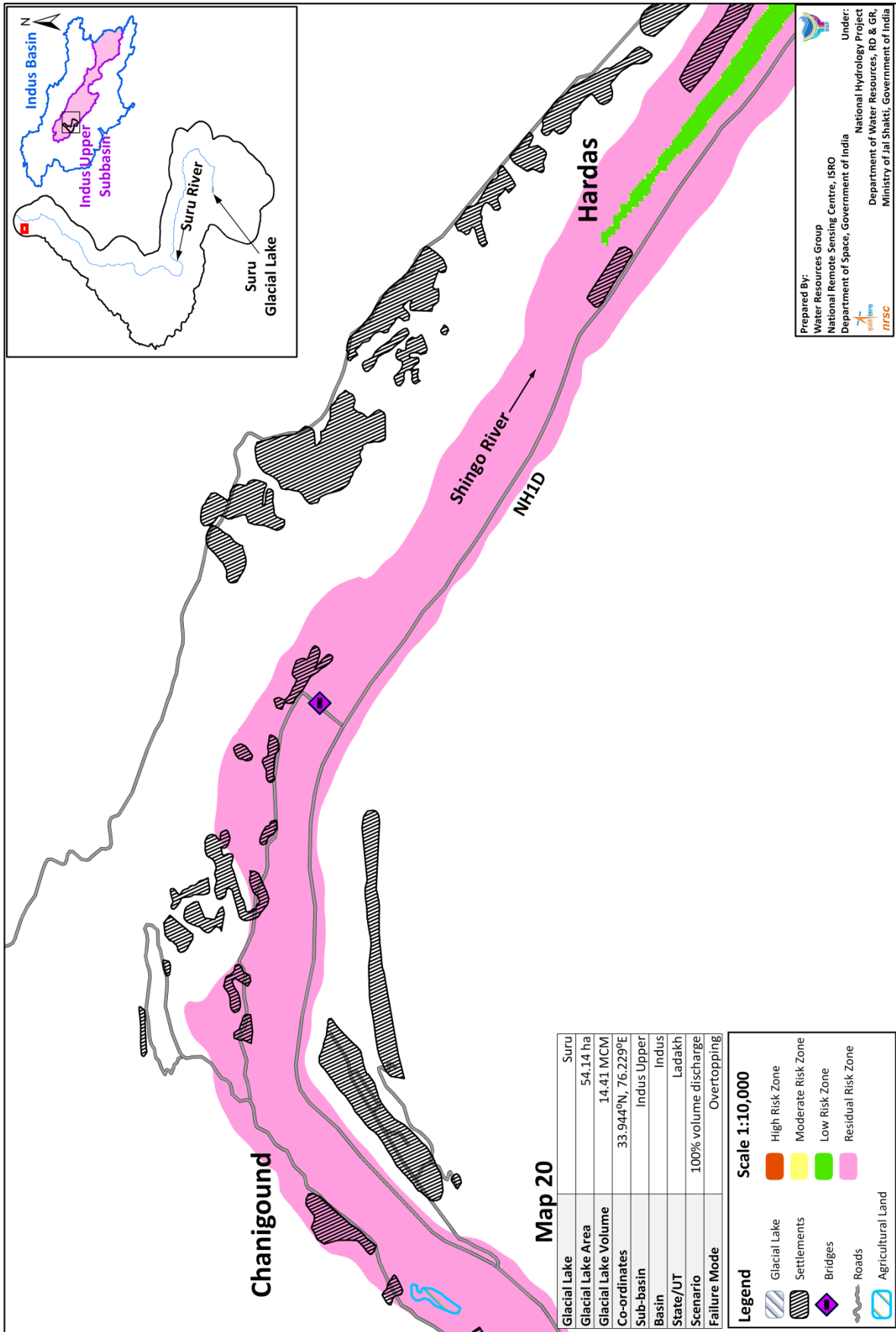














Ridge

Glacier

Hill shadow

Lake

Resourcesat 2
LISS IV MX